LONG RANGE NODAL SIGNALING IN VERTEBRATE LEFT-RIGHT SPECIFICATION

By

Yuki Ohi

Dissertation

Submitted to the Faculty of the

Graduate School of Vanderbilt University

in partial fulfillment of the requirements

for the degree of

DOCTOR OF PHILOSOPHY

in

Cell and Developmental Biology

May, 2007

Nashville, Tennessee

Approved:

Dr. David M. Bader

Dr. Mark P. de Caestecker

Dr. David M. Miller

Dr. Lilianna Solnica-Krezel

Dr. Christopher V.E. Wright

ACKNOWLEDGMENTS

Several people were instrumental in helping me complete this project. First, I would like to thank my mentor, Dr. Christopher V. E. Wright, for providing support and guidance throughout my training. Having entered his laboratory with zero developmental biology training, he took me under his wing and provided me with a fundamental knowledge base, as well as deeper understanding of the field. Chris also taught me the importance of paying attention to detail without losing sight of the bigger picture. His pursuit of excellence and demand for quality work will undoubtedly make me a better scientist in the future. Apart from my scientific training that I received in his lab, I will miss the challenging pool games as well as valuable advice that Chris provided me on how to become a better pool player. I will always fondly remember our first game of eight-ball, in which Chris demonstrated his billiards skills (and rightfully put me in my place). I would also like to thank my remaining committee members, Dr. David Bader, Dr. David Miller, Dr. Lilianna Solnica-Krezel, and Dr. Mark DeCaestecker for their kind words of encouragement and advice regarding the direction of my project. Additionally, I would like to thank both past and present members of the Wright lab for their assistance throughout the course of this project, in particular: Bonnie Cooper, Yoshiya Kawaguchi, Yoshio and Shuko Fujitani, Young Cha, Shuji Takahashi, Keely Solomon, JJ Westmoreland, Dan Boyer, Michael Ray, Lindsay Bramson, Xavier Stein, and Pan Fong Cheng deserve special thanks. My personal interactions with all of these wonderful individuals have made my time in the Wright lab enjoyable as well as productive.

On a personal note, I would also like to thank my family, Seigo, Norie, Keima, Ryoma, and Melanie Ohi for their support over the years. They have provided me with encouragement, advice, and love. In particular, I would like to acknowledge my mother's courage and grace in the face of adversity as an inspiration for me on both a personal and professional level. My father's tenacity and perseverance have served as a

model for me since childhood. I also want to thank my brothers and sister for always keeping me grounded, and helping to maintain a more global perspective.

Finally, I would like to acknowledge my husband, best friend, and confidant, Kevin Maas. He has supported me unconditionally with his love and devotion throughout my years in graduate school. I want to thank him for understanding the demands that go into working in a lab environment, and the unwavering support he has shown me despite the requirements of his own training as an M.D./Ph.D. I am grateful for how much he has enriched my life. I could not have made it through this process without him.

TABLE OF CONTENTS

Page

LIST OF TABLES

LIST OF FIGURES

CHAPTER I

INTRODUCTION

Cell-to-cell communication is crucial for promoting proper cell fate specification during early embryogenesis. This process entails secreted ligands that typically travel to responding cells where they bind to specific receptors on the cell membrane, resulting in intracellular signal transduction and activation of a particular repertoire of genes that are responsible for determining the fate of the cell. A large number of signaling pathways have been identified that are thought to play a role in cell fate determination, but the specific pathway that my studies have focused on is that of the Transforming Growth Factor-β (TGF-β) related molecule, Nodal. Nodal signaling has been implicated in several developmental processes that include mesendoderm specification and Left-Right (L-R) axis formation. Many findings suggest that the refinement of cell fate specification during these processes is achieved by a precise balance between both positive and negative influences from various factors that act on the Nodal signals. The experiments described in this thesis address the function of Nodal in L-R asymmetry specification and examine how Nodal signals are relayed within and between different tissues, as well as spatiotemporally regulated and globally integrated to pattern the tissues that will eventually undergo asymmetric morphogenesis. Although the Nodal signaling pathway is poorly defined at the biochemical level, there is much evidence suggesting that Nodal and TGF-β share common receptors and signal transducers. Therefore, I will first present a brief summary of what is known about TGF-β-like structure and signaling, as this information may become directly relevant to understanding the intricacies of how Nodal signaling is regulated. This will be followed by an overview of the recent discoveries that have been made in the areas of mesendoderm induction and L-R axis development, with a particular emphasis on the findings in *Xenopus*.

TGF-β superfamily

TGF-β structure

TGF-β signaling controls a large array of cellular processes that include cell proliferation, differentiation, and apoptosis. Mutations in various components of the TGF-β signaling pathway have been linked to several developmental defects, as well as particular disease states such as cancer. The TGF-β superfamily can be divided into two subgroups, the TGF-β /Activin/Nodal subfamily and the BMP (bone morphogenetic protein)/GDF (growth and differentiation factor)/MIS (Muellerian inhibiting substance) subfamily. Also included in the TGF-β superfamily are the more divergent Lefty-related molecules that are important regulators of Nodal signaling.

Although different TGF-β-related ligands play distinct and various biological roles, all members of the superfamily contain conserved sequences, structural features and undergo similar processing. TGF-β-related molecules are initially secreted as large pre-proproteins that are comprised of a hydrophobic signal sequence, an N-terminal prodomain, and a C-terminal mature ligand domain. The precursor molecules undergo proteolytic cleavage at a dibasic site by members of the subtilisin-like proprotein convertase (SPC) family to release the mature protein that is then able to bind to receptors and activate downstream signaling. Spc1 and Spc4 (also known as Furin and Pace4, respectively), for example, are two convertases that have been directly implicated in the maturation of the Nodal ligand (Beck et al., 2002). Most TGF-β family members contain 7-9 conserved cysteine residues and the active form of a TGF-β ligand is a homodimer that is stabilized by hydrophobic interactions and inter-subunit disulfide bridges. Each TGF-β monomer comprises several extended β strands that are interlocked by three conserved disulfide bonds that form a tight structure referred to as a "cysteine knot" (Sun and Davies, 1995). The more divergent Lefty-related proteins however lack a critical cysteine residue that is required for dimer formation and are therefore thought to

exist and/or function as a monomer. Lefty proteins also exhibit the distinct characteristic of having two proteolytic cleavage sites, so that the mature ligand may exist as two alternative forms (*e.g.,* a long and a short isoform).

Typically, after the mature TGF-β ligand is released it homodimerizes and functions to influence a number of biological processes by activating a specific downstream signaling pathway. However, studies on TGF-β1 have shown that after cleavage, the prodomain remains non-covalently associated with the mature protein as a "latency-associated polypeptide" (LAP). The LAP may be retained on the cell membrane by binding covalently with large secretory glycoproteins, known as latent TGF-β-binding proteins (LTBPs; Sterner-Kock et al., 2002; Yin et al., 1998; Giltay et al., 1997). It is thought that the LAP may be involved in regulating receptor activation by TGF-β1 (for review, see Massagué, 1998). In support of this notion, studies in *Xenopus* have shown that LTBP-1 potentiates Nodal and Activin signaling (Altmann et al., 2002).

TGF-β signal transduction

TGF-β-related ligands are thought to signal through a similar mechanism comprised of common intermediate steps. The common steps involved in TGF-β signal transduction are as follows (as illustrated by the Nodal signaling pathway in Fig. 1.1). TGF-β-related homodimers initiate signaling by binding to a type I serine/threonine kinase receptor on the membrane of receiving cells (**Fig. 1.1, step 1**; reviewed in Massagué, 1998). Ligand binding then leads to the recruitment of a type II receptor (**Fig. 1.1, step 2**), thereby forming an active signaling complex (**Fig. 1.1, step 3**). Studies in *Xenopus* and mouse largely suggest that Nodal signals through the type II activin receptors, ActRIIA and ActRIIB and the activin type I receptor, ActRIB (also known as ALK4) (Whitman, 2001). Nodal has also been shown to require an additional coreceptor (EGF-CFC, see below) for active signaling (for review, see Schier, 2003). Phosphorylation of the type I receptor in a highly conserved juxtamembrane position by

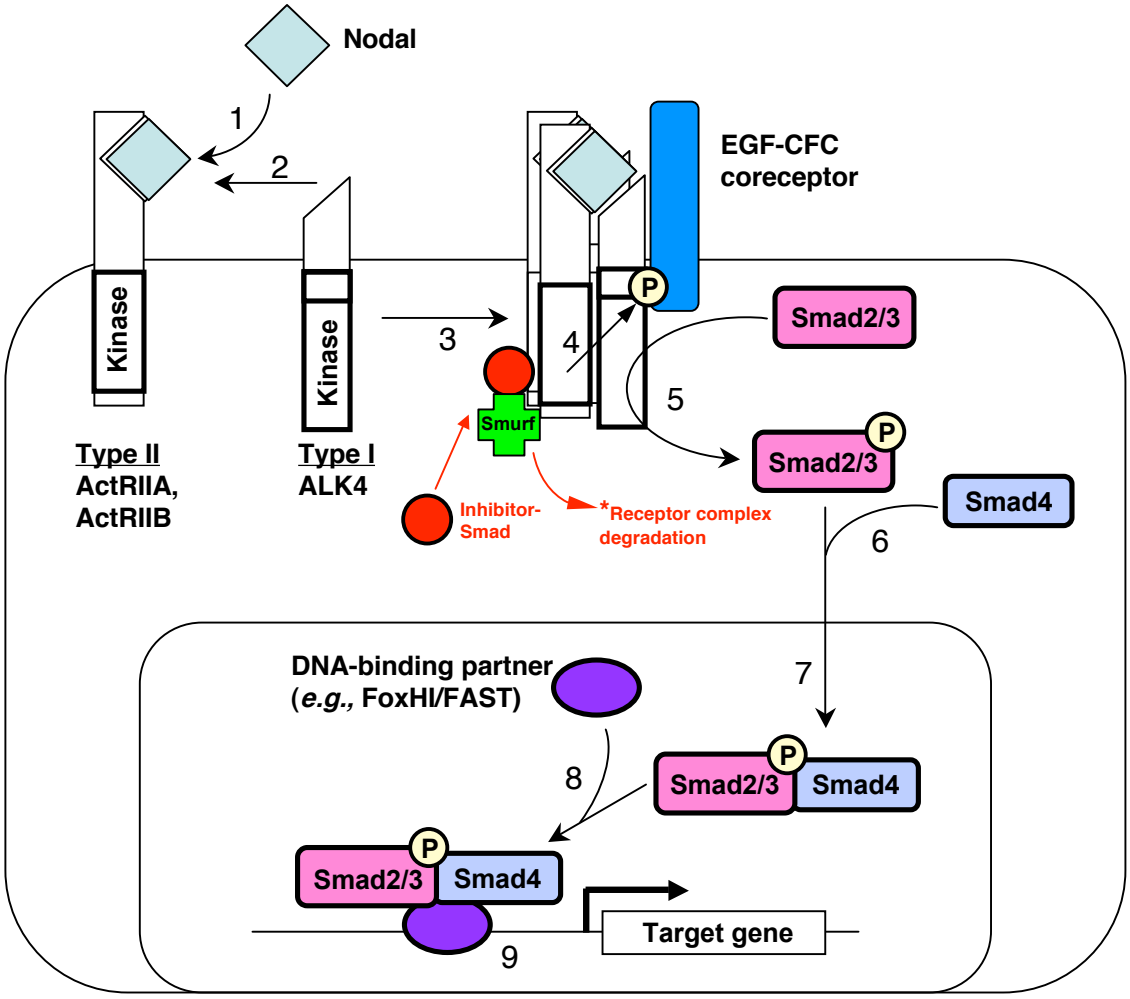

Fig. 1.1 Nodal signal transduction pathway. Binding of a Nodal homodimer (for simplicity, only one Nodal ligand is shown) to the ActRIIA/B type II receptor (1) together with the ALK4 type I receptor (2) and EGF-CFC coreceptor results in formation of an activated receptor complex (3) and phosphorylation of the type I receptor (4). The type I receptor then phosphorylates the Receptor-Smads, Smads2/3 (5), which then associate with the Co-Smad, Smad4 (6). The activated Smad complex translocates into the nucleus (7) and associates with DNA-binding cofactors, such as FoxHI/FAST (8) resulting in activation of downstream target gene expression (9). *Inhibitor-Smads, along with the E3 ubiquitin ligases (Smurfs), associate with activated receptor complexes and lead to their degradation. This figure is modified from Massagué (1998).

the constitutively active type II receptor (**Fig. 1.1, step 4**) subsequently results in the phosphorylation of specific receptor-regulated Smads (R-Smads) (**Fig. 1.1, step 5**). There are a number of different R-Smads that are activated by distinct signaling pathways. For example, the R-Smads, Smad2 and Smad3, specifically respond to TGF-β-mediated signaling whereas, R-Smads1, 5, and 8 primarily respond to BMP-related signaling. The phosphorylated R-Smads then complex with the Co-mediator Smad (Co-Smad), Smad4, in the cytoplasm (**Fig. 1.1, step 6**) resulting in the translocation of the activated Smad complex into the nucleus (**Fig. 1.1, step 7**). In conjunction with other cofactors such as FoxH1 (FAST) (**Fig. 1.1, step 8**), the active Smad complex leads to the transcription of target genes (**Fig. 1.1, step 9**). The inhibitory Smads (I-Smads), that include Smad6 and Smad7, in contrast, act to negatively regulate TGF-β signaling by competitively binding to activated receptor complexes (Kavsak et al., 2000; Suzuki et al., 2002). I-Smad interaction with activated receptors results in the ubiquitination of the complex, mediated by the E3 Smad ubiquitination regulatory factors (Smurfs), and eventual degradation via calveolin-positive vesicles by the 26S proteasome (Ebisawa et al., 2001; Tajima et al., 2003; Di Guglielmo et al., 2003).

R-Smad and Co-Smad proteins contain two conserved structural domains, an N-terminal MH1 and C-terminal MH2 domain (Mad-homology 1 and 2, respectively) that are separated by a less conserved linker region. The MH1 domain exhibits sequence-specific DNA binding activity, may function in nuclear import, and negatively regulates the MH2 domain. The MH2 domain, on the other hand, functions in receptor interaction, formation of homomeric as well as heteromeric Smad complexes, and directly contacts the nuclear pore complex for nucleocytoplasmic shuttling. Both of these domains are thought to interact with additional proteins in the nucleus for activating transcription of target genes (Shi and Massagué, 2003).

The interaction of Smads with an activated type I/type II receptor complex is a crucial step in the initiation of intracellular signal transduction. There is evidence that

adaptor proteins may facilitate the recognition of R-Smads by type I receptors. The SARA (Smad anchor for receptor activation) protein has been shown to immobilize Smad2 and Smad3 near the cell surface via an extended hydrophobic surface area of the proteins (Wu et al., 2000). SARA contains a phospholipid binding FYVE domain which targets the Smads to the membrane of early endosomes allowing more efficient recruitment to the signaling receptors for phosphorylation (Tsukazaki et al., 1998). After Smad2 phosphorylation, the interaction with SARA is destabilized allowing Smad2 to dissociate from the complex and exposes a nuclear import sequence present within the MH2 domain (Xu et al., 2000). Smad2 phosphorylation has also been shown to increase its affinity for Smad4 (Shi and Massagué, 2003). In addition to SARA, other adaptor proteins have been identified, such as Disabled-2 (Hocevar et al., 2001), Axin (Furuhashi et al., 2001), and ELFβ-spectrin (Tang et al., 2003). All have been shown to facilitate TGF-β signaling by promoting Smad2/3 and receptor interaction.

Upon nuclear translocation of activated Smad complexes, TGF-β-related signaling can result in both the activation, as well as repression of target gene expression depending on whether they become associated with co-repressor or co-activator molecules. Among the negative regulators of Smad transcriptional function are the co-repressors TG3-interacting factor (TGIF) and members of the Ski family of proteins. These proteins associate with histone deacetylases (HDACs) and lead to chromatin condensation of the DNA at target gene promoters. The co-activators, p300 and CBP, in contrast, exhibit histone acetyltransferase activities and therefore lead to the activation of target gene transcription when bound to an activated Smad complex (Shi and Massagué, 2003).

The Forkhead-related winged-helix transcription factor, FoxHI (formerly known as FAST1) is the most well characterized cofactor shown to interact with phosphorylated Smad2 and regulates Nodal downstream target gene expression (Whitman, 2001). FoxHI was originally identified through studies of mesodermal responsive genes in *Xenopus*. A

number of studies have shown that FoxHI, Smad2 and Smad4, form an ARF (Activin Response Factor) protein complex (Chen et al., 1996) that is capable of both positively and negatively regulating a variety of genes involved in the mesoderm induction program. Over the years, orthologs of FoxHI have been identified in other species including human (FAST-1/FOXHI), mouse (FAST1/FoxHI and FAST2/FoxH2) and zebrafish (Schmalspur/FoxHI), and have been shown to play a conserved role in Nodal signal transduction (Sirotkin et al., 2000; Pogoda et al., 2000; Boggetti et al., 2000; Zhou et al., 1998; Kaestner et al., 2000).

Once TGF-β-related signaling is complete within a cell, it is thought that dephosphorylation by as yet unidentified phosphatases (Randall et al., 2002), as well as ubiquitination of activated Smads followed by proteasome-mediated degradation leads to the termination of Smad signaling (Shi and Massagué, 2003). In support of the latter idea, it has been shown that activated Smad2 is ubiquitinated in the nucleus, which may involve the E3 ubiquitin ligase, Smurf2, and undergoes degradation through the 26S proteasome (Lo and Massagué, 1999).

Regulation of TGF-β signaling

Due to the involvement in many physiological processes, it is critical for TGF-β-related signaling to be tightly regulated. Numerous studies on TGF-β signaling have revealed that there appears to be regulation at each level of the pathway. For example, a large family of soluble proteins collectively known as "ligand traps" function to sequester TGF-β-related ligands and prevent them from binding to membrane receptors, thereby negatively regulating the overall strength of TGF-β signaling. Examples of known ligand traps are decorin and α2-macroglobulin that bind to TGF-β, follistatin which binds to Activin and BMPs, Noggin and Chordin/SOG that bind BMPs and Dan/Cerberus that also bind BMPs but also Nodal (Shi and Massagué, 2003). A truncated form of the Cerberus protein, Cerberus-short (Cer-S), has been shown to only block Nodal by direct

binding to the ligand (Piccolo et al., 1999). Overexpression of Cer-S in *Xenopus* embryos resulted in defects in mesendoderm induction and produced phenotypes closely resembling zebrafish and mouse mutants defective in Nodal signaling (Agius et al., 2000).

Membrane-anchored proteins, which act as accessory or coreceptors, function to positively promote TGF-β ligand binding to signaling receptors (Shi and Massagué, 2003). For example, the membrane-anchored proteoglycan betaglycan has been shown to specifically mediate TGF-β binding to the type II receptor (Brown et al., 1999; Massagué, 1998), whereas, members of the Epidermal-Growth-Factor-Cripto-FRL1-Cryptic (EGF-CFC), both in the secreted as well as membrane-bound form, mediate the binding of Nodal, Vg1, and GDF1 to Activin receptors (Cheng et al., 2003; Rosa, 2002; Shen and Schier, 2000). Members of the EGF-CFC family are extracellular, GPI-linked proteins. EGF-CFC homologs have been identified in all vertebrates examined and include zebrafish One-eyed pinhead (Oep), *Xenopus* xCR1-3, chick CFC, and mouse and human Cripto and Cryptic (Shen and Schier, 2000). The requirement for EGF-CFC coreceptors in Nodal signaling is clearly demonstrated by the observation that zebrafish embryos lacking both maternal and zygotic Oep activity are unresponsive to Nodals. Moreover, *oep*-deficient embryos appear phenotypically identical to double mutant embryos for the *nodal*-related genes *cyclops* (*cyc*) and *squint* (*sqt*) (Gritsman et al., 1999). Cripto mouse mutant embryos also exhibit similar characteristics to Nodal mutants (Ding et al., 1998). Biochemical studies have demonstrated that without Cripto, Nodal cannot form a complex with the type I/type II activin receptors (Bianco et al., 2002, Reissmann et al., 2001; Sakuma et al., 2002; Yan et al., 2002; Yeo and Whitman, 2001). Since Cripto can bind to ALK4 in the absence of Nodal, it is thought that Nodal assembles a complex of ActRIIB and pre-bound ALK4/Cripto to activate downstream signaling events (Schier, 2003). However, the precise mechanism of how EGF-CFC coreceptors mediate Nodal binding to its type I/II receptors still remains unclear.

It has also been shown that TGF-β-related signaling is regulated intracellularly. The DRAP1 protein has been demonstrated to inhibit Nodal signaling by binding to FoxHI, blocking its DNA binding activity. *DRAP1* mutants exhibit ectopic mesendoderm, consistent with an increase in Nodal signaling (Iratni et al., 2002). Other regulatory mechanisms and accessory proteins of Nodal signaling include the Nodal-induced Dpr2, which accelerates lysosome-mediated degradation of Nodal receptors (Zhang et al., 2004). Additional intracellular factors have recently been described that inhibit downstream activation of Nodal/Xnr signaling, including an E3 ubiquitin ligase molecule, ectodermin (Dupont et al., 2005). Clearly, a number of mechanisms exist at the extracellular level, at the level of the receptor and intracellularly to ensure the precise regulation of TGF-β-related signaling, enabling embryogenesis to proceed normally.

Nodal signaling and cell-fate specification

As development proceeds, the embryo becomes progressively more complex and cells must acquire specific fates to properly establish the mature body plan. One mechanism underlying cell fate specification is the preferential localization of particular determinants, as has been demonstrated by the formation of the early dorsal-ventral (D-V) axis during *Xenopus* embryogenesis (for review, see De Robertis et al., 2000). Alternatively, as I described above, the determination of cell fate can also be mediated by cell-to-cell communication, via extracellular secreted factors. Generally speaking, intercellular communication can be accomplished either by short range signaling, in which signals are transferred between neighboring cells that are directly in contact with each other, or by long range signaling, in which signals from a localized source travel quite far in order to induce responses in receiving cells. Long range signaling is often times achieved by the action of morphogens. A morphogen is classically defined as a signal that is produced from a localized source to form a concentration gradient through surrounding tissue, and instructing cells to adopt distinct fates, according to the

concentration of signal to which they are exposed to be integrated over time (Ashe and Briscoe, 2006). A number of significant studies over the years have demonstrated that embryogenesis proceeds through inductive interactions that are mediated by a key set of intercellular signaling factors including members of the Wnt, fibroblast growth factor (FGF), Hedgehog, Notch and TGF-β families (Shen and Schier, 2000). In the latter group, much evidence suggests that Nodal ligands form signaling gradients that are responsible for patterning the embryo at various stages of embryogenesis. One of the critical events to occur during development is the formation of the three germ layers, endoderm, mesoderm and ectoderm, during the process of gastrulation. I will now discuss the important findings made from studies in *Xenopus* that led to the notion that Nodal-related factors are the main endogenous inducers of mesoderm.

Mesoderm induction and patterning

Although activin was the first TGF-β molecule shown to have mesoderm-inducing activity in *in vitro Xenopus* explant assays (Smith et al., 1995), the subsequent finding that mice mutant for multiple *activin* genes form mesoderm and undergo normal gastrulation (Matzuk et al., 1995) argues against an *in vivo* role in the mesendoderm specification process. Experiments in *Xenopus* initially performed by Nieuwkoop in which vegetal explants were combined with animal tissue revealed that the endogenous mesoderm-inducing signal was derived from the endoderm after midblastula stages (Wylie et al., 1996). Pioneering experiments such as these, first implicated *Nodal*-related genes as the main mesoderm-inducing factors produced from the endoderm. When animal-vegetal recombinants were generated using a truncated form of Cerberus, Cerberus-short (Cer-S; Piccolo et al., 1999) to specifically inhibit *Xenopus* nodal-related factors (Xnrs), the induction of both dorsal and ventral mesoderm was blocked (Agius et al., 2000). It was shown that at late blastula/early gastrula stages *Xnrs* are expressed in a dorsal-to-ventral (D-V) gradient within the endoderm that was accompanied by a higher

level of phosphorylated Smad2 on the dorsal side of the embryo (Agius et al., 2000; Faure et al., 2000). This D-V gradient of *Xnr* expression in the endoderm is thought to be activated by three maternally provided factors: Vg1 (a TGF-β-related molecule), VegT (a T-box transcription factor) and β-Catenin. Vg1 and VegT are both localized to the vegetal pole of the *Xenopus* oocyte and are potent inducers of endoderm (Henry and Melton, 1998; Zhang et al., 1998). Studies have demonstrated that depleting *VegT* from embryos severely inhibits *Xnr* expression and mesoderm formation and can be rescued by injection of *Xnr* mRNA (Kofron et al., 1999). When *VegT* and *Vg1* mRNA is injected into normal embryos, only low levels of *Xnr* transcription is initiated; however, when β-Catenin is co-injected, it cooperates with VegT and Vg1 to induce high levels of *Xnr* expression resulting in Organizer induction (Agius et al., 2000).

The sum of these findings has led to the following model for mesoderm induction in *Xenopus*. At the midblastula stage, higher β-Catenin levels on the dorsal side of the embryo, together with the vegetally localized transcription factor VegT and the maternal growth factor Vg1, generate a gradient of *Xnrs* expressed in the endoderm. In turn, this gradient induces the formation of overlying mesoderm, with low doses of Xnrs inducing the formation of ventral mesoderm and high doses leading to formation of the Spemann/Mangold Organizer. The region of dorsal endoderm that induces the Organizer tissue is referred to as Nieuwkoop's center. Subsequently, at the gastrula stage, the Organizer is responsible for secreting a cocktail of factors that refine this initial D-V patterning (De Robertis et al., 2000). In the following section, I present direct evidence generated from studies in various species that strongly supports the idea that Nodal-related factors are the true mesoderm inducers *in vivo* during early embryogenesis.

Nodal as a mesendoderm inducer

Nodal was originally identified by the cloning of a mutation caused by a retroviral insertion in mice that resulted in defects in the formation of the primitive streak, from

which both mesoderm and definitive endoderm are derived (Zhou et al., 1993; Conlon et al., 1994). Subsequently, *Nodal* homologs have been identified in all vertebrate species examined to date. Specifically in *Xenopus*, six *nodal*-related genes (*Xnrs*1-6) have been isolated and of these, *Xnrs*1, 2, 4, 5 and 6 have been shown to possess mesoderm-inducing capabilities (Jones et al., 1995; Joseph and Melton, 1997; Takahashi et al., 2000). *Xnr3* is more divergent and does not appear to be involved in mesendoderm specification (Smith et al., 1995). There is much evidence demonstrating that Nodal-related proteins are conserved dose-dependent regulators of mesendoderm specification from studies in a number of species. For example, zebrafish mutants that are deficient for two *nodal*-related genes, *cyclops* (*cyc*) and *squint* (*sqt*) lack head and trunk mesoderm and fail to form the germ-ring, a structure analogous to the mouse primitive streak (Feldman et al., 1998). Moreover, gain-of-function studies have demonstrated that mouse *Nodal*, zebrafish *cyc* and *sqt*, and *Xnrs*1, 2, 4, 5, and 6 can respecify prospective ectoderm to dorsal mesendoderm (Jones et al., 1995; Rebagliati et al., 1998; Erter et al., 1998; Sampath et al., 1998; Joseph and Melton, 1997; Takahashi et al., 2000). *Nodal* genes are expressed in the vicinity of or overlapping with mesoderm progenitors, consistent with their role as mesendoderm inducers (Shen and Schier, 2000). Altogether, these findings firmly establish that Nodal signals are central to the formation of mesoderm in vertebrates.

Positive and negative regulation of Nodal signaling via FoxHI

Studies in mice, fish, chicken and *Xenopus* have demonstrated that the transcriptional cofactor FoxHI regulates the expression of both *Nodal* itself, as well as antagonists of Nodal (Osada et al., 2000; Pogoda et al., 2000; Saijoh et al., 2000). In all of these species, *Nodal*-related genes are initially expressed independent of FoxHI, however, the subsequent maintenance and/or enhancement of expression requires FoxHI activity. The situation is, however, more complicated in *Xenopus* due to the presence of

multiple *Xnrs*, some of which are positively autoregulated and some of which are not. For example, *Xnrs* 1, 2 and 4 have been shown to possess strong autoinductive capabilities, whereas *Xnr5* and *Xnr6* appear to be induced only in a cell-autonomous fashion (*e.g.*, by VegT during blastula/gastrula stages) (Takahashi et al., 2000). FoxHI has been shown to regulate *Nodal* expression both in prospective mesendoderm during early gastrulation stages and in lateral plate mesoderm (LPM) during later L-R patterning (see below), indicating that positive feedback regulation of *Nodal* is a common mechanism used at multiple stages during embryogenesis.

The conservation of FoxHI-mediated expression of *Nodal*-related genes is reflected in the conservation of FoxHI-regulated genomic regulatory elements. For example, a conserved intronic enhancer containing two FoxHI putative binding sites were identified in the *Nodal* orthologs from mouse, *Xenopus* and ascidian, strongly suggesting that FoxHI-mediated autoregulation of *Nodal* expression is broadly conserved among chordates (Osada et al., 2000). FoxHI also appears to regulate the expression of the Nodal antagonist *Lefty* in the early prospective mesoderm of zebrafish, *Xenopus* and mice (Pogoda et al., 2000; Watanabe and Whitman, 1999; Yamamoto et al., 2001), indicating that negative, as well as positive feedback regulation of Nodal signaling may be controlled by FoxHI, and that this role is conserved across species. As I will describe in more detail below, my studies directly address the functions of Nodal positive autoregulation and Lefty negative feedback inhibition during the process of L-R specification in *Xenopus*.

Negative feedback regulation of Nodal signaling by Lefty

A number of studies have led to the well-established idea that Lefty molecules act as antagonists of Nodal signaling. It is thought that Lefty-related proteins limit the strength, range and duration of Nodal signaling during mesendoderm induction, thereby regulating the extent of mesendoderm formation within the embryo. As for *Nodal*, *Lefty*

(also called *antivin* in zebrafish and *Xenopus*) genes have been identified in chordates as primitive as ascidians to higher vertebrates such as mouse and human. Whereas a single *Lefty* gene has been identified in the more primitive species, two *Lefty* genes (*Lefty1* and *Lefty2*) have been isolated in mouse. In the mouse embryo, *Lefty2* is co-expressed with *Nodal* at relatively high levels in the primitive streak. Accordingly, mice deficient for *Lefty2* exhibit an expansion of the primitive streak and excess formation of mesoderm. This phenotype can be partially rescued by reducing Nodal activity, indicating that the overproduction of mesoderm in *Lefty2* null mice is due to an increase in Nodal signaling (Meno et al., 1999). In contrast, overexpression of the *Lefty* genes in zebrafish induces a phenotype closely resembling both *cyc*;*sqt* double mutants and maternal zygotic *oep* mutants (Bisgrove et al., 1999; Meno et al., 1999; Thisse et al., 2000; Thisse and Thisse, 1999). Our laboratory was the first to isolate and characterize the *Lefty* homolog (*Xlefty*/*Xatv*) in *Xenopus* (Cheng et al., 2000). Due to the fact that *Xenopus laevis* is pseudotetraploid, two alloalleles, *XleftyA* and *XleftyB*, have been identified. Subsequent studies by a previous graduate student in the lab, Young Cha, demonstrated that simultaneous antisense oligonucleotide-mediated knockdown of both pseudoalleles resulted in the expansion of *Xnr* expression, as well as a dramatic increase in expression of Xnr downstream genes, such as the pan-mesodermal marker, *Xbrachyury* (*Xbra*) (Cha et al., 2006). These findings were consistent with, but arguably more convincing than the previous studies performed in *Xenopus* by Branford and Yost (2002).

Despite the convincing evidence that Lefty molecules inhibit Nodal signaling, the precise molecular mechanism underlying Lefty inhibition of Nodal activity is still unclear. It has been proposed that Leftys may directly bind to the Nodal ligand or competitively bind to common receptors to block downstream activation of the pathway. In support of the latter model, it has been shown that Lefty inhibition can be blocked by co-expression of the putative Nodal type II receptor, ActRIIB (Meno et al., 1999; Sakuma et al., 2002; Thisse and Thisse, 1999). However, a direct biochemical/physical

interaction between Lefty proteins and the ActRIIB receptor has not been demonstrated to date.

As mentioned above, Lefty proteins are distinct from other TGF-β superfamily members in that they possess two putative proteolytic cleavage sites, which would produce two alternative (a shorter and longer) forms of the mature ligand (Juan and Hamada, 2001). Studies by JJ Westmoreland in the lab have demonstrated that the Xlefty protein is indeed cleaved into a long ($Xlefty^{L}$) and short ($Xlefty^{S}$) form within blastula/gastrula stage embryos however only $Xlefty^{L}$ is capable of blocking Nodal signaling in mesoderm induction assays. These results suggest that $Xlefty^{L}$ is the form of the mature ligand that functions *in vivo*. Moreover, he has shown that only $Xlefty^{L}$ accumulates in embryonic-cell-conditioned medium, which has led to the hypothesis that $Xlefty^{S}$ may be a short-lived intermediate isoform that may be involved in clearing $Xlefty^{L}$ activity from embryonic tissue during early gastrula stages. It is, however, possible that $Xlefty^{S}$ may have a different function and/or longevity during later tailbud embryogenesis and play a role in L-R asymmetry patterning.

Nodal and Lefty as a 'reaction-diffusion system'

Because the levels and/or spatiotemporal extent of Nodal signals are critical for proper pattern formation during various stages of development, it is important to have a fundamental understanding of how these variables are altered by both positive and negative feedback autoregulation. It is thought that Lefty molecules act at a long distance to inhibit Nodal signaling. In support of this notion, studies in zebrafish have shown that the ectopic expression of *Lefty* at the animal pole can block Nodal signaling at the marginal region of the embryo (Chen and Schier, 2002). It has also been demonstrated that green fluorescent protein (GFP)-tagged mouse Lefty2, when introduced into chicken embryos, could travel farther away from the source of synthesis than a mouse Nodal-GFP fusion protein (Sakuma et al., 2002). From these data, the idea has been proposed that

Nodal and Lefty may constitute a classical 'reaction-diffusion system', as originally proposed by Turing (1952), as an *in vivo* mechanism for controlling pattern formation during both mesendoderm induction and L-R axis formation (for review, see Solnica-Krezel, 2003; Meinhardt, 2001; Tabin, 2006).

There are several principle tenets of a reaction-diffusion system, which are as follows: (1) the activator autoinduces its own production, (2) the activator also stimulates the production of an inhibitor, (3) the inhibitor blocks the autoinduction of the activator, (4) the inhibitor acts at a long range to restrict the short range self-enhancing feedback loop of the activator. The relationship between Nodal and Lefty appears to closely resemble this type of self-regulating mechanism and has been proposed to explain why, for example, during gastrula stages, *Nodal* expression remains limited to the prospective mesendoderm rather than propagating, via positive autoregulation, into prospective ectoderm. In this scenario, the long range diffusion of Lefty away from its site of production in the mesendoderm would permit Nodal signaling specifically in mesendoderm while restricting it in overlying ectoderm.

As I will discuss below (see–"Development of the L-R axis"), my findings during my thesis research, gathered concurrently but independently with those from studies in the mouse embryo, strongly suggest that a reaction-diffusion system (referred to as a Self-Enhancement and Lateral Inhibition or SELI mechanism) involving Nodal and Lefty-related molecules is responsible for initiating as well as maintaining L-R asymmetry during tailbud/early somitogenesis stages (Nakamura et al., 2006; Tabin, 2006).

Development of the L-R axis

In the previous section, I discussed how cell-to-cell communication plays an important role in germ layer specification during the early stages of vertebrate embryogenesis. Now I will discuss the role of intercellular signaling in the context of

specifying the L-R axis. All vertebrates establish anatomical L-R asymmetry during embryogenesis, which is apparent in the final body plan in the placement and stereotypical looping of the heart and visceral organs, asymmetric lung lobation, and in the structure of the cardiovascular system. In some vertebrates, such as zebrafish, anatomical asymmetries have also been identified in the brain. Variation from this normal asymmetric arrangement (situs solitus) results in heterotaxy, seen either as randomization or complete reversal (situs inversus) of normal organ position. Although the complete reversal of asymmetric situs is not harmful, the incomplete reversal of situs, in which some tissues are oriented correctly while others are reversed in the same individual, can result in severe medical complications, such as congenital heart abnormalities (Casey, 1998). For example, individuals affected with X-linked heterotaxy (HTX1), caused by mutations in the *ZIC3* gene, suffer from congenital heart disease as a result of cardiac malformation, and show alterations in visceral situs. *ZIC3*, which encodes a zinc-finger protein, was the first gene identified to have a causal role in human laterality defects (Casey et al., 1993; Gebbia et al., 1997). Precisely how ZIC3 influences L-R axis determination, however, still remains unclear.

The formation of L-R asymmetric anatomy can be conceptually divided into 4 distinct phases: 1) the breaking of global embryonic symmetry, 2) transfer of asymmetric information (either directly or indirectly) to the L LPM, 3) propagation and reinforcement of asymmetric information via networks of asymmetric gene expression, and 4) the interpretation of asymmetric signals by the organ primordia through the activation of morphogenesis effector programs. I will now present an overview of the pertinent findings that have served to provide insight into the underlying mechanisms that influence and/or regulate the process of L-R asymmetry specification during embryogenesis.

Initial Breaking of Embryonic Symmetry

The developmental mechanism by which L-R asymmetry is initiated, and the degree to which it is conserved between species, remains unclear (Burdine and Schier, 2000; Capdevila et al., 2000; Levin, 2005). Studies in some embryos such as chicken and *Xenopus*, suggest that broad L-R biasing may occur very early in development as a result of, for example, asymmetric gap junctional communication and/or localization of mRNAs encoding proteins that generate ion flux (Bunney et al., 2003; Levin and Mercola, 1998; Levin and Mercola, 1999; Levin et al., 2002). Gain-of-function experiments in *Xenopus* implicate the spatially restricted activity of Vg1, a TGFβ-like ligand likely acting during gastrulation, as a dominant L-R coordinator (Hyatt et al., 1996; Hyatt and Yost, 1998; Kramer et al., 2002; Kramer and Yost, 2002). As I will discuss in the second part of this section, a body of evidence gathered from studies in the mouse embryo, however, suggests that the initial symmetry breaking event occurs somewhat later, around the onset of somitogenesis, and is in some way linked to a net leftward fluid flow at the surface of the node ("nodal flow"), which is generated by motile monocilia. I will now discuss the pertinent findings that have led to the different models of asymmetry initiation in vertebrates.

Cell-Cell Communication and Distribution of Left-Right Information

A role for intercellular gap junctional communication in the chicken and frog embryo has been proposed to contribute to the breaking of initial embryonic symmetry by asymmetrically distributing a L-R specifier molecule(s) on the left and right side of the embryo, subsequently resulting in the activation of asymmetric gene expression pathways (Levin and Mercola, 1998; Levin and Mercola, 1999). Pharmacological blocker experiments showed that gap junctional communication begins to function during *Xenopus* early cleavage stages, and is upstream of asymmetric *Xnr1* expression and

cardiac looping (Levin and Mercola, 1998). Expression by microinjected RNA of either dominant negative connexin protein (a component of gap junctions) into dorsal blastomeres or wild-type connexins into ventral blastomeres resulted in the randomization of *Xnr1* expression, as well as anatomical asymmetry defects (*i.e.,* heterotaxia) (Levin and Mercola, 1998). Similarly, studies in the chicken embryo have shown that knockdown of one particular connexin, *Connexin43* (*Cx43*), using either antisense oligonucleotide injection or blocking antibodies, caused disruption of L-R asymmetry patterning thereby implicating an important role for gap junctional communication (Levin and Mercola, 1999). The same basic model for a gap junctional communication system seems to apply to both *Xenopus* and chicken embryos, in that correct laterality determination upstream of asymmetric gene expression depends on an uninterrupted region of gap junctional communication around a barrier "zone of isolation" (*e.g.,* the ventral midline and primitive streak in frog and chick, respectively) (Levin and Mercola, 1999). Whether gap junctional communication initiates L-R asymmetry patterning in other species still remains an issue of debate. For example, mice in which *Cx43* is either misexpressed or absent do not exhibit significant laterality defects (Ewart et al., 1997; Reaume et al., 1995), suggesting that the mechanism underlying asymmetry determination may differ in mice. However, it has been proposed that redundancy of connexin proteins in the mouse embryo may allow for compensation of lack of *Cx43*.

Levin and Mercola (1998, 1999) proposed that an energy source would be required to drive a net unidirectional distribution of small molecules through the circumferential gap junctional communication path. It was, therefore, hypothesized that left versus right-sided voltage differences exist within the embryo to provide an electrophoretic force that would push charged molecules in preferred directions through gap junctional paths (Levin, 2005). A pharmacological screen to identify potential candidate molecules (*e.g.,* ion channels, pumps, co-transporters) that may be involved in

generating ion flux within the embryo was performed and implicated several genes (Levin et al., 2002). Among these genes identified was *H+/K+ ATPase*, which was found to function during early cleavage stages in *Xenopus* (Levin et al., 2002; Bunney et al., 2003). It was shown that maternal *H+/K+ ATPase* mRNA was asymmetrically distributed within the 2-4 cell stage embryo, demonstrating that asymmetry is generated within two hours after fertilization. Moreover, pharmacologically inhibiting H+/K+ ATPase activity in the early embryo resulted in aberrant asymmetric expression of *Xnr1*, *Xlefty* and *XPitx-2* (Levin et al., 2002). Gain-of-function experiments using H+/K+ ATPase and K+ channel overexpression, which would equalize H+ and K+ flux on the left and right sides of the embryo, were also shown to disrupt L-R axis formation (Levin et al., 2002). In agreement with the findings in *Xenopus*, blocking H+/K+ ATPase function in the chicken embryo prior to gastrulation randomized the asymmetric expression of *Shh*, *cWnt-8C* and *Cerberus* (Levin et al., 2002).

Interestingly, it was found that, in contrast to the asymmetric expression in *Xenopus*, *H+/K+ ATPase* mRNA is distributed symmetrically within the early chicken embryo (Levin et al., 2002). These results suggested that while both species use gap junctional communication and differential ion flux to asymmetrically pattern the embryo, the regulation of the mechanisms differ. Whereas in early frog embryos asymmetric ion flux is provided by the asymmetric localization of mRNA, this differential flux appears to be established in the chicken embryo by a post-translational mechanism that may involve gating of electrogenic activity of mature pump complexes (Levin, 2005).

L-R coordinator in *Xenopus*

In *Xenopus*, gain-of-function experiments implicate the spatially restricted activity of Vg1, a divergent TGFβ-like ligand likely acting during gastrulation, as a dominant L-R coordinator (Hyatt et al., 1996; Hyatt and Yost, 1998; Kramer et al., 2002; Kramer and Yost, 2002). Vg1, like other TGF-β-related proteins, is synthesized as an

inactive precursor protein during oogenesis and stored as a maternal RNA for use during early embryogenesis (Weeks and Melton, 1987). The Vg1 precursor protein is uniformly expressed in both left and right vegetal cells of the early *Xenopus* blastula stage embryo. Studies in *Xenopus* have demonstrated that ectopic expression of the mature form of Vg1 in right, but not left, vegetal cells of the 16-cell blastula embryo resulted in altered L-R anatomical situs. The degree of L-R patterning defects observed in these experiments depended upon which right blastomeres were injected, such that injection into right dorsovegetal cells at the 16-cell stage caused heterotaxia, whereas Vg1 overexpression in more ventral-lateral right blastomeres resulted in a complete inversion of the L-R axis at later stages (Hyatt et al., 1996; Hyatt and Yost, 1998). Ectopic expression of Vg1 in the complementary left-sided blastomeres did not have an effect on L-R asymmetric situs (Hyatt et al., 1996; Hyatt and Yost, 1998). Because overexpression of mature Vg1 affects L-R development only when introduced to the right side of the embryo, it has been proposed that the activity of Vg1 is normally spatially restricted to cells of the left vegetal region, perhaps through a mechanism involving asymmetrical processing of the Vg1 precursor protein into the mature ligand (Hyatt et al., 1996; Hyatt and Yost, 1998). In support of this hypothesis, it has been shown that a dominant-negative TGF-β receptor that inhibits Vg1 signaling can cause reversal of asymmetric situs if introduced into the left but not right lateral vegetal cells (Hyatt et al., 1996; Hyatt and Yost, 1998). The consequences of right-side overexpression of Vg1 are thought to be specific, since the results cannot be replicated using Activin. Because Vg1 and Activin both signal through a Smad2/3-dependent pathway, it has been proposed that the difference in activity between the two proteins may reflect ligand-binding specificity of signaling receptors (Mercola and Levin, 2001). The "left-right coordinator" (LRC) model therefore proposes that Vg1 activity in left lateral vegetal cells induces a left-sided identity in these cells. The ectopic expression of mature Vg1 in right lateral cells is thought to override endogenous Vg1 signaling that occurs on the left side of the embryo, by placing an

ectopic LRC on the right (Ramsdell and Yost – review, 1998). Furthermore, the LRC model proposes that global L-R asymmetric patterning of the embryo is achieved by left-side LRC activity, perhaps by transmission of this information to the organizer/node (Hyatt and Yost, 1998), as occurs in the chicken embryo (see below).

It is important to note, however, that even though the Vg1 overexpression data is consistent with an early L-R pattern in the pre-gastrula stage *Xenopus* embryo, the precise timing of global symmetry breaking remains unclear due to the potential persistence of the injected mRNA to later stages and raises the possibility that injected Vg1 simply mimics a later endogenous signal. This issue is compounded by the difficulty to detect the endogenous, mature form of Vg1 in early stage *Xenopus* embryos (Mercola and Levin, 2001).

Additional early mechanisms for L-R asymmetry setting

More recently, a role for heparan sulfate proteoglycans (HSPGs) associated with the extracellular matrix (ECM) on the basal surface of the ectoderm has been implicated in the transmission of L-R information to the mesodermal primordia during *Xenopus* gastrulation (Kramer and Yost, 2002). Using dominant-negative and loss-of-function approaches, it was shown that a cytoplasmic domain of Syndecan-2 was asymmetrically phosphorylated in cells on the right but not left half of the embryo during gastrulation (Kramer and Yost, 2002). Furthermore, evidence was provided that showed the attachment of multiple heparan sulfate glycosaminoglycans on Syndecan-2 and that the functional interaction of these sites with the cytoplasmic domain were an obligate part of L-R patterning during gastrulation at a stage immediately prior to the migration of mesoderm across ectoderm. In line with the Vg1/LRC model, it was demonstrated that Syndecan-2 could directly interact with Vg1 (Kramer and Yost, 2002), suggesting that these two proteins may function together during L-R patterning at gastrulation stages.

Transfer of L-R information to and from the node

From studies in the chicken and frog embryo, it is thought that the initial L-R asymmetric information established during early cleavage stages (as discussed above) is relayed to the node/Organizer, which then sets up asymmetric gene expression within the tissues of the node. Node rotation studies in chicken have shown that the molecular asymmetry of *Sonic hedgehog* (Shh) expression in the node, one of the earliest asymmetrically expressed genes in chicken, is induced/polarized by influences from adjacent neighboring tissues (Pagan-Westphal and Tabin, 1998). The pivotal discovery that asymmetric Sonic hedgehog (Shh) signaling from the chicken node induced left-sided *Nodal* expression, and that misexpression of *Shh* on the right side resulted in right-sided *Nodal* expression and the subsequent reversal of embryonic situs, provided the first molecular entrypoint into the L-R specification pathway (Levin et al., 1995). Subsequent to this discovery, there has been a rapid expansion of the number of molecular players found to be involved in this pathway. However, despite the significant advancements in the field, only a rough framework exists of a conserved pathway that regulates L-R asymmetry determination in the vertebrate embryo.

Establishing node asymmetry

As mentioned above, studies focused on identifying the mechanism underlying the initial breaking of symmetry in mice have led to the idea that L-R asymmetry specification does not occur until after gastrulation. In the mouse embryo, it has been demonstrated that monocilia present on the ventral surface of the node project into the extraembryonic space and exhibit a directional rotation that generates an apparent leftward flow of extraembryonic fluid in the node region ("nodal flow") (Nonaka et al., 1998; Okada et al., 1999). It has been proposed that this nodal flow may initiate L-R asymmetry by distributing a putative morphogen to the left (Nonaka et al., 2002; Nonaka et al., 1998; Okada et al., 1999), or by inducing flexion of immotile cilia at the left node

periphery, which triggers an intracellular Ca^{2+} wave that leads to the induction of L-sided gene expression (McGrath and Brueckner, 2003; McGrath et al., 2003; Tabin and Vogan, 2003). Recent additions to this model include the possibility of flow-induced accumulation of Shh- and retinoic acid-containing vesicles, released from node cells in an FGF-dependent manner, with L-sided delivery of their cargo causing the asymmetric Ca^{2+} transient and subsequent gene expression (Tanaka et al., 2005). The nodal flow model attractively links L-R asymmetry to the fundamental molecular chirality of ciliary proteins, and to L-R asymmetry abnormalities associated with mutations in their genes (McGrath and Brueckner, 2003; Yost, 2003). For example, the two mutant mouse strains, iv (inversus viscerum) and inv (inversion of turning), exhibit drastic asymmetric situs defects. The products of the iv and inv loci are L-R dynein (Lrd), an axonemal-type dynein heavy chain molecule, and an ankyrin-repeat protein, respectively. Lrd is expressed in the ventral node cells and mice lacking a functional Lrd have immotile nodal cilia, thus failing to produce any nodal flow (Okada et al., 1999).

Experiments in fish, chick, and frog provide initial evidence that cilia are present on the functional analogs of the mouse node in these species, but whether they function in the same manner as in mouse (*i.e.*-to produce nodal flow) still remains to be determined (Essner et al., 2002). However, even more recent evidence suggests that ciliary proteins may actually have earlier cytoplasmic roles in establishing L-R asymmetry during pre-node stages of development (Qiu et al., 2005; Wright, 2001).

Transference of L-R information from the node to LPM

A model for the flow of L-R information from the node to the LPM has been proposed from studies in chicken and mouse embryos (Levin et al., 1995; Levin and Mercola, 1998; for review, see Levin, 2005). Specifically in chicken, after the asymmetric influences from outlying tissues (see above) are registered at the node, a complex cross-regulatory network of interactions among several signaling molecules

(including Shh, BMP, FGF, RA, and Notch) produces strong node-intrinsic L-R biases. These biases are transmitted laterally to instruct L or R side-selective gene expression patterns (Burdine and Schier, 2000; Krebs et al., 2003; Levin, 2005; Pagan-Westphal and Tabin, 1998; Raya et al., 2003; Raya et al., 2004; Wright, 2001). It is thought that asymmetric Activin signaling on the right side of the node induces the expression of *BMP4*, which subsequently inhibits Shh. BMP4 simultaneously activates the expression of *FGF8*, thus activating downstream right-sided components such as the *snail-related* (*SNR*) gene. In contrast, the enrichment of *Shh* expression at the left of the node is thought to induce the expression of *Caronte* (*Car*), a BMP inhibitor (Rodriguez-Esteban et al., 1999; Yokouchi et al., 1999).

Experiments in the chicken embryo suggest that *Nodal* expression is repressed on both sides of the LPM by BMP signals and that the left-sided expression of *Car* is responsible for releasing this repression, resulting in the left side-specific expression of *Nodal* (Rodriguez-Esteban et al., 1999; Yokouchi et al., 1999). Several lines of evidence suggest that the repression of Nodal by BMPs may be a conserved feature of the vertebrate L-R cascade. In the mouse, a deficiency of *Smad5*, a gene that encodes an intracellular mediator of BMP signaling, results in bilateral expression of *Nodal* in the LPM (Chang et al., 2000). Similarly, in *Xenopus*, it has been shown that a BMP-dependent pathway functions to repress Nodal on the right side of the embryo (Hyatt and Yost, 1998; Ramsdell and Yost, 1999). However, this model of BMP repression of *Nodal* expression in the LPM has been presented with some conflicting data, which suggests that BMP signaling positively regulates Nodal during L-R axis specification (Piedra and Ros, 2002; Schlange et al., 2002; Fujiwara et al., 2002). The precise relationship between BMPs and Nodal, therefore, still remains somewhat elusive and requires further examination.

Whether the same genetic cascade functions to activate *Nodal* expression in other species remains unclear. For example, there is no evidence to date suggesting that *Shh* is

asymmetrically expressed in any other species besides chicken (Burdine and Schier, 2000). Moreover, studies in mice have shown that although Shh and FGF8 are involved in L-R asymmetry patterning, their roles are reversed compared to what is observed in chicken, such that FGF8 acts as a left-side determinant and Shh is required to prevent left determinants from being expressed on the right (Meyers and Martin, 1999).

Conservation of asymmetric gene expression in the LPM

There is currently no unifying "L-R specification model" that applies well to all species (Burdine and Schier, 2000; Capdevila et al., 2000; Whitman and Mercola, 2001). It is possible that different embryos have developed variations on a central theme that are necessary to accommodate their size, architecture, or overall developmental strategy. Despite the possible divergence in early mechanisms, they culminate in all vertebrate model systems examined so far in the transient asymmetric LPM expression of a "L-side gene cassette": *Nodal*, *Lefty*, and *Pitx2* (Fig. 1.2). Such asymmetric expression may precede vertebrate evolution, as it is observed in ascidians and amphioxus (Boorman and Shimeld, 2002; Chea et al., 2005; Hudson and Yasuo, 2005; Morokuma et al., 2002; Yu et al., 2002), even if "L-sidedness" seems to be carried in a different germ layer. It is plausible that this gene cassette's role in L-R asymmetry arose by redirecting a primitive role in specifying the oral-aboral axis, as in sea urchins (Chea et al., 2005; Duboc et al., 2005).

In the following sections, I will describe the findings that have led to the well-established notion that Nodal acts as a true L-side determinant across species. I will also discuss recent important findings from studies in the mouse embryo that have led to an integrated model for L-R asymmetry specification during vertebrate embryogenesis. The relationship of Nodal and Lefty as a reaction-diffusion system, as described earlier with respect to the process of mesendoderm specification, underlies the basic mechanism of this recently proposed SELI (Self-Enhancement and Lateral Inhibition) model for L-R

asymmetry patterning of the embryo (Nakamura et al., 2006; Tabin, 2006). As I will highlight throughout my thesis, my findings in *Xenopus*, which were gathered concurrently but independently, strongly support this recently proposed model and demonstrate further conservation in the L-R asymmetry specification program.

Nodal-related genes & L-R Axis Specification

Nodal-related proteins have been implicated as crucial determinants of L-R patterning during vertebrate embryogenesis. In zebrafish and *Xenopus*, several *nodal* homologs have been identified that can regulate the expression of genes involved in L-R axis specification (Saijoh et al., 2000; Sampath et al., 1998; Shiratori et al., 2001; Wright, 2001). Aberrant patterns of *Nodal* expression in the LPM (from which heart and visceral organ precursors are derived) are closely correlated with situs abnormalities (Levin et al., 1995; Collignon et al., 1996; Lohr et al., 1997; Lowe et al., 1996) and misexpression of *Nodal* on the right side of the embryo is sufficient to either randomize situs determination in multiple organ systems or completely reverse situs in some situations (Levin et al., 1997; Sampath et al., 1997; Toyoizumi et al., 2005). The conserved expression of *Nodal* and its target genes *Lefty* and *Pitx2* in the left LPM of all vertebrates examined to date suggest an intimate relationship between L-R specification and asymmetric morphogenesis. In *Xenopus*, *Xnr1* expression in the left LPM is dynamic and transient with a stereotypic forward shifting of the expression domain (Lowe et al., 1996; Lustig et al., 1996). Of the six identified *Xenopus nodal*-related genes (*Xnrs*), only *Xnr1* is asymmetrically expressed in the left LPM during neurula/tailbud stages, appearing first as bilateral symmetric stripes flanking the posterior notochord, then in the left LPM (Lowe et al., 1996; Sampath et al., 1997). Whether this posterior-to-anterior (P-to-A) directional spread of the *Nodal*/*Xnr1* expression domain is intrinsic to the left LPM is an intriguing question, since it opposes the normal rostral to caudal sequence of development observed

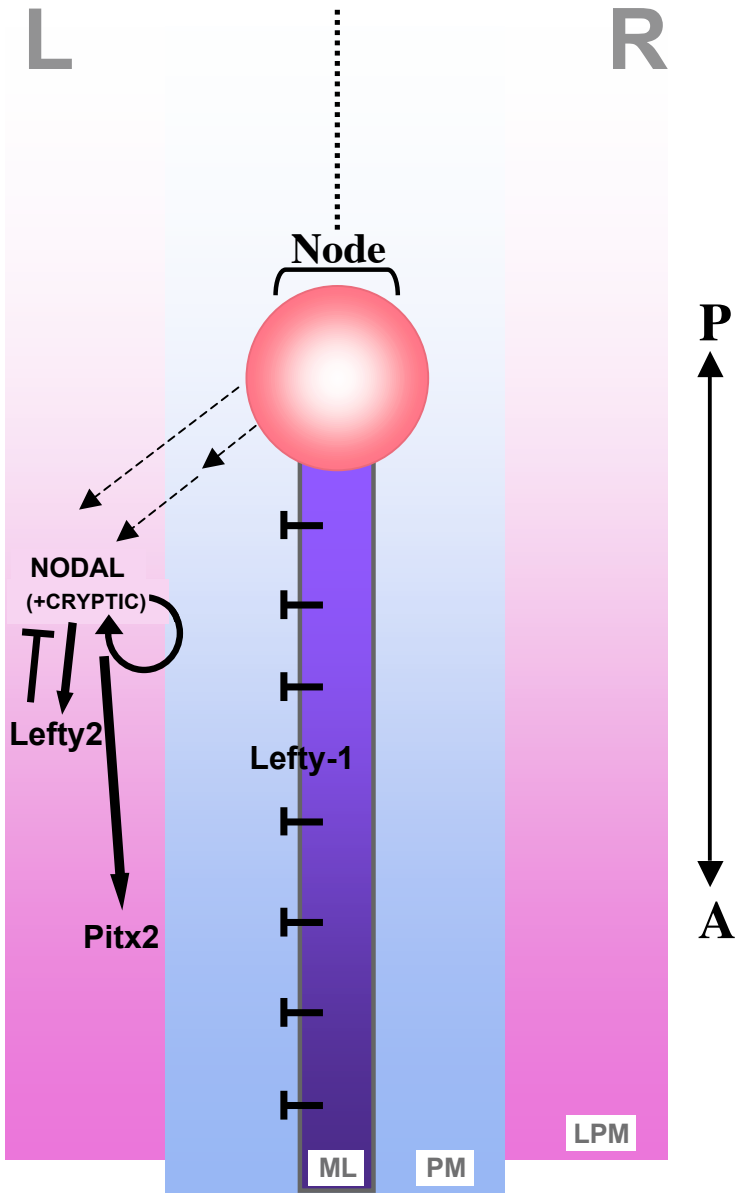

Fig. 1.2 L-R specification pathway. Formation of L-R anatomy can be divided into 4 distinct phases: 1) breaking of global embryonic symmetry, thought to occur in or around the node, 2) transfer of asymmetric information (either directly-single dotted arrow or indirectly-double dotted arrows) to L LPM, 3) propagation and reinforcement of asymmetric information via L-side gene cassette (Nodal, which induces its own expression as well as its negative feedback inhibitor, *Lefty2* and the transcription factor *Pitx2*), 4) interpretation of asymmetric signals by organ primordia and activation of morphogenesis effector programs. *Lefty1* expression in midline is thought to prevent activation of *Nodal* on R side. L, left; R, right; P, posterior; A, anterior; ML, midline; PM, paraxial mesoderm; LPM, lateral plate mesoderm. Time progresses from top to bottom of page.

in many instances during embryogenesis, such as in the development of somites (Pourquie, 2001; Tajbakhsh and Sporle, 1998). In Chapter III, I report on the molecular and cellular mechanisms that underlie this anteriorwards shifting of *Xnr1* expression within the L LPM and provide evidence suggesting that Xnr1 autoregulation that relies on planar tissue communication is required for the propagation of the Xnr1 signal.

Lefty-related molecules

In the mouse embryo, two *Lefty* genes have been identified, *Lefty1* and *Lefty2* (Meno et al., 1996), whereas in *Xenopus*, only one *Lefty* homolog, *Xlefty/Xatv*, has been identified to date (Cheng et al., 2000; Branford et al., 2000). Mouse *Lefty1* is expressed in the anterior visceral endoderm (AVE) and during early somitogenesis on the left side of the prospective floor plate (PFP) and at lower levels in the LPM. Asymmetric expression of *Lefty1* in the midline was initially thought to prevent the inappropriate crossing of L-specifying signals to the right side of the embryo (Meno et al., 1998). As discussed below, a more updated model for Lefty function suggests that Lefty1 inhibition from the midline plays a role in the initial activation of L-specific *Nodal*. Additionally, Lefty1/2 from both the L LPM and midline are subsequently thought to maintain asymmetric expression by contralaterally suppressing R side activation of *Nodal* (Nakamura et al., 2006). *Lefty2* expression, like *Nodal*, is dynamic and transient being initially expressed symmetrically in the primitive streak then broadly expressed in the left LPM during early somitogenesis (Juan and Hamada, 2001). An additional mechanism that appears to restrict the range of Nodal signaling is the putative negative feedback role of Lefty2 in the L LPM. Inactivation of *Lefty2* results in gastrulation-stage defects involving broadened *Nodal* expression and excess mesoderm induction (Agathon et al., 2001; Meno et al., 2001). *Xlefty/Xatv* misexpression on the left side of the frog embryo blocks L-sided *Xnr1* and *XPitx2* expression, and leads to severe organ malformations at later stages of development, although overall A-P and D-V axis development is normal

(Cheng et al., 2000). My high-resolution analysis of *Xnr1* and *Xlefty* expression during tailbud stages (shown in Chapter III) demonstrated that *Xlefty* expression spatially mimics *Xnr1* within the L LPM but with a temporal delay. My current hypothesis, therefore, is that Xlefty feedback inhibition results in the progressive P-to-A shutdown of *Xnr1* expression within the L LPM during tailbud embryogenesis, thereby ensuring its transient expression during L-R specification.

Contralateral communication allows for pan-embryonic integration of L-R information

Although it has been known that the midline plays an important role in regulating L-R asymmetry patterning (see below), the precise mechanism underlying midline function has remained unclear. One of the significant findings of my thesis research was that contralateral communication between the L and R sides of the embryo, which occurs by intermediate signaling through the midline, allows for the regulation and maintenance of asymmetric *Xnr1* expression during L-R asymmetry specification. As presented in Chapters III and IV, I used a grafting strategy to ectopically introduce Xnr1 on the R side of *Xenopus* embryos and showed that *Xnr1*-expressing grafts caused a robust induction of *Xnr1* expression in the R LPM that recapitulated the anteriorwards shifting that normally occurs on the L side. A second significant finding was that when *Xnr1*-grafts were placed in a mid-trunk position (which I subsequently found gave the R-side *Xnr1* expression a spatial advantage – refer to Chapter IV for further details) on the right side, I observed an ectopic induction of *Xlefty* in the midline, as well as a reduction in the levels and/or anterior extent of endogenous *Xnr1* expression in L LPM. But perhaps the most important result from these experiments was that R-side, mid-trunk *Xnr1*-engraftment caused a concordant reversal of anatomical situs in all embryos examined at later stages, which demonstrated that the engrafted R-side had been converted to a dominant left. Altogether, these findings led to a model in which Xnr1 signals from the LPM to the

midline to induce *Xlefty* expression. Xlefty produced from the midline and/or LPM, in turn, spreads contralaterally to suppress *Xnr1* expression on the opposite side by inhibiting the Xnr1 positive autoregulatory loop. In normal embryos, this mechanism would ensure the continuous suppression of potentially self-amplifying low levels of *Xnr1* expression within the R LPM and maintain L-R compartmentalization during the period of tailbud embryogenesis (refer to Fig. 4.6).

My findings directly support very recent findings from studies in the mouse embryo that have led to a SELI (Self-Enhancement and Lateral Inhibition) model for specifying the L-R axis (Nakamura et al., 2006; Tabin, 2006 – Fig. 1.3). These findings in mouse were gathered concurrently but independently and also show contralateral communication between the L and R sides during the process of L-R asymmetry patterning. The SELI model proposes the following. A L-R biasing mechanism, which is thought to be leftward nodal flow in the mouse embryo, functions to initially activate *Nodal* at higher levels on the L versus the R side (**Fig. 1.3A**; reviewed in Tabin, 2006). In *Xenopus*, this L-R biasing step may occur much earlier as compared to the mouse as I have alluded to above. It is important to note here that similarly to the Nakamura *et al.* (2006) results, our laboratory has also observed low levels of *Xnr1* expression in the R LPM during tailbud stages, suggesting that the R side initially tries to mount a *Nodal*/*Xnr1* response. *Nodal* then autoregulates its own expression and induces *Lefty* expression in the midline (**Fig. 1.3B**). *Nodal* is only able to expand and self-amplify on the L side because, due to the principles of a reaction-diffusion mechanism, the inhibitory influence of midline Lefty is stronger than the R-side inductive signal but weaker than the autoregulatory signal on the left (**Fig. 1.3C**). Consistent with this hypothesis, I showed in explants that the levels and timing of *Xnr1* expression in the L and R LPM depends on the length of association with the midline (see Chapter III). Nodal activity in the L LPM autoactivates its own expression, as well as that of *Lefty*, resulting in the rapid expansion of both domains (**Fig. 1.3D**). Lefty produced in the L LPM and midline then functions

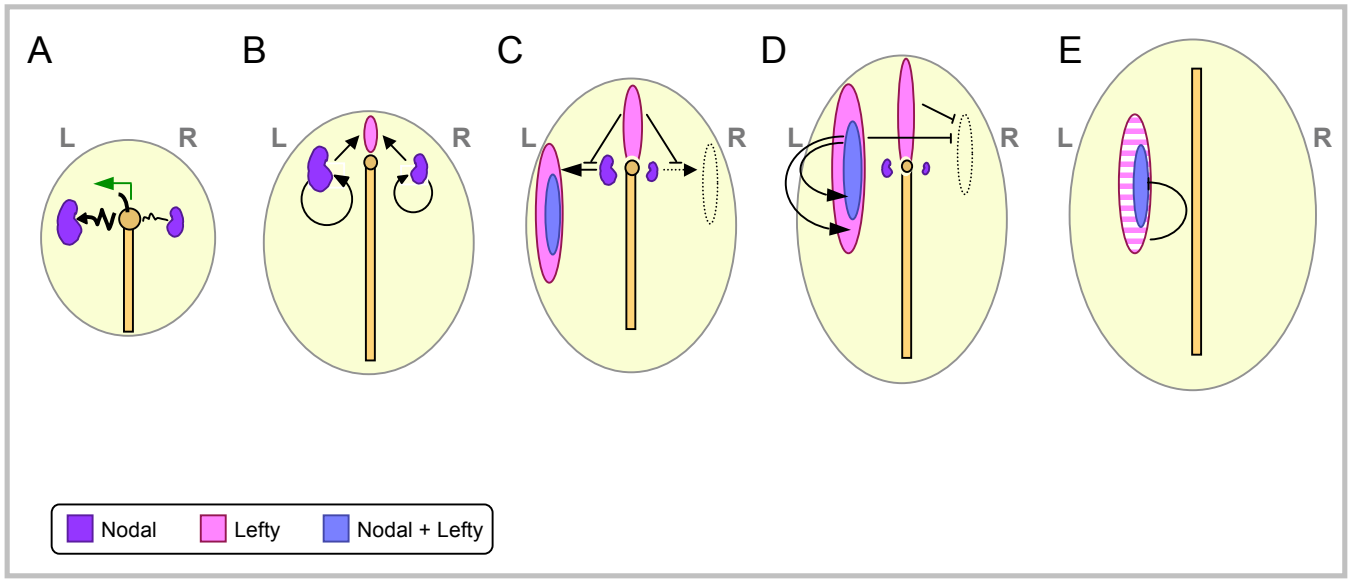

Fig. 1.3 SELI (Self-Enhancement and Lateral Inhibition) model for pan-embryonic integration of L-R asymmetry by communication across the midline. Our data gathered concurrently with those of Nakamura *et al.* (2006) show that asymmetric threshold-dependent activation of *Xnr1* expression in the LPM of *Xenopus* embryos leads to the same situation shown here for mouse. The node here is equivalent to the *Xenopus* tailbud region with bilateral *Xnr1* expression. A) Node cilia drive leftward fluid flow (green arrow), biasing signaling to the node's L side (black squiggly arrows), & causing unequal activation of *Nodal* expression (purple). B) Nodal autoregulates, and induces midline expression of its feedback antagonist, *Lefty* (pink). C) Nodal adjacent to the node induces *Nodal* (blue) and *Lefty* (pink) in LPM, only on the L because, in a reaction-diffusion mechanism, inhibtion by midline Lefty is stronger than the R-side inductive signal, and weaker than the L-side autoregulatory inductive signal. D) Nodal in LPM induces both *Nodal* and *Lefty* expression, with subsequent rapid expansion of both domains. Lefty from L LPM and midline acts contralaterally to prevent R-sided activation of *Nodal* expression. E) Inhibitory activity of Lefty in L LPM contributes to transient nature of *Nodal* expression, as it blocks the Nodal autoregulatory loop. This figure is modified from Tabin (2006).

contralaterally to prevent the R-sided activation of *Nodal* expression (**Fig. 1.3D**). Finally, negative feedback regulation of Nodal by Lefty in the L LPM then leads to the shutdown of *Nodal* expression, ensuring its transient nature (**Fig. 1.3E**).

The consistency in the findings in mouse and *Xenopus* demonstrate further conservation in the L-R specification program. These studies also lend mechanistic insight into how the midline functions to regulate L-R asymmetry patterning. I will now present the findings that originally led to the notion that the midline plays a direct role in regulating L-R asymmetry.

Asymmetric gene expression is dependent upon an intact midline

The first indication that the embryonic midline was important for proper L-R axis formation was the observation that decreased development of axial midline structures (that is, including notochord and neural floorplate) was correlated with an increased incidence of cardiac situs reversals across a population of embryos (Danos and Yost, 1995). It was subsequently shown by removal of midline tissues in *Xenopus* embryos that midline integrity is important during early neurula stages, prior to neural tube closure, for the development of proper L-R asymmetry (Danos and Yost, 1996; Lohr et al., 1997). Mutant analyses in zebrafish and mouse have also indicated that the midline is crucial for L-R asymmetry patterning (Danos and Yost, 1996; Izraeli et al., 1999; Melloy et al., 1998; Rebagliati et al., 1998). For example, *no tail* (*ntl*) and *floating head* (*flh*) zebrafish mutants that are defective in notochord development also exhibit randomized cardiac situs (Danos and Yost, 1996). Observations of human, frog, and chicken conjoined twins led to the speculation that the midline may produce a R side-directed repressive signal that inhibits L-sided gene expression in the adjacent lateral regions of the twin, since asymmetry defects are only observed in the R-sided individual (Hyatt et al., 1996; Levin et al., 1997; Levin et al., 1996; Nascone and Mercola, 1997). These

observations can readily be explained by taking into account the SELI model for L-R axis specification, as discussed above.

Conversion of unilateral gene expression into asymmetric situs

Very little is currently known about how asymmetric gene expression cascades within the LPM are translated into asymmetric organ *situs*. In contrast to *Nodal* and *Lefty*, *Pitx2* expression persists on the left side of the mesodermal compartment of several asymmetric organs, such as the heart and gut, until the onset of asymmetric morphogenesis. Studies have demonstrated that *Pitx2* is a direct transcriptional target of Nodal signaling (Shiratori et al., 2001). Therefore, it has been proposed that Pitx2 may act as a "molecular bridge" connecting the intermediate phase of asymmetric *Nodal* expression to the final phase of asymmetric morphogenesis, whereby Pitx2 would activate tissue specific asymmetric morphogenetic programs (Mercola and Levin, 2001).

Pitx2 is a member of the bicoid class of paired homeodomain transcription factors. The human *pitx2* gene was originally identified by a positional cloning strategy that mapped the gene to a locus that is associated with Axenfeld-Rieger syndrome, a rare autosomal-dominant disorder characterized by abnormalities in eye, tooth and abdominal organ development (Semina et al., 1996). Severely affected individuals display defects in ventral body closure superficially reminiscent of ventral body closure deficits that accompany certain severe laterality disturbances (Mercola and Levin, 2001). Pitx2 homologs have been identified in chicken, mouse, *Xenopus*, and zebrafish and in all species, *Pitx2* has been shown to be asymmetrically expressed in the L LPM (Essner et al., 2000; Logan et al., 1998; Piedra et al., 1998; Ryan et al., 1998; Schweickert et al., 2000; St. Amand et al., 1998; Yoshioka et al., 1998). *Pitx2* mutant mice exhibit laterality defects that include arrested embryonic turning and right pulmonary isomerism (Gage et al., 1999; Kitamura et al., 1999; Lin et al., 1999; Lu et al., 1999). Studies in the chicken embryo have shown that depletion of Pitx2c function (the *Pitx2* isoform expressed

asymmetrically in L LPM) using either antisense oligonucleotides or an engrailed repressor-Pitx2c fusion protein unbiased the direction of heart looping (Yu et al., 2001). However, the directionality of cardiac looping and expression of *eHAND* and *dHAND*, two markers of late asymmetric development, were normal in *Pitx2* mutant mice (Gage et al., 1999; Kitamura et al., 1999; Lin et al., 1999; Lu et al., 1999). These findings indicate that although Pitx2 is a necessary component of downstream L-R determination, other factors must be involved in activating downstream asymmetric morphogenetic programs within the organ primordia. Two additional genes that are asymmetrically expressed downstream of Nodal are *nkx3.2* and *snail*, which encode a homeodomain and zinc finger transcription factor, respectively (Schneider et al., 1999; Isaac et al., 1997; Patel et al., 1999; Sefton et al., 1998). The precise role that these factors play in L-R asymmetry specification still remains elusive and requires further investigation. Our future goals include identifying additional factors that lie downstream of *Nodal* and/or *Pitx2* that are involved in initiating and/or executing asymmetric morphogenesis.

Aims of the dissertation

The broad goal of this thesis was to examine how Nodal/Xnr1 signals are transmitted and spatiotemporally regulated during L-R axis formation in *Xenopus laevis*. The overall finding is that L-R specification during tailbud embryogenesis arises as a result of a constant competition between inductive and repressive signals from posterior and lateral tissues of the embryo, and asymmetric signals need to reach particular thresholds in order to activate asymmetric gene expression in the L LPM. In Chapter III of this dissertation, I describe the characterization of the cellular mechanisms underlying the dynamic, unidirectional posterior-to-anterior shifting of *Xnr1* expression that occurs during late neurula/early tailbud stages. Based on these findings, I propose that positive inductive signals emanating from the posterior tailbud (the functional equivalent of the node at these stages in *Xenopus*) are required to initiate asymmetric *Xnr1* expression in

the L LPM. This expression is then maintained and propagated by a rolling wave of Xnr1-Xnr1 autoactivation that occurs in an L LPM-autonomous fashion. In Chapter IV, I describe my experiments that address how asymmetry of *Xnr1* expression within the LPM is regulated and ensured during L-R patterning. I propose that orthogonal Xnr1 signaling from the LPM induces *Xlefty* in the midline that, in turn, functions to inhibit activation of *Xnr1* contralaterally on the R side. In Chapter V, I describe my preliminary experiments using a pharmacological approach to further investigate the role that Xnr1 autoregulation plays in maintaining and propagating its own expression within the L LPM. I present evidence demonstrating that *Xnr1* and *Xlefty* transcripts are rapidly downregulated within cells of the L LPM, suggesting that they are either intrinsically unstable or actively targeted for degradation. In Chapter VI, I present a brief synopsis on the significance of my findings and include my future goals and perspectives.

CHAPTER II

MATERIALS AND METHODS

Embryo manipulations

Fertilized embryos were obtained by in vitro fertilization of eggs from hormonally induced *Xenopus laevis* females (Kay and Peng, 1991). Embryos were dejellied in 1% Thioglycolic Acid in 1X Steinburg's solution (SS; Kay and Peng, 1991) pH 6.0 plus 1M NaOH for 1-2 minutes and subsequently cultured in either 1X SS (1X SS pH 7.4: 58 mM NaCl, 0.67 mM KCl, 0.34 mM $Ca(NO_3)_2 \cdot 4H_2O$, 0.83 mM $MgSO_4 \cdot 7H_2O$, 4.6 mM Tris) or 0.1X SS. Embryos were staged according to Nieuwkoop and Faber (1967).

Fertilized embryos were transferred to 5% Ficoll/1X SS and injected with 10 nl of total RNA/DNA solution into four blastomeres at the 8-cell stage using a Narashige gas driven microinjector. Injected embryos were allowed to recover at room temperature in 5% Ficoll/1X SS until stage 9-9.5 and then transferred into 0.1x SS for the remainder of the culture period.

Embryo injections

For the 8-cell stage injections, embryos with differential dorsal/ventral pigmentation (Nieuwkoop and Faber, 1967) were injected into the right or left four blastomeres with CsCl-purified plasmids (in water) containing either *β-galactosidase* (150 pg total), *Xnr1* (80 pg), *Xlefty* (150 pg), or *Cerberus-short* (*Cer-S*; Piccolo et al., 1999; 150 pg). *Xnr1*, *Xlefty*, or *Cer-S* were placed in pCSKA plasmids to drive expression from early gastrulation (Condie et al., 1990). Injections were ~30° from the dorsal midline and ~20° above/below the equatorial cell boundary. Capped *LacZ* RNA (1.5 ng total; mMESSAGE mMACHINE kit; Ambion) was injected alone or together with plasmids for host-donor

demarcation. pCSKA-*β-galactosidase* (pCSKA-*497*) encodes a nuclear-targeted form of *β-galactosidase* (gift from Richard Harland, UC Berkeley). pCSKA-*Cer-S* contained *Cer-S* protein-coding region in the pCSKA *Sma*I site, and pCSKA-*Xnr1* and pCSKA-*Xlefty* were as published (Cheng et al., 2000; Sampath et al., 1997).

Microdissections and LPM Transplantation

Embryo dissections used a Gastromaster® dissector with 400, 800, or 1500 μm size square loop tips, to cut square (*i.e.,* box-shaped) or, by tilting, V-shaped explants. Dissections and culturing were in 0.75X normal amphibian medium (NAM; Sive et al., 2000). For LPM grafts, a square-shaped piece of donor LPM + ectoderm (~200 cells total area; ~12-15 cells wide) was excised; endoderm was carefully detached before transplantation. Explants were therefore somatopleure (LPM plus overlying ectoderm); they are referred to as "LPM" for simplicity because *Xnr1* is only expressed within that tissue layer. In hosts, a shallow pocket of similar size, shape, and depth to the graft was prepared in the L or R flank. Engrafted embryos were healed for 5 minutes before transferring to fresh 0.75X NAM. Good engraftment was assured by quality of edge matching and rapid healing; only high quality embryos were maintained and analyzed. For midline extirpations, 400 μm square tips were tilted to remove a segment with a V-shaped cross-section, aiming to remove neural tube floorplate, notochord, and hypochord, as checked by serial histochemical analysis of post-fixed embryos.

β-galactosidase activity staining

Red-gal (6-chloro-3-indolyl-β-D-galactoside; Research Organics) staining was a modification of standard protocols: embryos were MEMFA-fixed for 1 hour at room temperature, washed 3-4 times in phosphate-buffered saline (PBS) containing 0.1% Triton X-100, and stained with 1.0 mg/ml Red-gal in PBS/0.1% Triton X-100, 5 mM potassium ferro/ferricyanide, 2 mM $MgCl_2$ for 1 hour at room temperature. Embryos were washed 3

times in 1X PBS, MEMFA post-fixed, and stored at -20ºC in 100% methanol until *in situ* hybridization analysis.

In situ hybridization analysis

Whole-mount *in situ* hybridization was performed as described previously (Harland, 1991). Briefly, embryos were re-hydrated in a methanol: PBTw (1X PBS, 0.1% Tween 20) series, treated with proteinase K/PBTw (17 minutes – 10 μg/ml) and rinsed in 0.1 M triethanolamine (pH 7.5). Embryos were then treated with acetic anhydride, re-fixed with 4% paraformaldehyde/ PBTw and pre-hybridized at 65°C for 5-6 hours. Embryos were changed into fresh hybridization buffer (50% formamide, 5X SSC, 1 mg/ml Torula RNA, 100 μg/ml heparin, 0.1% CHAPs, 0.1% Tween 20, 10 mM EDTA•$2H_2O$, and 1X Denhardt's: 2% BSA, 2% polyvinyl pyrrolidone, 2% Ficoll 400) containing 1μg/ml antisense digoxygenin RNA probe and incubated overnight at 65°C. The following day, the embryos were washed 3 times with 2X SSC for 20 minutes at 65°C and treated with RNase A (20 mg/ml) and RNase T1 (10U/ml) in 2X SSC for 30 minutes at 37°C. Subsequently, the embryos were washed once in 2X SSC for 10 minutes at room temperature and then twice in 0.2X SSC for 30 minutes at 65°C. The samples were then rinsed 2 times with Maleic Acid Buffer pH 7.5 (MAB; 100 mM maleic acid, 150 mM NaCl) at room temperature for 15 minutes. The embryos were blocked with MAB/2% BMB (Boehringer Manheim Blocking reagent) and MAB/2% BMB/20% heat inactivated lamb serum at room temperature for 1 hour each. After blocking, the embryos were incubated with a 1/2000 dilution of anti-digoxygenin antibody conjugated to alkaline phosphatase (pre-blocked with frog embryo powder) in MAB/2% BMB/20% heat inactivated lamb serum overnight at 4°C. The next day, embryos were washed 5-6 times in MAB for 1 hour at room temperature to remove excess antibody and then 2 times for 5 minutes in alkaline phosphatase buffer (100 mM Tris pH 9.5, 50 mM $MgCl_2$, 100 mM

NaCl, 0.1% Tween 20, 5 mM Levamisol) before the color reaction. BM Purple (Roche) was used as a substrate.

Antisense *Xnr1*, *Xlefty* and *XPitx2* full length probes were generated from pSKII$^+$ CsCl purified cDNA plasmids by linearizing with *Xba*I, *Bam*HI and *Not*I, respectively, and transcribing with T7 RNA polymerase as previously described (Cheng et al., 2000; Jones et al., 1995; Ryan et al., 1998).

Frog embryo powder

Wild type or albino embryos were collected between stages 25-30 (100 at a time) and homogenized in 1X PBS by vigorous vortexing. Ice-cold acetone was then added to the embryo homogenate, vortexed and incubated on ice for 30 minutes. Samples were centrifuged at 10,000 rpm for 10 minutes and the pellet rinsed with cold acetone. After removal of the supernatant, the pellet was dried at room temperature for approximately 20-30 minutes. The dried pellet was then crushed to a fine powder with a mortar and pestle and stored at -20°C.

Histological analysis

After *in situ* analysis, embryos were re-fixed for 1 hour at room temperature in Bouin's fixative (LabChem, Inc.), dehydrated and equilibrated to Histoclear:paraplast (National Diagnostics; 1:1 ratio), and paraplast-embedded. 8-10 μm microtome sections were counterstained with a 3:1 mixture of 95% ethanol:eosin (Sigma).

Immunohistochemistry

Stage 42-45 embryos were MEMFA-fixed for 2 hours at room temperature and washed 3-4 times in 1X PBS. Whole-mount immunohistochemistry (Harland, 1991) used a 1:5 dilution (in PBS, 2 mg/ml BSA, 0.1% Triton X-100) of MF20 monoclonal antibody against all sarcomeric myosin heavy chains (Bader et al., 1982). Secondary antibody was

Alexa Fluor 594-conjugated anti-mouse IgG (Molecular Probes, Eugene, OR) used at a 1:200 dilution. Embryos were placed in PBS and immunofluorescent images recorded by an Olympus DP70 camera and Olympus BH2 microscope with appropriate filters. Images from any single experiment were post-processed identically.

SB-inhibitor treatment

Solid anhydrous SB-431542 and SB-505124 (Sigma) were dissolved at a concentration of 52 mM and 64 mM, respectively, in DMSO. Titration experiments were performed for each of the SB-inhibitors to determine the optimal concentrations to be used to completely block Xnr1 signaling during tailbud stages (see Fig. 5.1; Table 5.1). 50 μM, 100 μM and 150 μM concentrations were tested for SB-431542 and 10 μM, 30 μM and 50 μM concentrations were tested for SB-505124. Although 100 μM of SB-431542 and 50 μM of SB-505124 inhibited the majority of Xnr1 signaling, low levels of *Xnr1* expression within the L LPM was still observed after treatment. 150 μM and 75 μM concentrations of SB-431542 and SB-505124, respectively, were therefore used in all experiments to completely inhibit Xnr1 autoregulatory signaling within the L LPM. SB-431542 and SB-505124 inhibitor stocks were diluted to a final concentration of 150 μM and 75 μM, respectively, in 0.75X NAM for all experiments described. 0.75X NAM containing the same concentration of DMSO or 0.75X NAM alone was used as positive controls in each experiment.

CHAPTER III

INDUCTION AND DYNAMICS OF ASYMMETRIC *XNR1* EXPRESSION WITHIN L LPM DURING L-R SPECIFICATION

Introduction

Vertebrates exhibit conserved anatomical left-right (L-R) asymmetry in, for example, the placement and anatomy of the cardiovascular system, visceral organs, and the number of lung lobes. In some species, such as zebrafish, L-R asymmetry is also apparent in the brain. The developmental mechanism by which L-R asymmetry is initiated, and the degree to which it is conserved between species, remains unknown (see general introduction) (Burdine and Schier, 2000; Capdevila et al., 2000; Levin, 2005). Although a number of signaling molecules, including Shh, BMP, FGF, RA, and Notch, have been implicated in some vertebrates in the stage-setting phase of asymmetry establishment, there is currently no unifying "L-R specification model" that applies well to all species (Burdine and Schier, 2000; Capdevila et al., 2000; Whitman and Mercola, 2001). Despite the possible divergence in early mechanisms, however, they culminate in all species examined so far in the transient asymmetric LPM expression of a "L-side gene cassette": *Nodal*, *Lefty*, and *Pitx2*. Such asymmetric expression may precede vertebrate evolution, as it is observed in ascidians and amphioxus (Boorman and Shimeld, 2002; Chea et al., 2005; Hudson and Yasuo, 2005; Morokuma et al., 2002; Yu et al., 2002), even if "L-sidedness" seems to be carried in a different germ layer. It is plausible that this gene cassette's role in L-R asymmetry arose by redirecting a primitive role in specifying the oral-aboral axis, as in sea urchins (Chea et al., 2005; Duboc et al., 2005).

Gain-of-function experiments show that Nodal has asymmetry-instructive effects, and genetic loss-of-function experiments indicate its essential nature (Brennan et al., 2002; Capdevila et al., 2000; Cheng et al., 2000; Levin et al., 1997; Lowe et al., 2001;

Saijoh et al., 2003; Sampath et al., 1997; Shiratori et al., 2001; Vincent et al., 2004). Asymmetric Nodal signaling directly induces *Lefty* and *Pitx2* expression, which encode an antagonist and effector of L-R asymmetric signaling, respectively (Cheng et al., 2000; Juan and Hamada, 2001; Logan et al., 1998; Meno et al., 1999; Meno et al., 1998; Meno et al., 2001; Ryan et al., 1998; Yoshioka et al., 1998).

Probably because of its highly dynamic expression pattern, combined with the substantial tissue movement and posteriorward node regression seen in some vertebrate embryos during early somitogenesis, there have been no concerted studies in mouse, chicken or zebrafish of the spatiotemporal pattern of *Nodal* expression in the LPM relative to anatomical landmarks. Expansion of *Nodal* expression, however, definitely occurs in other species, such as mouse and chicken, despite the current poor characterization of the direction and dynamics involved (Lowe et al., 1996; Murray and Gridley, 2006; Levin et al., 1995). In Medaka, there is anterior-shifting of expression of the *Nodal*-related gene *southpaw* (*spaw*) (Soroldoni et al., 2006), and the same phenomenon also occurs in zebrafish (Long et al., 2003). It is important to characterize how *Nodal* expression in the L LPM is initiated and spatiotemporally regulated along the A-P axis as an instructor of asymmetric morphogenesis to the various organ primordia, and how the underlying molecular mechanisms are coordinated across the embryo to ensure an integrated morphogenetic process.

In all species, the mechanism initiating *Nodal* expression in the L LPM is poorly defined. In experiments in *Xenopus*, both the L and R LPM expressed *Xnr1* when explanted away from axial midline tissues (Lohr et al., 1997). The addition of notochord to these explants suppressed expression (Lohr et al., 1998), which led to the proposal that LPM expresses *Xnr1* by default, and that midline-derived tissues actively repress R-sided *Xnr1* expression (Lohr et al., 1998; Lohr et al., 1997). However, Levin and Mercola (1998) showed that midline/node-type tissue could be formed in the "LPM-alone" explants, and suggested that positive-acting signals caused *Xnr1* expression in both L and

R LPM explants. The inference from these studies was that inductive signals are normally deployed specifically leftward in whole embryos, consistent with results from manipulating chicken embryos (Levin, 2005). In the mouse embryo, it has been suggested that Nodal itself is the node-derived positive inducing factor that travels to the L LPM to initiate *Nodal* expression (Yan et al., 1999; Lowe et al., 2001; Brennan et al., 2002; Saijoh et al., 2003). In support of this hypothesis, Nodal can exhibit long-range movement (Chen and Schier, 2001; Sakuma et al., 2002; Williams et al., 2004).

The ability of Nodal to autoinduce its expression in LPM may differ across species. In chicken embryos, Nodal-expressing cell pellets did not induce *Nodal* expression (Levin and Mercola, 1998). More recent studies, however, in early somitogenesis stage mouse embryos showed that *Nodal*-expressing tissue grafts, or electroporated expression vectors, did induce LPM expression of *Nodal* (Yamamoto et al., 2003). While the response to Xnr1 itself has not been demonstrated previously in *Xenopus* embryos, there is evidence that other TGFβ-related factors, which likely mimic Xnr1 to some degree, can induce *Xnr1* expression when introduced into the LPM (Mogi et al., 2003; Toyoizumi et al., 2000; Toyoizumi et al., 2005). There is, however, no current evidence that these factors are normally expressed in or involved in L-R specification during tailbud stages; one issue addressed in the studies reported herein is the ability of Xnr1, specifically, to autoactivate its own expression within the LPM.

A body of evidence from studies in the mouse suggests that a net leftward fluid flow at the surface of the node ("nodal flow"), which is generated by motile monocilia, is responsible for breaking embryonic symmetry in this species and initiating asymmetric gene expression in the L LPM (for review, see Raya and Belmonte, 2006). Recent studies in mice have led to a Self-Enhancement Lateral Inhibition (SELI) model that proposes that the L-sided initiation of *Nodal* expression in the LPM is dependent upon asymmetric threshold-dependent induction. More specifically, this model proposes that nodal flow occurring at the node causes an initial L-R bias that results in *Nodal* being

expressed at higher levels on the L versus the R side of the embryo. Subsequently, *Nodal* in the L LPM self-amplifies its own expression through positive autoregulation, as well as induces *Lefty* in the midline. The inhibitory action of Lefty, in turn, suppresses the lower levels of *Nodal* on the R side, thereby not allowing self-enhancement and expression in the R LPM. As I will discuss in more detail in reference to the data presented in the next chapter, the SELI model also proposes that contralateral inhibition by Lefty induced in both the L LPM and the midline by Nodal signaling, results in the continued suppression of *Nodal* in R LPM, thereby maintaining asymmetry of expression. Lefty is also thought to progressively shut down *Nodal* expression in the L LPM ensuring its transient expression during L-R asymmetry specification (Nakamura et al., 2006; Tabin, 2006).

In this chapter, I will describe studies on the initiation of *Xnr1* expression in the L LPM, its spatiotemporal expression pattern and the mechanism underlying its dynamic directional shift, and its subsequent inactivation. I present evidence suggesting that the initiation of *Xnr1* in the L LPM relies on inductive signaling from the posterior tailbud (the functional equivalent of the node at this stage in *Xenopus*) and that proper L-sided activation of *Xnr1* requires a particular time of association with the midline, in keeping with a SELI mechanism for L-R asymmetry patterning. Here, I also show results suggesting that planar tissue communication, operating independent of axial tissues, underlies the rapid anteriorward expansion of *Xnr1* expression, and that this process requires intercellular *Xnr1* autoactivation. Finally, I will discuss how my findings demonstrate plasticity in L-R asymmetry specification at relatively late stages of embryogenesis.

Results

Anterior shifting and transient expression of *Xnr1* and *Xlefty* in the left LPM

We previously described L-sided *Xnr1* expression in *Xenopus* embryogenesis and noted a general anteriorward shift of expression during tailbud stages (stage 19/20-25; Lowe et al., 1996). We characterized this pattern at higher resolution and at more stages and compared it to *Xlefty*, which encodes a major feedback inhibitor of Nodal/Xnr1 signaling (Fig. 3.1A). After downregulation of gastrula stage *Xnr1* expression (Jones et al., 1995; Lustig et al., 1996), expression appears posteriorly in small bilateral perinotochordal domains near the chordoneural hinge. Shortly thereafter, *Xnr1* is first expressed in posterior L LPM relatively close to these domains. L LPM expression subsequently undergoes a large-scale, posterior-to-anterior (P-to-A) shift. A stage of broad expression encompassing much of the embryo's flank, in both splanchnic and somatic mesoderm (Lowe et al., 1996), is followed by an anterior/ventralward shift, and progressive P-to-A shutdown of expression, which results in the *Xnr1* signal becoming restricted to a small territory just posterior to the presumptive heart anlage. This signal disappears at stage 26-27. The *Xlefty* expression pattern follows the dynamic *Xnr1* shift, consistent with the idea that *Xlefty* is a direct response gene of Nodal/Xnr1 signaling (Cheng et al., 2000; Tanegashima et al., 2000).

Requirement of posterior tissue for asymmetric activation of *Xnr1* in LPM

We first readdressed the issue of whether asymmetric *Xnr1* expression results from unilaterally directed positive signaling or R-side-specific inhibition, as proposed by Levin and Mercola (1998) and Lohr *et al.* (1997), respectively, as discussed in the Introduction. We found that two types of explants produced relevant information. The

Fig. 3.1 Anteriorwards shifting of *Xnr1* expression in L LPM requires tissue communication. (A) Anterior shifting and transient expression of *Xnr1* and *Xlefty* in L LPM. The dynamic expression pattern of *Xnr1* in L LPM is mimicked with a temporal delay by *Xlefty*. The first *Xnr1* expression at neurula/early tailbud is bilateral, flanking posterior notochord (yellow arrowheads). Asymmetric LPM expression begins at ~stage 19/20, shifts rapidly, and disappears by stage 27. Green arrowhead, axial *Xlefty* expression. Stage 18, dorsal view; other panels, lateral view. Anterior, left. (B) Transecting embryos (stage 18/19) prevents *Xnr1* expression in anterior halves at all stages analyzed (stages indicated, panel top left). (Black arrowheads, perinotochordal *Xnr1* expression; white arrowhead, L LPM *Xnr1* expression). (C) LPM explants after neural tube closure, including tissue close to the bilateral posterior *Xnr1* expression region, were marked anteriorly (Neutral Red; red arrowhead). *Xnr1* expression shifted forward and showed graded expression as diagrammed. (D) *Xnr1* expression in anterior explants (2) depends upon attached posterior tissue (1). Note perdurance of strong signal in posterior L explants at stage 24. A, anterior; P, posterior.

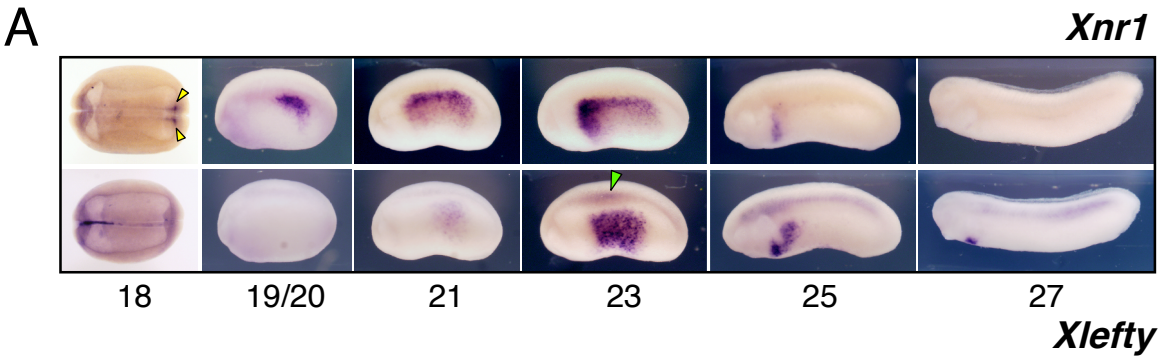
A
Xnr1
18
19/20
21
23
25
27
Xlefty

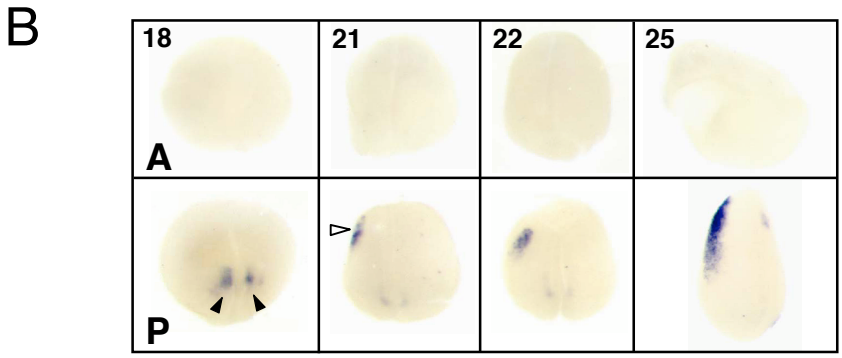
B
18
21
22
25
A
P

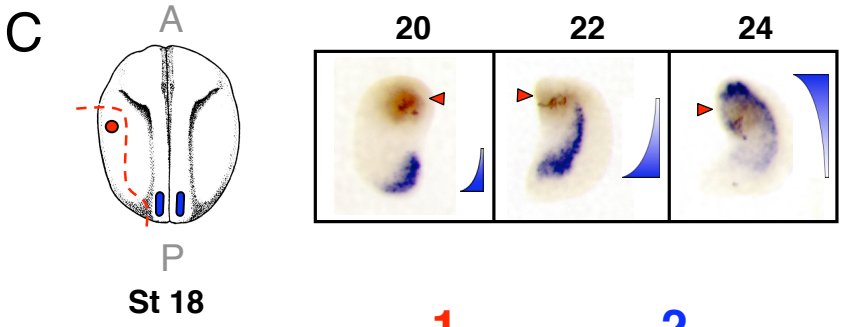
C
A
P
St 18
20
22
24

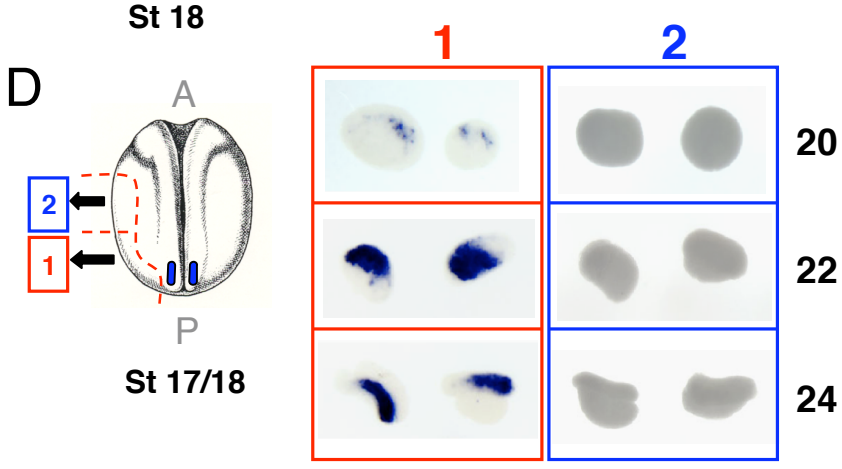
D
A
2
1
P
St 17/18
1
2
20
22
24

first explant type, from stage 15/16 embryos, was L or R mid-trunk LPM from the middle third of the embryo, with a dorsal limit ~20-25 cells below the intermediate mesoderm and a ventral limit approximately one-third from the embryo's keel. Neither L nor R explants of this type developed *Xnr1* expression at sibling stage 24 (Fig. 3.2A). The second explant type included the same mid-trunk region, except that it was extended posteriorly to include a region approaching the tailbud and posterior-most axial tissue (Fig. 3.2B). These explants therefore contained tissue encroaching upon the location where posterior bilateral *Xnr1* expression develops at stage 17. In this case, both L and R explants expressed *Xnr1*, but we found L/R differences that varied with explantation stage. Stage 15/16 and stage 17 explants showed equivalently strong L and R expression when scored at sibling stage 24. Beginning at stage 18, R explants showed much less extensive and weaker *Xnr1* expression than L explants, and this difference was more pronounced at stage 19 (Fig. 3.2B). If explanted at stage 21/22, at a time when asymmetric *Xnr1* expression in whole embryos is broad along the L LPM (Fig. 3.1A), R LPM explants did not develop *Xnr1* expression (data not shown). Bisecting whole embryos along the axial midline at stage 15/16 led to L-sided *Xnr1* expression only, despite the presence in both embryo-halves of the posterior perinotochordal *Xnr1* expression domain (Fig. 3.2C).

These data agree with the finding that removing the tailbud region encompassing the posterior bilateral *Xnr1* expression from late neurula/early tailbud embryos (stage 17) led to the absence of asymmetric *Xnr1*, *Xlefty*, and (except as noted below) *XPitx2* expression (Fig. 3.3A). The lack of L-sided *Xnr1* and *Xlefty* expression was associated with a lack of axial midline *Xlefty* expression. Control stage 20 extirpations, done just after asymmetric *Xnr1* expression has initiated in posterior L LPM, developed robust expression of all three genes, including axial midline *Xlefty* (Fig. 3.3B). In addition, in batches of embryos that lacked asymmetric *Xnr1* expression, a substantial proportion (representative experiment, n=4/7) showed some L-sided *XPitx2* expression that was

Fig. 3.2 Explantation of different regions of LPM affects ability to express *Xnr1*. (A) Approximately the middle one-third of L and R LPM was explanted at either (a) stage 15/16 or (d) 19/20, and cultured to sibling stage 24. (b,c) L or R LPM explanted at stage 15/16 failed to develop *Xnr1* expression. (d,e,f) Only L LPM explanted at stage 19/20 developed *Xnr1* expression. The *Xnr1* expression territory observed at stage 19/20 is schematized in blue. (B) (b,c,e,f,h,i) Explanting L or R LPM that extended more posteriorly, approaching the bilateral *Xnr1* expression domain, resulted in L- and R-sided *Xnr1* expression when explanted at (a,d,g) stages 17, 18, or 19/20 and developed to stage 24. *Note stronger intensity of Xnr1 signal in L LPM explanted at stages 18 and 19/20.* (C) (a) Bisections down the midline from stage 15/16 embryos that were then cultured to stage 24 (b,c) led to only L-specific *Xnr1* expression, despite presence in L and R embryo-halves of the respective posterior perinotochordal *Xnr1* expression domain (c, black arrowheads). Red dotted lines, region of explanted LPM. L, left; R, right.

A

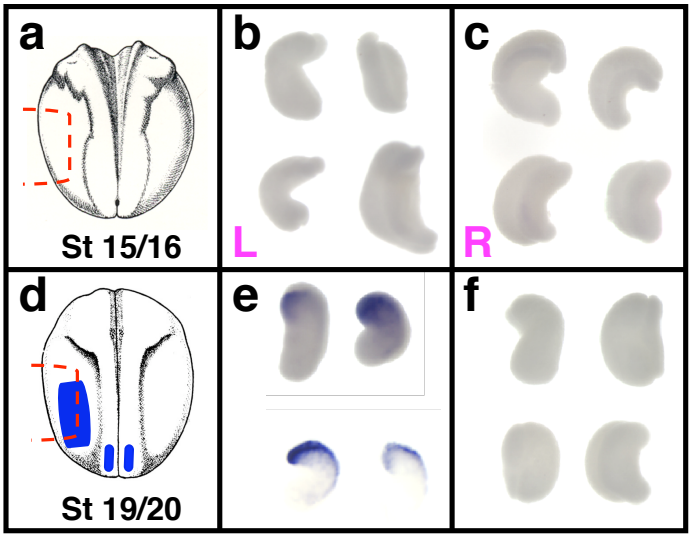
a
b
c
St 15/16
L
R
d
e
f
St 19/20

B

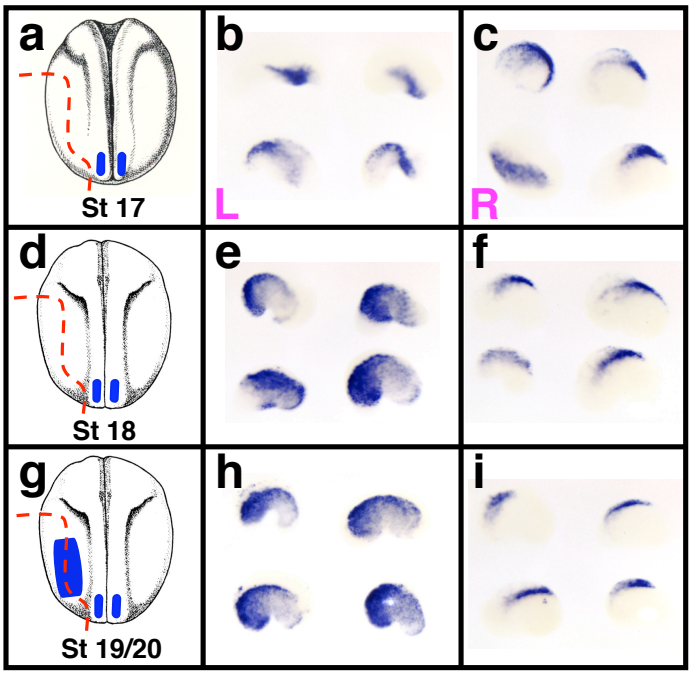
a
b
c
St 17
L
R
d
e
f
St 18
g
h
i
St 19/20

C

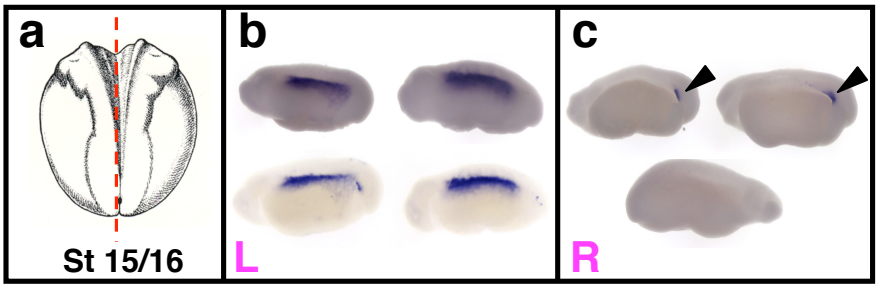
a
b
c
St 15/16
L
R

much weaker than in sibling controls (Fig. 3.3A). This result implies that non-Nodal-signaling mechanisms can induce L-sided *Pitx2* expression, as reported in some genetic situations in the mouse (Constam and Robertson, 2000a; Constam and Robertson, 2000b; Meyers and Martin, 1999; Pennekamp et al., 2002).

The cardiac situs of posteriorly-cropped embryos was assessed at stage 43-45. In a population of embryos cropped at stage 17, heart looping was normally directed (22%), reversed (56%), or incomplete (22%) (Fig. 3.3C). Our data are consistent with previous findings in the mouse, in which the absence of L LPM *Nodal* expression led to cardiac situs randomization (Brennan et al., 2002; Lowe et al., 2001; Saijoh et al., 2003). Cardiac situs remained normal in all control stage-20-cropped embryos (Fig. 3.3C).

Preliminary data using pharmacological inhibitors of the Nodal signaling pathway support the idea that Xnr1 signaling from the posterior tailbud is required to initiate asymmetric *Xnr1* expression in L LPM. Exposure of stage 18 embryos to SB-431542, a specific inhibitor of Type 1 Activin-Like Kinase receptors (ALK-4, -5, -7), prevented L LPM *Xnr1* expression at later stages, without affecting the posterior bilateral *Xnr1* expression (Fig. 5.2B).

Overall, we conclude from these data that an inductive process involving Nodal/TGFβ signaling activates *Xnr1* expression in L LPM, with the signal emerging from the region of the posterior tailbud that is the functional equivalent of the mouse and chicken embryonic node.

Directional expansion of *Xnr1* expression is independent of the axial midline

One way of generating anteriorward-propagating *Xnr1* expression in the L LPM could be that a developmental timing mechanism results in progressively anterior regions of the LPM activating *Xnr1* expression slightly later than posterior neighboring tissue, with the activation not requiring contact with or signals from posterior tissue. In contrast, our results suggest a rolling-wave mechanism in which progressively anterior cell fields

Fig. 3.3 Posterior tailbud induces asymmetric *Xnr1* expression. Tissue encompassing the posterior bilateral *Xnr1* expression area was removed at (A) stage 17 or (B) stage 20, and posteriorly-cropped embryos analyzed for *Xnr1*, *Xlefty*, and *XPitx2*. In (A), asymmetric gene expression was absent, except for occasional weak *XPitx2* signal (stage 34 shown, black arrowhead). Note absence of midline *Xlefty* expression (red arrowheads, compare to Fig. 2B). (B) Unilateral induction occurs by stage 20, and midline *Xlefty* expression develops. (Anterior, left; stages analyzed indicated) The removed posterior tissue from both stages showed the bilateral *Xnr1* expression. (C) L-R anatomy after cropping (MF20 immunofluorescence analysis for heart, brightfield analysis for gut). Stage 17 cropping produced (from left to right) normal, reversed, and indeterminate heart looping at percentages indicated (n=18); stage 20 cropping (rightmost panel) all had normal looping (n=21). Yellow arrowheads, cardiac outflow tract; inset, diagram of heart looping. Stage 17 posterior cuts damaged posterior endoderm more than at stage 20, the gut is more normal in the latter.

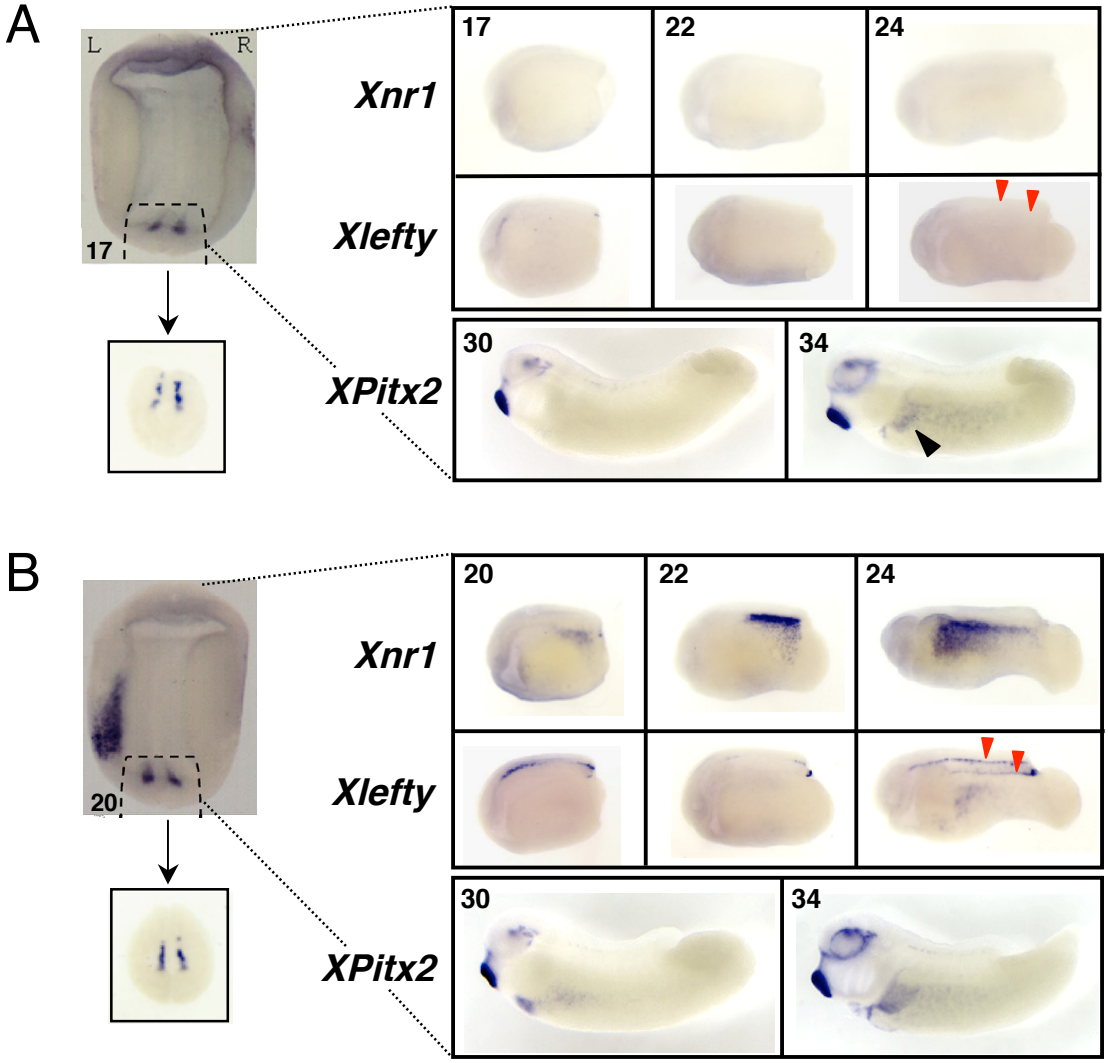
A
L
R
17
Xnr1
Xlefty
XPitx2
17
22
24
30
34
B
20
Xnr1
Xlefty
XPitx2
20
22
24
30
34
C
cut at St 17
cut at St 20
22%
56%
22%
100%

activate *Xnr1* expression after induction from Xnr1 that is produced just-posteriorly. First, simple mid-trunk transection of stage 18/19 embryos, when *Xnr1* expression has just begun in posterior L LPM, into anterior and posterior halves (which all developed well) prevented *Xnr1* expression in anterior half-embryos (Fig. 3.1B). Stage 22 transections, performed when *Xnr1* expression has just shifted into the anterior half, showed robust expression in both half-embryos. Subsequently (stages 23, 25, and 27 analyzed), there was expression domain shifting in the anterior half and downregulation in both the anterior and posterior half-embryos, similar to whole embryos (not shown). This result also shows that the development of anterior L LPM expression occurs via signaling from posterior LPM tissue, and does not require orthogonal induction from the trunk axial midline. The similar results obtained when L LPM explants alone were anterior-posterior transected (Fig. 3.1D) show that LPM integrity is required for anteriorward-propagating *Xnr1* expression (Fig. 3.1C). We conclude that the directional P-to-A propagation of asymmetric *Xnr1* expression requires planar tissue communication through the LPM and results from posteriorly-originated signals.

Autoregulation controls forward expansion of *Xnr1* in L LPM

Further evidence that an intercellular "rolling-wave" of *Xnr1* autoinduction occurs in the L LPM came from the finding that small LPM transplants expressing Nodal-specific inhibitors could block the shift of *Xnr1* expression. CerS, the short isoform of the secreted factor Cerberus, inhibits Nodal/Xnr signaling (Agius et al., 2000; Piccolo et al., 1999), and *Xlefty* was shown previously to block *Xnr1* and *XPitx2* expression in L LPM (Cheng et al., 2000). Each factor was encoded in pCSKA plasmids, to drive expression after gastrulation, and injected as a mixture with *lacZ* RNA lineage tracer. Control grafts were from embryos injected with *lacZ* RNA alone, or pCSKA-*497* (encoding nuclear-targeted β-galactosidase). Based upon the fate maps, 8-cell-stage donor embryos were injected to enrich delivery to LPM (Methods). pCSKA-*CerS* or

pCSKA-*Xlefty* LPM from stage 17 donor embryos was transplanted to a mid-trunk L-side location in stage 17 wild-type hosts (Fig. 3.4A). Engrafted embryos were cultured to stage 24/25 and analyzed for asymmetric *Xnr1* expression.

Grafts expressing either inhibitor blocked the forward expansion of *Xnr1* expression (Fig. 3.4C,D; Table 3.1). The suppression of L-sided *Xnr1* expression in host embryos receiving *CerS*- or *Xlefty*-expressing LPM grafts was of two types: complete absence of *Xnr1* signal, or partial suppression in which *Xnr1* expression shifted up to the posterior edge of the graft, and very seldom into its posterior margin (Fig. 3.4C,D; Table 3.1). In CerS-grafting experiments, ~75% of embryos showed complete or partial suppression. For *Xlefty*-expressing grafts, ~73% of embryos showed no signal or anteriorly halted expression (Fig. 3.4C,D; Table 3.1). The proportion of embryos (~20-30% overall) showing no effect on anteriorly shifting *Xnr1* expression could reflect a dependence of the graft's ability to block *Xnr1* autoregulation upon the level of CerS and Xlefty produced from it, very likely including problems caused by the inevitable large-scale mosaic inheritance pattern of the non-chromosomally integrated factor-producing plasmids (*e.g.,* see embryos in Fig. 3.5B). In embryos showing no L-sided expression, a high inhibitor level might have caused an early block to the beginning-stage rolling wave of *Xnr1* expression within the L LPM (adding to the suppression caused by endogenous Xlefty expression). Alternatively, it may have completely prevented *Xnr1* expression from initiating in the posterior L LPM. The control grafts did not perturb the *Xnr1* expression pattern (Fig. 3.4C,D; Table 3.1). We conclude that once its asymmetric expression is initiated in L LPM, Nodal/Xnr1 signaling is required for the forward propagation of *Xnr1* expression (Fig. 4.6).

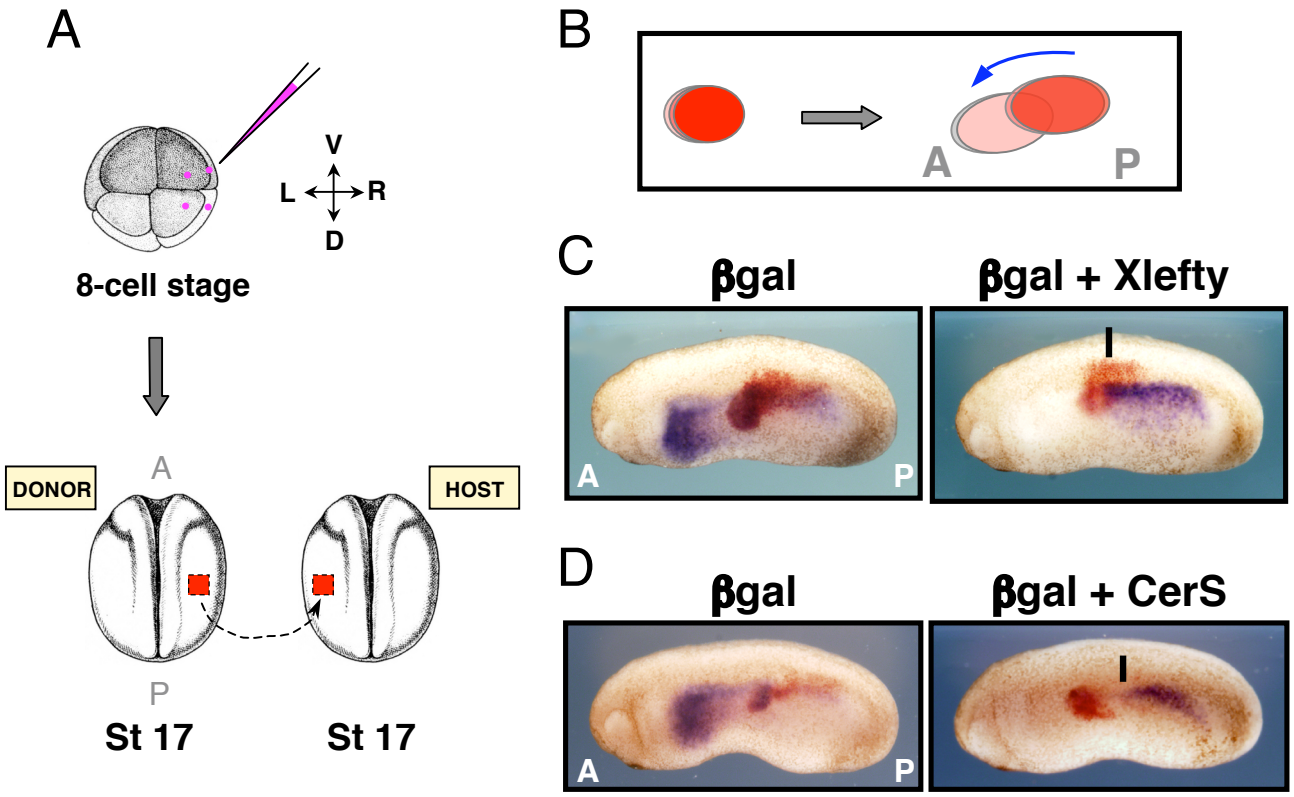

Fig. 3.4 Xnr1 inhibitors Xlefty and Cer-S suppress anteriorward shift of L-sided *Xnr1* expression. (A) 8-cell embryo injection with *LacZ* RNA +/- pCSKA-*Xlefty* or pCSKA-*Cer-S* enriched for LPM delivery (pink dots, injection points). R LPM was grafted mid-trunk into L LPM of host embryos. (B) Cartoon shows forward/ventral dislocation of graft LPM layer relative to overlying ectoderm that occurs after integration. (C,D) Stage 24/25 embryos showed shifting of *Xnr1* expression through βgal-alone transplants, but suppressed or delayed shifting for Xlefty or Cer-S (black lines, anterior limit of *Xnr1* expression). L, left; R, right; D, dorsal; V, ventral; A, anterior; P, posterior.

Table 3.1. *Xnr1*-specific inhibitors suppress anteriorward shifting of *Xnr1* expression

Donor graft	*n* embryos (# expts. pooled)	*n* (%) complete suppression	*n* (%) partial suppression	*n* (%) no suppression
LacZ alone	49 (6)	-	-	49 (100)
p497/LacZ	9 (1)	-	-	9 (100)
pCerS/LacZ	28 (3)	3 (11)	18 (64)	7 (25)
pXlefty/LacZ	30 (3)	5 (17)	17 (57)	8 (27)

Donor grafts injected with *LacZ* RNA lineage tracer plus pCSKA/497, pCSKA/CerS, pCSKA/Xlefty; or *LacZ* alone were transplanted to the left side of host embryos at stage 17 and engrafted embryos were analyzed for *Xnr1* expression at stage 24-25. All data refer to Figure 3.4.

Xnr1 induces *Xnr1* in tailbud stage LPM

Although it has been demonstrated that various TGFβ-related factors (Activin, TGF-β5, and mouse Nodal), can induce robust *Xnr1* expression in *Xenopus* embryos (Mogi et al., 2003; Toyoizumi et al., 2000; Toyoizumi et al., 2005), the response to Xnr1 itself has, however, not been demonstrated. As described below, our experiments go further than those previously published and, in some cases, have distinctly different findings.

Using the grafting method described above, we targeted pCSKA-*Xnr1* to the L or R LPM of donor embryos, transplanted *Xnr1*-expressing grafts at stage 17 to a R-side mid-trunk location in wild-type hosts (Fig. 3.5A), and analyzed *Xnr1* expression at various stages thereafter. Host *Xnr1* expression was first detected both anteriorly and posteriorly of the graft at stage 22/23 (Fig. 3.5C; Table 4.1), slightly later than the time when endogenous *Xnr1* expression is initiating in the posterior L LPM in normal embryos (Fig. 3.1A). Because the pCSKA-derived *Xnr1* expression in donor embryos was strong at all stages between 12/13 and 19/20 (Fig. 3.5B), the stage 17 grafts were likely already producing significant amounts of Xnr1. We therefore attribute the inability to induce earlier R-sided endogenous *Xnr1* expression to either an intrinsic competence window in the LPM to respond to Xnr1, or a requirement to reach a specific (unknown) threshold of graft-derived Xnr1.

By stage 24/25, the induced R-sided *Xnr1* expression had shifted substantially anterior of the graft but minimally, if at all, posteriorly. Under these conditions, the induced R-sided *Xnr1* expression extended farther forward than the endogenous L LPM expression, which itself had become stalled (extended less anteriorly) in comparison with unmanipulated or βgal control embryos (Fig. 3.5C,D; Table 4.1). For example, while R-sided expression abutted the presumptive heart anlage, L LPM expression had extended only mid-way through the LPM (Fig. 3.5C,D; Table 4.1). Another outcome occasionally

observed (not shown) was that endogenous L-sided *Xnr1* expression, in addition to anterior stalling, was overall significantly weaker than that induced on the R side, or seen in the L LPM of control embryos (Table 4.1). At stage 26/27, pCSKA-*Xnr1*/LPM engrafted embryos showed prolonged *Xnr1* expression specifically in the anterior region of the R LPM, but *Xnr1* expression was not detected around or within the graft, and there was no L-side signal (Fig. 3.5C; Table 4.1). It should be noted that L-sided *Xnr1* expression disappears by this stage in normal embryos. LPM grafts from the L or R side of donor embryos induced R-sided host *Xnr1* expression equivalently (not shown), suggesting that the meaningful signal is the ectopic Xnr1, with no requirement for additional L LPM tissue-derived signals.

Fig. 3.5 Xnr1 induces R LPM *Xnr1* expression, which undergoes stereotypic P-to-A shifting. (A) 8-cell embryos injected as in Fig. 2 produced L LPM grafts that were placed into mid-trunk R LPM locations in stage 17 hosts. Right panel: engrafted embryo shortly after healing (red-gal stained), demonstrating medial placement. (B) Donor embryos injected with pCSKA-*Xnr1* showed mosaic strong *Xnr1* expression in L LPM from early neurula stage onward. Bracketed area (stage 15/16 panel) indicates explant size used in grafts. (C) βgal-alone engraftment did not induce R-sided *Xnr1* expression at any stage (stages indicated left of panel). *Xnr1*-engrafted hosts showed extensive, anterior shifting, R LPM *Xnr1* expression. At stage 23, R-sided *Xnr1* expression had begun to shift significantly anterior-ward, with only limited posterior shifting. Red lines, A-P boundaries of graft. Purple arrowheads, A-P limits of induced *Xnr1* expression. At stage 24/25, the anterior limit of R-sided *Xnr1* expression was farther anterior than the endogenous L expression, as indicated by yellow arrowheads (dorsal view, embryo shown in panel above). At stage 26, R-side induced *Xnr1* expression was prolonged compared to L side expression (red arrowhead). (D) Transverse sections, stage 24/25 *Xnr1*-engrafted embryo: grafts showed good laminar alignment with host tissues. Induced *Xnr1* expression was restricted to R LPM. Sections as indicated demonstrate that R-sided induced *Xnr1* expression progressed farther anterior than endogenous L-side expression, with minimal posterior shifting of *Xnr1* expression. L, left; R, right; D, dorsal; V, ventral; A, anterior; P, posterior.

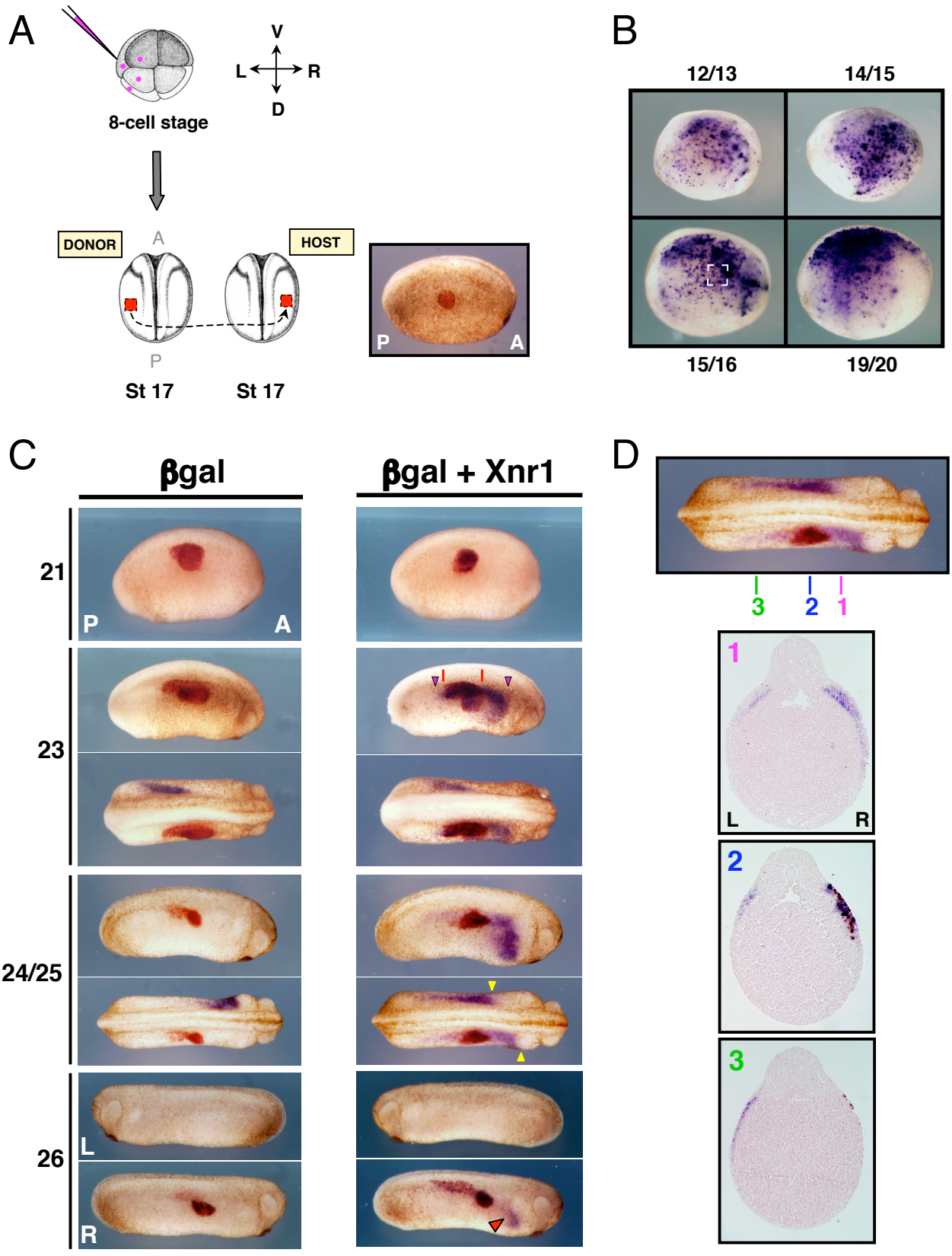
A
V
L
R
D
8-cell stage
DONOR
A
HOST
P
St 17
St 17
P
A
B
12/13
14/15
15/16
19/20
C
βgal
βgal + Xnr1
21
23
24/25
26
P
A
L
R
D
3
2
1
1
L
R
2
3

Discussion

My finding that posterior inductive signals from the tailbud region of *Xenopus* embryos induce L-sided *Xnr1* expression supports the idea that a conserved asymmetrically directed inducer emanates from the node or its functional equivalent in all vertebrate species. While studies on various *Nodal* and *Cryptic* mutants in the mouse suggest that Nodal signaling from the node is involved in initiating *Nodal* expression in the L LPM, there has, however, been little to no study in any vertebrate of the mechanism underlying the spreading of *Nodal* expression within the LPM after its initiation. My inhibitor results suggest that *Xnr1* autoregulation is a required component of the mechanism for the rapid and unidirectional anteriorward propagation of its expression domain. I also provided evidence that embryonic L-R asymmetry, determined by Xnr1 signaling activity from the LPM, remains plastic until stages that are close to the actual onset of asymmetric morphogenesis. In this latter respect, it is possible that there is no specification of definitive L or R fates, but that the earlier L-R biases only becomes fixed by the structurally irreversible process of asymmetric morphogenesis.

Induction of asymmetric *Xnr1* expression during *Xenopus* embryogenesis

Lohr *et al*. (1997) proposed that L or R LPM expresses *Xnr1* by default, and that R-side specific inhibition causes the L-specific expression seen in normal embryos, while Levin and Mercola (1998) suggested that asymmetric L-specific positive induction is involved. My results are largely consistent with, but extend the findings of, Levin and Mercola (1998). I showed that *Xnr1* expression does not develop simply as a default condition within LPM removed from the repressive influence of the midline, but that an inductive signal is asymmetrically deployed from the tailbud region, the area of nascent mesoderm formation and bilateral *Xnr1* expression. These conclusions were generated from both posterior cropping and LPM explantation experiments (Figs. 3.2 and 3.3).

The recent studies by Nakamura *et al.* (2006) showed that *Nodal* is initially activated in both L and R LPM but with stronger expression on the L side, due to an asymmetric biasing caused by leftward nodal flow. Our laboratory has also found in *Xenopus*, both by RT-PCR and *in situ* hybridization analyses, that low levels of *Xnr1* expression can be detected in the R LPM. The SELI model proposes that Lefty from the midline acts to suppress *Nodal* only in the R LPM and not the left because, in a reaction-diffusion system (of which Xnr1 and Xlefty are thought to comprise, see general introduction), the inhibitory influence of Lefty produced in the midline is relatively stronger than the inductive signal on the right but weaker than the Nodal autoregulatory signal on the left (Nakamura et al., 2006; Tabin, 2006). Therefore, my findings that the levels of *Xnr1* expression in L and R lateral explants differs depending on the stage of isolation fits well with the SELI model, in that earlier explantation would remove the inhibitory influence of midline Xlefty that occurs in whole embryos, resulting in equivalent bilateral expression (Fig. 3.2B). The importance of an inhibitory role for the midline was also demonstrated by the finding that in lengthwise-bisected embryos (down the midline) only left half-embryos developed broad LPM expression of *Xnr1* even though both halves contained its posterior perinotochordal domain of *Xnr1* expression (Fig. 3.2C).

Studies in the mouse embryo suggest that Nodal signals originating from the node are involved in initiating *Nodal* expression in the L LPM. Embryos lacking node *Nodal* expression because of a deletion of specific *cis*-regulatory regions show an absence of L LPM *Nodal* expression (Brennan et al., 2002; Saijoh et al., 2003). Consistent with these findings, I showed that disruption of Xnr1 signaling from the posterior tailbud, either by extirpation or pharmacological approaches, abolished L LPM *Xnr1* expression. These results imply that the posterior bilateral perinotochordal *Xnr1* expression domains are functionally equivalent to the bilateral *Nodal* expression in the 0-7 somite-stage mouse node (Lowe et al., 1996). In contrast to the spreading of *Xnr1* expression through the L

LPM, *Xnr1* autoregulation is apparently not involved in maintaining the posterior bilateral tailbud expression, because it was unaffected by the Nodal receptor inhibitor SB-431542.

Dynamics of asymmetric *Xnr1* expression and LPM plasticity during L-R specification

Yamamoto *et al*. (2003) showed that *Nodal*-expressing LPM grafts or *Nodal* expression vectors could induce *Nodal* expression in the LPM of early somite-stage mouse embryos. Intriguingly, the electroporation of *Nodal* expression vectors into the R LPM caused an extensive spreading of *Nodal* expression along the A-P axis, although the authors did not speculate on the underlying mechanism. Based on their report, one cannot conclude that the locally electroporated vectors induced bidirectionally shifting *Nodal* expression, or the degree to which the expression in the LPM became expanded by the rearward movement of *Nodal*-expressing cells in association with the movements driving node regression. Future time-course studies of the expansion of *Nodal* expression with respect to the position of the node might gain insight in this respect.

I demonstrated that *Xnr1*-expressing grafts caused R-sided induction of *Xnr1*, which underwent the dynamic directional shift that occurs in the L side of normal embryos (I note here the substantially prolonged *Xnr1* expression observed at the end phase; Fig. 3.5C). While mid-trunk *Xnr1*-expressing grafts did initially induce host *Xnr1* expression both posterior and anterior of the graft, the subsequently induced host *Xnr1* expression shifted only anteriorly, revealing an inherent directionality within the LPM in the ability to propagate an *Xnr1* autoregulated expression wave. Further work will be needed to determine if a specific repressive influence works to oppose a posteriorward *Xnr1* expression wave. We speculate that anterior cues may somehow be given by the anterior movement of the graft's LPM layer relative to the overlying epidermis (*e.g.*, Fig. 3.4B), a movement of the interior germ layer that could be considered similar to that

undergone by the endoderm relative to the rest of the tailbud-stage embryo (Chalmers and Slack, 2000). It is, however, not known how this displacement might orient the *Xnr1* autoregulatory wave. Another possibility is that Xnr1 is somehow moved vectorially within the plane of the LPM through the anteriorly-disposed cell surfaces in association with some form of planar cell polarity.

A potential limitation of the rolling-wave Xnr1-to-Xnr1 model comes from considering the observed speed of *Xnr1* expression shifting in the LPM as compared to the time required for transcription, translation, propeptide processing and secretion, ligand diffusion/transport, receptor binding and intracellular signal transduction. The time from posterior initiation of *Xnr1* expression to the maximal forward progression of expression in the L LPM can be estimated at ~6-8 hours. Studies on TGF-β signaling have shown that peak levels of phosphorylated Smad2 are detected as soon as 0.5-1 hour after ligand addition (Di Guglielmo et al., 2003; Lo and Massagué, 1999). The 8-hour expression-shift-period could be sufficient if the underlying mechanism was not a long series of individual cell-to-cell signaling events along the entire LPM, but as a smaller number of "block steps" between broad fields of cells. While our data strongly support the idea that Xnr1 autoregulation is a required part of the anteriorward-shifting process, there may be an additional and faster tissue communication process, acting synergistically with Xnr1 autoactivation, which contributes to the rapid field-propagation.

Following the P-to-A expression shift, *Xnr1* expression is progressively downregulated in the same direction. The inactivation wave may be directly connected with the induced expression of *Xlefty*, which mimics *Xnr1* with a spatiotemporal delay, as expected for a direct target of Xnr signaling. The model arising is that Xlefty inhibits the *Xnr1* autoregulatory loop and shuts off *Xnr1* expression, thereby ensuring transient Nodal signaling. While delayed expression of *Lefty2* with respect to *Nodal* was noted during gastrulation stages in the mouse embryo (Juan and Hamada, 2001), more precise

comparative studies will be needed to determine if this relationship holds true during early somitogenesis stages.

CHAPTER IV

ORTHOGONAL INDUCTION OF MIDLINE *XLEFTY* AND CONTRALATERAL COMMUNICATION IN *XENOPUS*

Introduction

In the previous chapter, I discussed my findings on the mechanisms underlying the initiation and propagation of *Xnr1* expression within the L LPM during late neurula/early tailbud stages in *Xenopus*. Briefly, I found that the initiation of L-sided *Xnr1* expression relies on inductive signaling from posterior tailbud tissues. My explant data, in combination with the additional finding that low levels of R-sided *Xnr1* expression can also be detected in *Xenopus* embryos, is consistent with the SELI model's proposal that the R side initially attempts to mount a *Nodal/Xnr1* response, which is suppressed by Lefty/Xlefty inhibition from the midline in normal embryos. I also demonstrated that Xnr1-to-Xnr1 autoinduction is required for the unidirectional, dynamic progression of *Xnr1* expression within the L LPM. In support of this idea, I showed that *Xnr1*-expressing grafts could induce robust *Xnr1* expression in the R LPM of host embryos, which recapitulated the rapid anteriorward shifting of L-sided expression observed in normal embryos. Moreover, a significant finding, which prompted us to perform the next set of experiments that I will present in this chapter, was that the mid-trunk placement of R-sided *Xnr1* grafts caused a strong reduction in the level and/or anterior extent of endogenous L-sided *Xnr1* expression. These results suggested that there was a long-distance contralateral effect on the endogenous L-sided gene expression program of these graft-recipients. In the following chapter, I provide evidence that this L-to-R contralateral communication is dependent on the midline and allows for pan-embryonic integration of asymmetric patterning information.

Embryological manipulations in *Xenopus* and mutant analyses in zebrafish and mouse have indicated that midline integrity is crucial for the development of proper L-R asymmetry (Danos and Yost, 1995; Danos and Yost, 1996; Izraeli et al., 1999; Lohr et al., 1997; Melloy et al., 1998; Rebagliati et al., 1998; Sampath et al., 1998). For example, extirpation of midline tissues that include the notochord from *Xenopus* embryos results in randomization of the direction of cardiac looping and gut coiling, as well as bilateral expression of *Xnr1* in the LPM (Danos and Yost, 1996; Lohr et al., 1997). Furthermore, zebrafish and mouse mutants defective in notochord development (*no tail* and *floating head* in zebrafish and *No turning* and *SIL* in mouse) also exhibit randomized heart looping and express *nodal* genes symmetrically (Danos and Yost, 1996; Rebagliati et al., 1998; Sampath et al., 1998; Melloy et al., 1998; Izraeli et al., 1999). Analysis of mice deficient for *Lefty1*, a Nodal antagonist, indicated that L-sided *Lefty1* expression in the prospective neural tube floor plate contributes to a midline barrier function that is proposed to prevent the wrong-sided diffusion of L-specifying signals (Meno et al., 1998). Observations of conjoined twins in human, frog, and chicken have led to the additional speculation that the midline may produce a R side-directed repressive signal that inhibits L-sided gene expression in the adjacent lateral regions of the twin, since asymmetry defects are only observed in the right-sided individual (Hyatt et al., 1996; Levin et al., 1997; Levin et al., 1996; Nascone and Mercola, 1997). While the midline seems to play a key role in the early establishment of asymmetry, it is uncertain if, and how, the midline plays a longstanding function in ensuring that L-R asymmetry is maintained in an integrated way across the entire embryo. I address this function during the phase of transient expression of the *situs*-instructive Nodal signal.

The mechanism underlying the establishment of midline barrier function during L-R patterning has also remained largely unknown. Recent studies in mice showed that exogenously introduced Nodal induced endogenous *Nodal* expression in the LPM of early somitogenesis-stage embryos and subsequently caused the induction of *Lefty1*

expression in the midline. These results led to the proposal that in the mouse embryo Nodal travels from the LPM to the midline to induce midline barrier function (Yamamoto et al., 2003).

In *Xenopus*, midline *Xlefty* expression occurs during two sequential phases of development. *Xlefty* expression is detected during gastrulation stages in the prospective dorsal midline tissues. This expression is maintained through early neurulation but becomes downregulated around the time of neural tube closure. Beginning at around stage 21, strong midline *Xlefty* expression, in a somewhat discontinuous pattern, is then re-established in the neural floorplate and hypochord (and transiently in notochord), in a P-to-A direction (Branford et al., 2000; Cheng et al., 2000). At these stages, *Xnr1* is being expressed in L LPM. After completion of the mesendoderm inductive process, Organizer-derived Xnr signaling may be responsible for maintaining *Xlefty* expression in the prospective midline cells. This early-phase midline expression may contribute midline barrier function during the period when asymmetric LPM gene expression is first being activated, as has been proposed by others (Danos and Yost, 1996; Lohr et al., 1997; Meno et al., 1998). In this chapter, I show data strongly supporting the idea that orthogonal Xnr1 signaling from the LPM is responsible for the second-phase induction of midline *Xlefty* during late neurula/tailbud stages, in agreement with the published data in mouse mentioned above (Yamamoto et al., 2003).

The SELI model proposed by Nakamura *et al.* (2006) suggests that once asymmetric threshold-dependent initiation of *Nodal* occurs in the L LPM (as described in Chapter III), that contralateral Lefty-mediated inhibition from both the L LPM and the midline (induced by L LPM Nodal) functions to continuously suppress R-sided activation of *Nodal*, thereby maintaining L-R compartmentalization within the embryo during the asymmetry-setting process. My findings that I will present in this chapter, which were gathered concurrently but independently, strongly support a SELI mechanism in *Xenopus*, demonstrating further conservation in the L-R developmental program. Herein,

I show evidence for tailbud-stage contralateral communication between the L and R LPM, via the orthogonal induction of midline *Xlefty* by Xnr1 generated from the LPM, and discuss how this process may ensure that asymmetric morphogenesis occurs as a coordinated process between both sides of the embryo.

The conservation of a SELI mechanism for L-R specification in mouse and *Xenopus* raises important questions that I will address in the Discussion section of this chapter. For example, especially in reference to the large *Xenopus* embryo, how does Xnr1 move a relatively far distance to induce *Xlefty* in the midline and subsequently, how is Xlefty able to spread from the L LPM and/or midline to the opposite side to elicit an inhibitory effect on R-sided *Xnr1*? I will discuss how these questions set the stage for future experiments to address the cell biological and/or biochemical mechanisms for long range movement of Xnr1 and Xlefty ligands during tailbud stage embryogenesis.

Results

Xnr1 activates L-sided gene expression program in R LPM and inverts situs

I previously demonstrated that the mid-trunk placement of R-sided *Xnr1* grafts caused a strong reduction in the intensity and/or anterior extent of L-sided *Xnr1* expression, suggesting that a long-distance contralateral effect was registered on the endogenous L-sided gene expression program of the engrafted embryos. In order to investigate the mechanism underlying this contralateral effect, I analyzed the downstream consequences of the R-side *Xnr1*-engraftment both at the gene expression as well as anatomical level.

The graft-induced *Xnr1* activated a robust L-side gene expression program in the R LPM as judged by the induced expression of *Xlefty* and *XPitx2* at stage 25 and 28, respectively (Fig. 4.1A,B). As observed for *Xnr1*, R-side LPM *Xlefty* expression in engrafted embryos extended more anteriorly than the endogenous L LPM expression, although I noted that suppression of the level of L-sided *Xlefty* expression was not observed (Fig. 4.1A; Table 4.2). βgal controls showed the anterior-ventral localization of *Xlefty* expression within L LPM that is normally observed at stage 25 (Fig. 4.1A).

In the *Xnr1*-engrafted embryos, a strikingly high level of *Xlefty* expression was detected in the midline perpendicularly closest to the graft, most notably enhanced in the notochord in cleared whole-mounts (Fig. 4.1A; Table 4.2). This effect was not observed in βgal controls, in which midline expression was restricted primarily to the neural tube floorplate and hypochord, and was very comparable to the pattern and level seen in unmanipulated sibling stage embryos (Fig. 4.1A; Table 4.2). These results strongly suggest that the mid-trunk region R-sided LPM *Xnr1* expression signals orthogonally, and over a long range, to induce midline *Xlefty* expression. The result is also consistent with my findings in posteriorly cropped embryos. First, midline *Xlefty* expression was

Fig. 4.1 R-sided Xnr1 activates L-side gene expression program, midline *Xlefty* expression and inverts situs. (A) While stage 25 βgal control-engrafted embryos (red-gal stained) showed no *Xlefty* expression, robust R-sided LPM expression (red arrowhead) was induced by *Xnr1* grafts. Similar to *Xnr1*, R-sided *Xlefty* expression extended farther anterior than endogenous L-side expression. Strong induction of midline *Xlefty* expression orthogonal to the *Xnr1*-expressing grafts was detected (black arrowhead). (B) *XPitx2* expression was induced in R LPM of stage 28 *Xnr1*-engrafted host embryos (red arrowhead), not by β-gal controls. (C) All embryos receiving βgal alone R-side grafts had normal cardiac and gut situs (stage 43-45: top panels, indirect immunofluorescence, MF20 antibody; middle panels, brightfield ventral views; bottom panels, lateral views, same embryos). All *Xnr1*-engrafted embryos showed concordant reversal of heart and gut looping, otherwise appearing normal (bottom panels). Careful gut uncoiling showed an overall reversed chirality, but with some disruption of architecture, although it did not resemble an inverted earlier-stage gut. Because grafts healed well, and control βgal engrafted embryos had normal gut coiling, this defect is likely not associated with the surgery *per se*, but because R-sided expression of *Xnr1*, and potentially its downstream targets, was prolonged compared to endogenous L-sided expression. Yellow arrowheads, outflow tract; inset, diagram of heart looping; line drawings, gut tube coiling after partial unwinding. RO, right origin; LO, left origin; CCW, counter-clockwise; CW, clockwise. L, left; R, right; A, anterior; P, posterior.

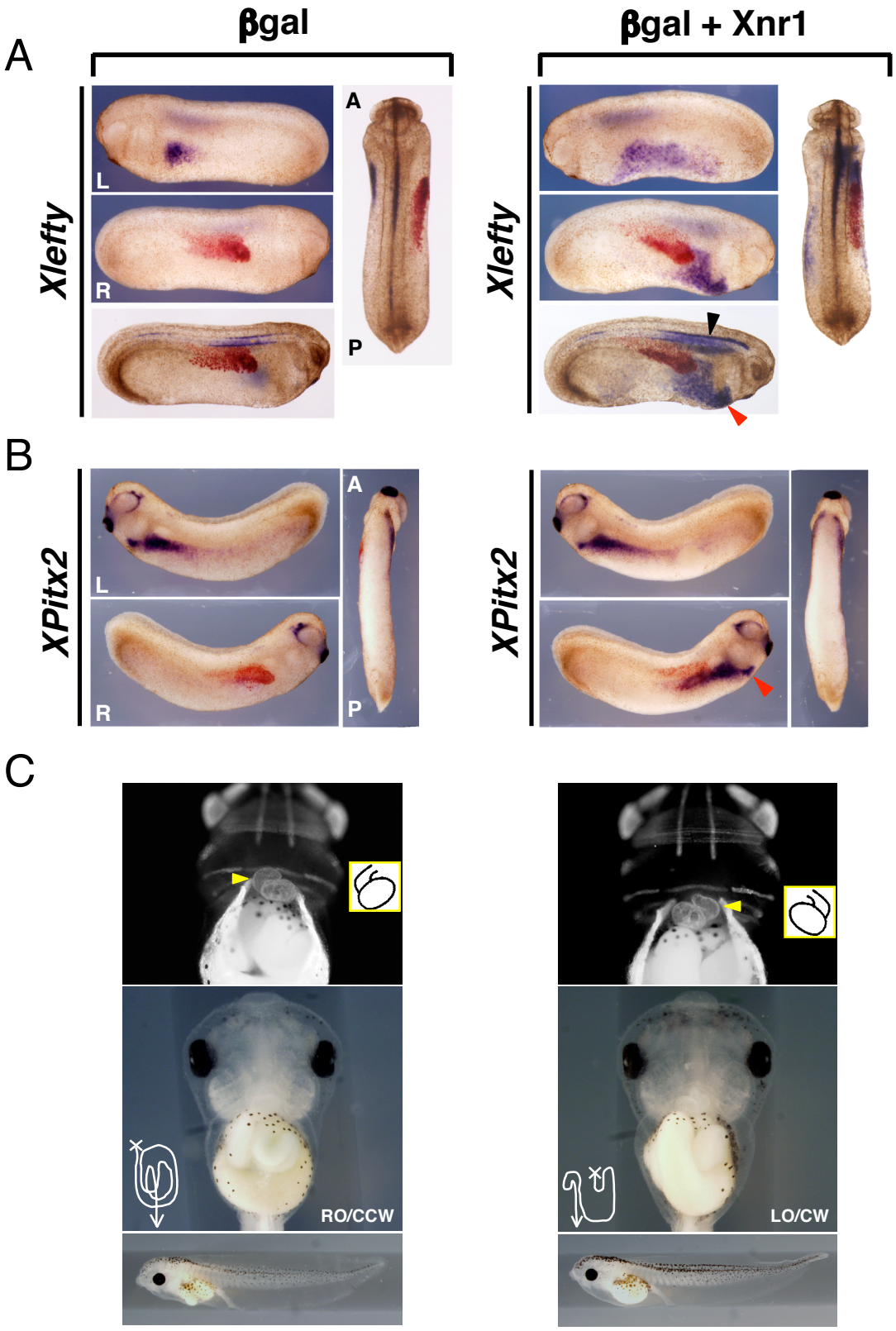
A
βgal
βgal + Xnr1
Xlefty
Xlefty
L
R
A
P
B
XPitx2
XPitx2
L
R
A
P
C
RO/CCW
LO/CW

absent in posteriorly cropped embryos that lack L LPM *Xnr1* expression. Moreover, engraftment of *Xnr1*-expressing LPM into posteriorly cropped embryos induced robust and anteriorly shifting *Xnr1* and *Xlefty* expression, but also restored an extremely high level of axial *Xlefty* expression (Fig. 4.2).

Additionally, whereas βgal-engrafted control embryos all showed the L-sided dorsal anterior endoderm expression that is normally detected between stages 22-25 (Cheng et al., 2000), R-sided *Xnr1*-expressing grafts inverted this expression domain to the R anterior dorsal endoderm (Fig. 4.1A; Table 4.2).

XPitx2 was expressed at relatively equal intensities on both the L and R sides of *Xnr1*-engrafted embryos, although a substantial proportion showed induced R-sided *XPitx2* expression that had progressed more anteriorly than on the left, as noted for *Xnr1* and *Xlefty* (Fig. 4.1B; Table 4.2). Again, we infer that *XPitx2* expression, induced in the R LPM by the robust and anteriorward-shifting *Xnr1* expression, because of the mid-trunk graft placement, had a head-start in progressing anteriorly compared to the endogenous L LPM expression. In contrast, however, to the anterior truncation observed for L-sided *Xnr1* and *Xlefty* expression in mid-trunk R side *Xnr1*-engrafted embryos, there was only an incremental difference in the anterior limits of the L versus R side *XPitx2* expression domains.

Figure 4.1C shows that while embryos receiving control grafts exhibited normal cardiac and gut situs, there was a concordant reversal of heart and gut asymmetry in all pCSKA-*Xnr1*/LPM engrafted embryos (Table 4.1). This result is consistent with the idea that the induced R LPM *Xnr1* expression, which is stronger, reaches more anteriorly, and is longer lasting than the endogenous L-sided expression, converts the R side to a dominant "L-sided specification state", in accordance with the idea that Xnr1 is a true L-side instructive signal.

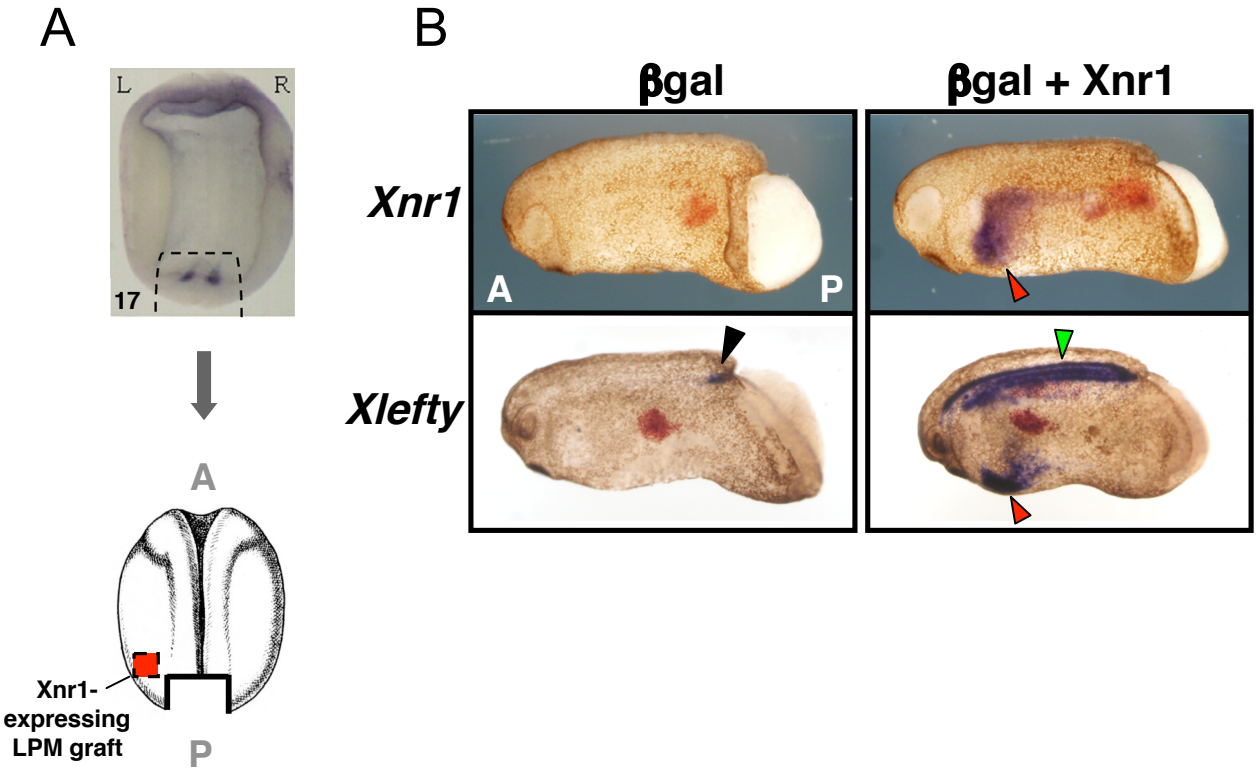

Fig. 4.2 *Xnr1*-expressing grafts restore LPM *Xnr1*, *Xlefty* expression and midline *Xlefty* in posterior cropped embryos. (A) Posterior tailbud tissues encompassing the posterior bilateral *Xnr1* expression area were removed at stage 17. *Xnr1+βgal*-expressing L LPM was then grafted to L side of posterior cropped embryos, which were analyzed for *Xnr1* and *Xlefty* expression at stage 24/25. (B) *Xnr1* and *Xlefty* expression was absent in LPM of βgal control-engrafted embryos that also lacked axial *Xlefty* expression, except for occasional small fleck of expression observed in posterior midline tissues, most likely due to incomplete posterior tailbud cropping (black arrowhead). Robust L-sided *Xnr1* and *Xlefty* expression was observed in *Xnr1*-engrafted hosts (red arrowheads), as well as restoration of midline *Xlefty* (green arrowhead). *Xlefty* expressing embryos were cleared. A, anterior; P, posterior.

Xnr1-mediated L-R switching depends upon the *Xnr1*-expressing graft location

The dominant L-R inversion caused by R-sided *Xnr1* grafts depended upon their A-P location. Our working hypothesis was that the mid-trunk placement caused orthogonal midline induction of high levels of Xlefty, which by long-range leftward movement preconditioned the L LPM and interfered with the autoregulation-based anteriorward propagation of L-sided *Xnr1* expression (Fig. 4.6). Our prediction was that more posterior engraftment would limit the "head-start" situation and allow the L-sided *Xnr1* expression to escape contralateral blocking, and to undergo a more normal anteriorward shift. In this situation, a competitive "double-left" situation might develop with respect both to *Xnr1* expression and L-R morphogenesis. Figure 4.3 shows that more posterior grafts indeed led to mirror-image L- and R-sided *Xnr1*, *Xlefty*, and *XPitx2* expression (Table 4.2). Randomization of heart and gut looping was observed in these embryos (50% normal: 50% reversed across the group, but concordant within each embryo; Fig. 4.4, Table 4.1). We conclude that a competitive double-left situation leads to a stochastic choice of one side or the other as the dominant left.

Extirpation experiments showed that the axial midline was required for the contralateral suppressive effect on L-sided *Xnr1* expression by the mid-trunk R-sided grafts (Fig. 4.5). *Xnr1*-expressing grafts were placed in the mid-trunk R LPM at stage 17 and the embryos developed until stage 19/20, when approximately half of each group underwent localized midline extirpation (Fig. 4.5A). *Xnr1* expression was then compared later (stage 24/25), when its expression has shifted relatively far forward (Fig. 3.1), between extirpated and non-extirpated Xnr1/βgal or βgal-alone-engrafted embryos, and to unmanipulated siblings. The posterior limit of the removed midline region was set approximately to the posterior graft margin. The anterior limit was just anterior of the graft's anterior margin, to take into account the forward dislocation of the graft LPM relative to the ectoderm (*e.g.,* Fig. 3.4B). Embryos with midline integrity reproduced the

Fig. 4.3 Posterior placement of R-side *Xnr1* grafts causes mirror-image expression of L-side genes. (A) Plasmids were targeted to the LPM as in Fig. 3.4. Compare posterior placement shown to medial location in Fig. 3.5 (engrafted embryo shortly after healing, red-gal stained). (B) βgal control-engrafted embryos (red-gal stained) showed endogenous L-sided expression of *Xnr1*, *Xlefty*, and *XPitx2* in LPM, and no R-sided expression. Host embryos carrying posterior R-side *Xnr1* grafts developed mirror-image *Xnr1*, *Xlefty*, and *XPitx2* expression with equivalent anterior limits in L and R LPM (pink arrowheads). Same embryos shown have been cleared in bottom panels and dorsal views of *Xlefty* expressing embryos to show axial expression. Black arrowheads, endogenous *Xlefty* expression in anterior regions of the neural floorplate and hypochord with weak expression in the notochord, as normally observed at stage 25. Embryo stages indicated. L, left; R, right; D, dorsal; V, ventral; A, anterior; P, posterior.

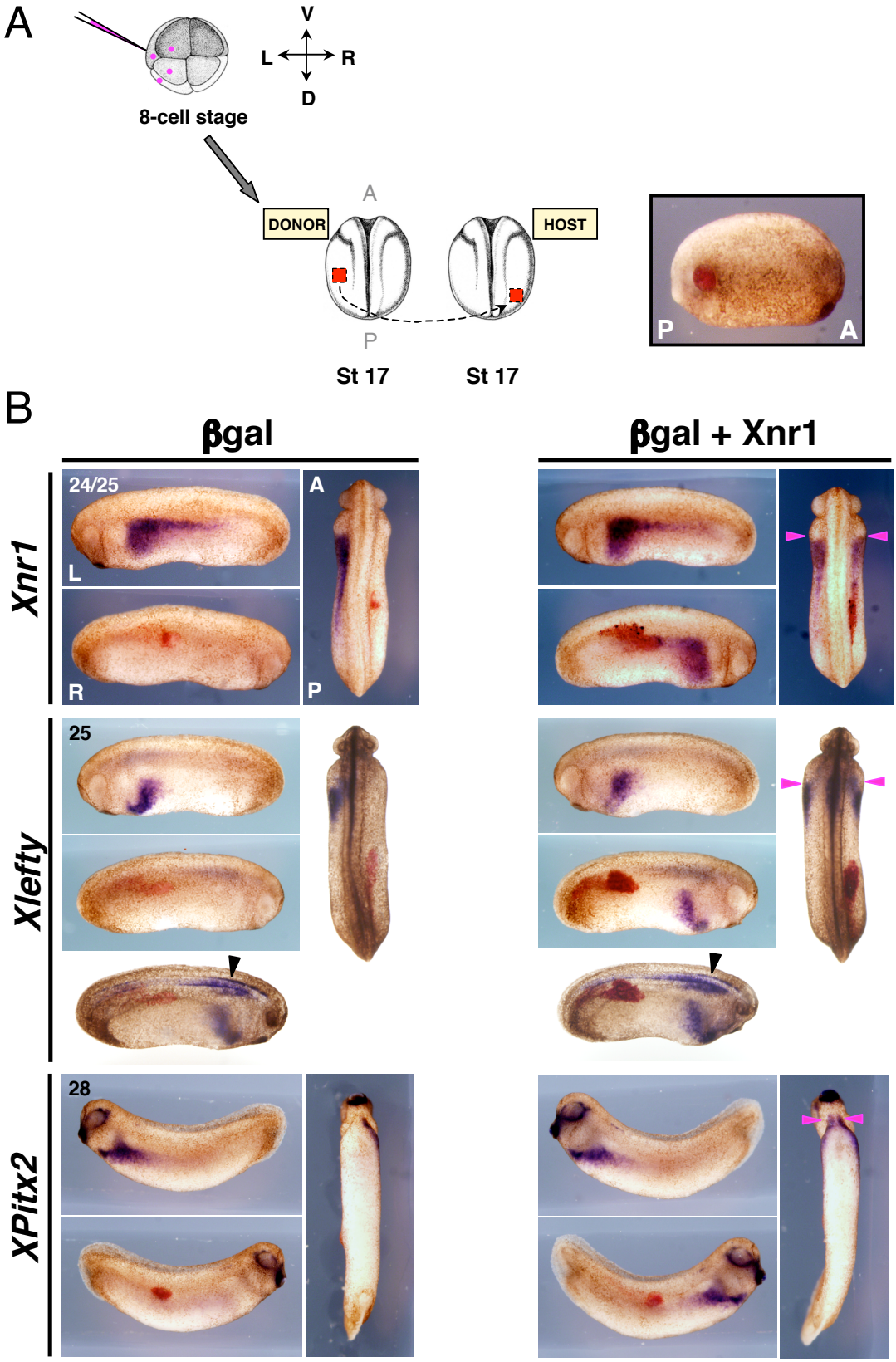
A
V
L
R
D
8-cell stage
A
DONOR
HOST
P
St 17
St 17
P
A
B
βgal
βgal + Xnr1
Xnr1
Xlefty
XPitx2
24/25
L
R
A
P
25
28

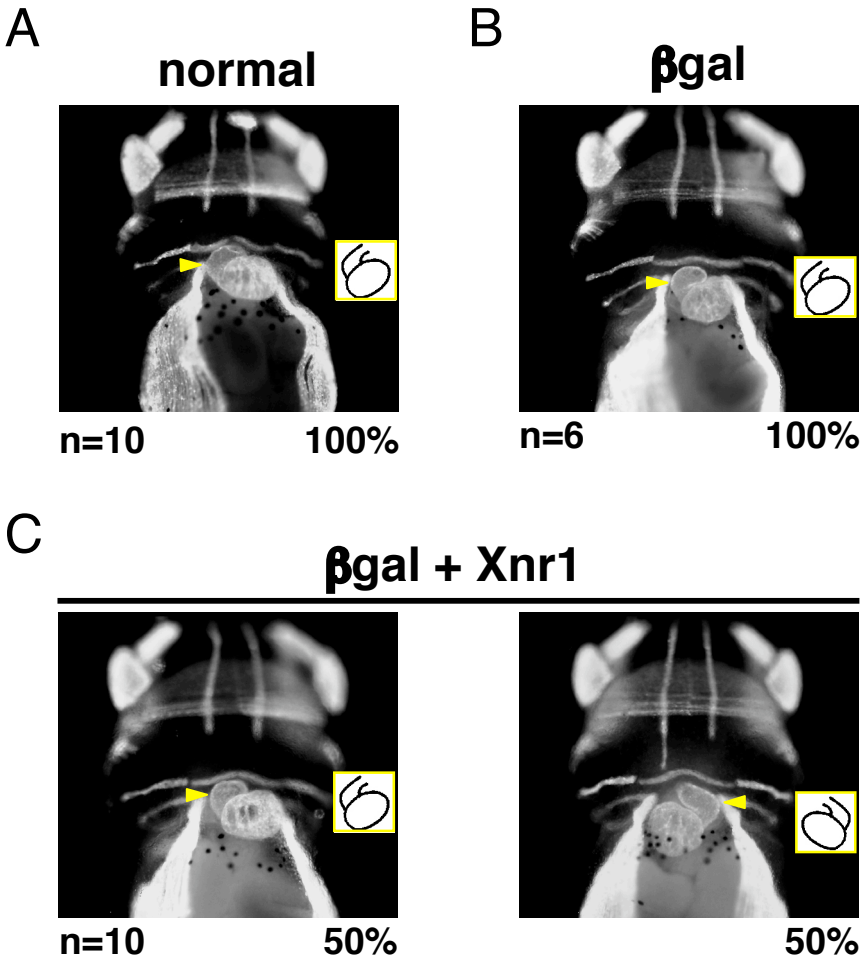

Fig. 4.4 Loss of *Xnr1*-engrafted R-to-L dominance with posterior engraftment. (A) All unmanipulated sibling embryos and (B) βgal-alone-engrafted embryos had normal heart and gut looping. (C) Posterior R-sided *Xnr1* grafts caused randomization of heart and gut situs across the population, but situs concordance within each embryo was noted (stage 43-45 embryos analyzed, MF20 immuno-fluorescence shown; gut analysis not shown; yellow arrowheads, cardiac outflow tract; insets, schematic representation of heart looping).

Table 4.1. Morphological consequences of R side *Xnr1*-engraftment

Donor graft	Graft position	*n* embryos (# of expts.)	*n* (%) Heart/ gut normal	*n* (%) Heart/ gut reversed*	Figure
LacZ alone	mid-trunk	6 (1)	6 (100)	-	Fig. 4.1
pXnr1/LacZ	mid-trunk	8 (1)	-	8 (100)	Fig. 4.1
LacZ alone	posterior	6 (1)	6 (100)	-	Fig. 4.4
pXnr1/LacZ	posterior	10 (1)	5 (50)	5 (50)	Fig. 4.4

Embryos engrafted at stage 17 in either a mid-trunk or posterior position of the R LPM were scored at stage 43-45 for heart and visceral orientation.

*In cases where situs was inverted, both heart and gut situs were concordantly reversed (*i.e.*, in one embryo both heart and gut were reversed).

contralateral block on the anterior shift of L-sided *Xnr1* expression (as in Fig. 3.5). In contrast, midline removal prevented communication between the L and R sides; extirpated embryos showed bilateral *Xnr1* expression of equivalent intensity and anterior progression (Fig. 4.5B; Table 4.2). Extirpations from R-side βgal control-engrafted embryos did not affect L-sided *Xnr1* expression compared to non-extirpated βgal control or unmanipulated embryos (this latter result agrees with findings that extirpating midline tissues after neural plate closure (stages 20-28) does not significantly alter cardiac situs (Danos and Yost, 1996). The result with *Xlefty* and *XPitx2* was similar: anteriorward shifting was blocked on the L side without midline extirpation (except not as noticeably for *XPitx2*, as mentioned previously), but became bilaterally equivalent with extirpation (Fig. 4.5B; Table 4.2). The finding that the ability of the R-sided graft to suppress the forward propagation of *Xnr1* expression within the L LPM is prevented by the local removal of a strip of midline tissue orthogonally closest to the *Xnr1*-expressing graft supports the idea that the relevant event is the induced high level of midline *Xlefty* expression (Fig. 4.6).

Fig. 4.5 Midline extirpation blocks the spatial advantage of mid-trunk grafts in dominantly converting R to L. (A) Stage 17 *Xnr1+βgal*-expressing L LPM was mid-trunk grafted to the R LPM as in Fig. 3. At stage 19, midline orthogonal to the graft was removed (*i.e.,* neural floorplate, notochord, and hypochord; A-P limits indicated by blue hatched bar). Right-hand panel, diagrammatic representation of tissue removed (neural tube, dark blue; notochord, red; paraxial mesoderm, purple; intermediate mesoderm, green; LPM, pink; endoderm, yellow; ectoderm, light blue). Top right panel in (B), transverse section (eosin stained) at plane indicated (white lines) demonstrating extirpation of midline tissues. (B) βgal control-engrafted embryos showed normal L-specific gene expression. Midline extirpated embryos with mid-trunk placed R-side *Xnr1*-expressing grafts developed equivalent anterior limits of expression of *Xnr1*, *Xlefty*, and *XPitx2* in both L and R LPM (pink arrowheads). Same embryos shown have been cleared in bottom panels and dorsal views of *Xlefty* expressing embryos to show axial expression. Black arrowheads, relatively broad *Xlefty* expression in dorsal endoderm that is anterior of extirpated region. Green arrows, midline area removed. *Note increased curvature of stage 28 embryos related to midline extirpation (compare to Fig. 4.3).* Stages indicated in top left of panels. L, left; R, right; A, anterior; P, posterior.

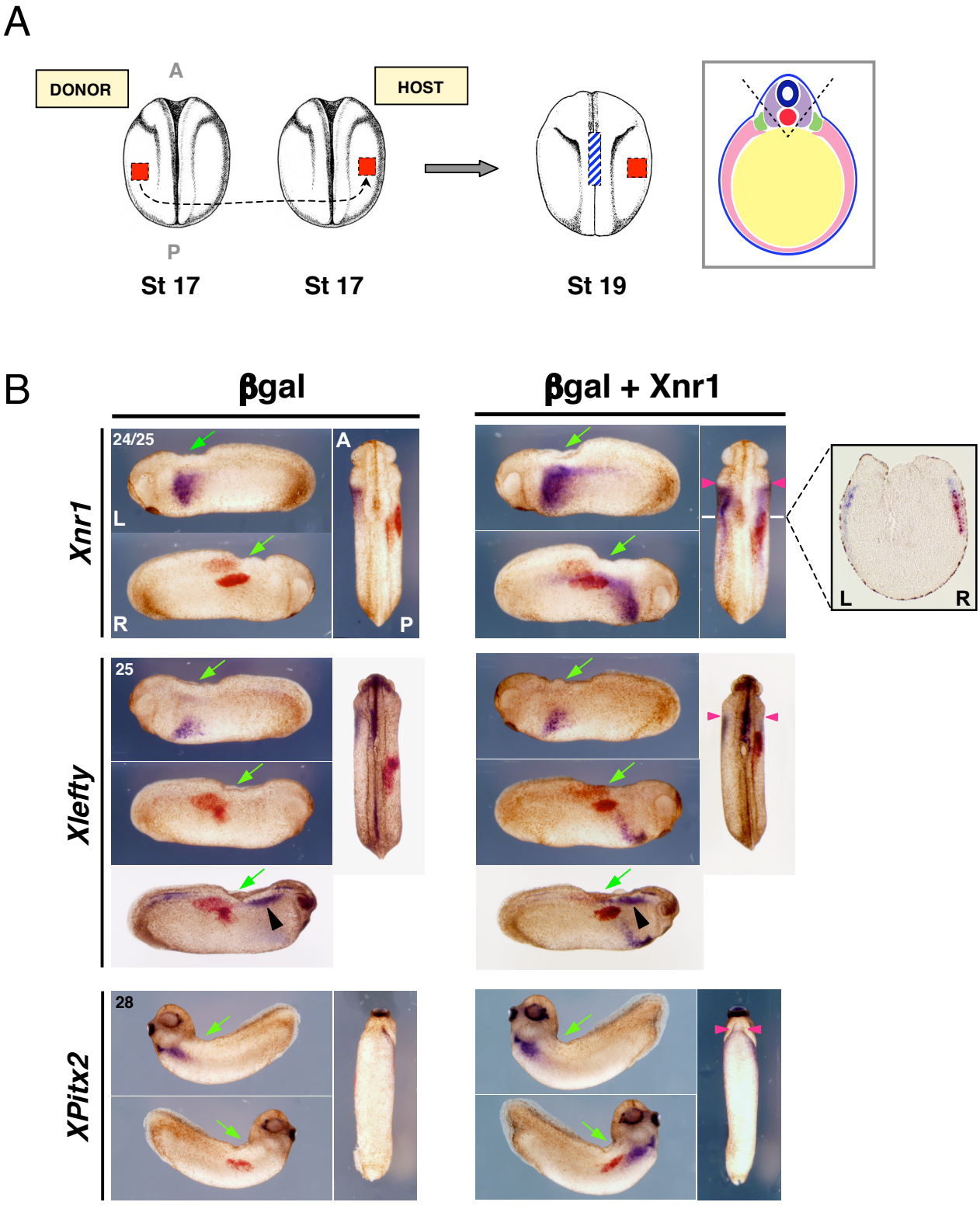
A
DONOR
A
P
HOST
St 17
St 17
St 19
B
βgal
βgal + Xnr1
Xnr1
24/25
L
R
A
P
L
R
Xlefty
25
XPitx2
28

Table 4.2. Gene expression data, R side *Xnr1*-engrafted embryos

A) Mid-trunk placement

Stage	Gene	*n* embryos (# expts. pooled)	*n* (%) L-sided	*n* (%) R-sided	*n* (%) bilateral	% Anterior truncation (% truncated plus suppressed)	Figure
St. 23	Xnr1	12 (2)	2 (17)	-	10 (83)	-	Fig. 3.5
St. 24/25	Xnr1	21 (3)	-	-	21 (100)	90 (47)	Fig. 3.5
St. 26	Xnr1	9 (1)	-	9 (100)*	-	-	Fig. 3.5
St. 24/25	Xlefty	16 (3)	2 (12)	-	14 (88)†	100 (0)	Fig. 4.1
St. 28	XPitx2	13 (2)	2 (15)	1 (8)	10 (77)	60 (0)	Fig. 4.1

R-side βgal-engrafted controls showed normal L-side expression and anteriorward progression of *Xnr1* (at St.24/25), *Xlefty* and *XPitx2*, respectively: n=14/14; n=12/12; n=9/9.

*All R-side mid-trunk *Xnr1*-engrafted embryos at stage 26 showed perdurant *Xnr1* expression in R LPM whereas endogenous L-sided expression had disappeared.

†Ectopic midline and R side dorsal endoderm expression was also observed in 100% of engrafted embryos showing bilateral *Xlefty* expression (see text).

B) Posterior placement

Stage	Gene	*n* embryos (# expts. pooled)	*n* (%) L-sided	*n* (%) R-sided	*n* (%) bilateral*	Figure
St. 24/25	Xnr1	10 (1)	2 (20)	-	8 (80)	Fig. 4.3
St. 24/25	Xlefty	11 (2)	1 (9)	2 (18)	8 (73)	Fig. 4.3
St. 28	XPitx2	5 (1)	-	-	5 (100)	Fig. 4.3

*Posterior placement of R side *Xnr1*-graft resulted in mirror image L & R expression. Of embryos with bilateral expression, no suppression of anterior progression or intensity of L-sided expression was observed compared to the graft-induced R side expression.

C) Mid-trunk placement plus midline extirpation

Stage	Gene	*n* embryos (# expts. pooled)	*n* (%) L-sided	*n* (%) R-sided	*n* (%) bilateral*	Figure
St. 24/25	Xnr1	6 (1)	-	-	6 (100)	Fig. 4.5
St. 24/25	Xlefty	13 (2)	-	1 (8)	12 (92)	Fig. 4.5
St. 28	XPitx2	6 (1)	-	-	6 (100)	Fig. 4.5

*Removal of midline tissues in mid-trunk R side *Xnr1*-engrafted embryos led to mirror image L & R expression.

Discussion

In addition to the role that the midline plays in preventing the inappropriate initial activation of R-sided *Nodal/Xnr1* expression in the LPM, my results support the idea that, in normal embryos, Xlefty, induced orthogonally by L LPM-derived Xnr1, diffuses from the midline into the R LPM and helps to maintain suppression of ectopic expression of "L-specifying" genes. My findings described in this chapter are again consistent with those in mouse recently reported by Nakamura *et al*. (2006), and strongly support a conserved SELI mechanism for L-R asymmetry specification in *Xenopus*. Such a process is particularly important in suppressing the R-sided activation of genes whose expression is subject to self-amplification, such as *Xnr1* (Fig. 4.6). As mentioned briefly in the introduction of this chapter, these findings of contralateral communication between the L and R sides, by way of the midline, as a way of maintaining L-R compartmentalization raise important issues with regard to how Nodal/Xnr1 and Lefty/Xlefty ligands can move such far distances within the embryo. This is of particular relevance, especially when considering the relatively large size of the *Xenopus* embryo. At the end of this section, I will discuss factors that may contribute to and/or facilitate the long range movement of Xnr1 and Xlefty through the LPM and/or across the embryo during tailbud stages.

Xnr1 functions as a true L-side determinant

I showed that *Xnr1*-expressing LPM grafts could induce the full L-side gene expression cassette in the R LPM of host embryos. My results disagree with those of Toyoizumi *et al*. (2005), who use hypodermic injection to deliver bacterially expressed and refolded mouse Nodal to the R LPM of neurula/tailbud stage *Xenopus* embryos. Toyoizumi *et al*. detected the induced expression of *Xnr1* and *XPitx2*, but not of *Xlefty*, a surprising finding as Xlefty is a direct downstream target of Xnr1 signaling (Cheng et al., 2000; Tanegashima et al., 2000). Toyoizumi *et al*. (2005) also concluded that mouse Nodal could not activate the autoregulatory *Xnr1* expression loop in the R LPM. While

their hypodermic delivery method allows easier control over the time of ligand presentation than our plasmid expression/grafting methods, my method may be advantageous in misexpressing Xnr1 itself from its normal source tissue, thereby presumably presenting this intercellular signal in a state much closer to that encountered in normal embryos.

My results further confirm the view that unilateral *Xnr1* expression is the asymmetry-instructive event that the preceding L-R biases converge towards. I have found conditions in which altering the relative level of *Xnr1* expression, or the timing of its production from LPM to the organ primordia, can dominantly invert L-R anatomy. These findings led to our current hypothesis that it is the level of Xnr1 and/or integrated time of receipt of this signal that determines how "leftness" information is imparted to and registered by the LPM. Mogi and Toyoizumi (2000, 2003) showed a rapid decline at stages 26-28 in the ability of Activin or TGFβ5 to reverse embryonic situs. Their observations support the model that it is the transient *Xnr1* wave in the LPM that is the main determinant of asymmetry, because at this stage the asymmetric *Xnr1* expression wave would be becoming extinguished, and asymmetric expression of downstream effectors, such as *XPitx2*, would be beginning in the organ primordia to drive the chiral morphogenetic program. The inability of inducers placed on the R-side to invert situs at even later stages might reflect the closing of a window of competence for LPM responsiveness. But, it is also possible, even if older R LPM maintains its competence to activate *Xnr1* expression, that the earlier passage of a L-sided *Xnr1* expression wave would have already initiated the asymmetric morphogenetic program, and that this would maintain a temporal advantage over any effects induced in the R LPM.

Fig. 4.6 Model for asymmetric Nodal/Xnr1 signaling during L-R specification. The transfer and propagation of L-R asymmetry is divided conceptually into three steps (arrows, direction of signal transfer. (1) Stage 17/18 normal embryos (top row), *Xnr1* is first expressed symmetrically flanking posterior notochord (purple crescents). (2) At stage 19/20 an asymmetric inducing factor (X) initiates *Xnr1* expression in posterior L LPM. (3) Between stages 21 and 25 a rolling wave autoactivation loop expands *Xnr1* expression anteriorward. Orthogonal Xnr1 signaling from L LPM induces *Xlefty* expression in the midline (light blue bar) and rightward transfer of Xlefty prevents inappropriate activation of an Xnr1 autoregulatory loop in R LPM (SOM, somitic mesoderm; IM, intermediate mesoderm; LPM, lateral plate mesoderm). Middle row: effect of R-side mid-trunk *Xnr1* grafts. Xnr1 induced in the R LPM causes orthogonal induction of robust ectopic midline *Xlefty* expression (turquoise bar); Xlefty travels contralaterally and suppresses the anterior shifting *Xnr1* expression on the L. Accordingly, the R side becomes the dominant L side, and causes a concordant reversal of anatomical *situs*. Bottom row: with posterior *Xnr1* grafts, orthogonal *Xlefty* induction does not precondition L LPM against the continued expansion of endogenous L-sided *Xnr1* expression. The lack of a spatial advantage of R over the L (i.e., no "head-start") leads to a competitive double-left situation; across the population, either side adopts "dominant L" status, causing randomization of situs that is concordant within each embryo.

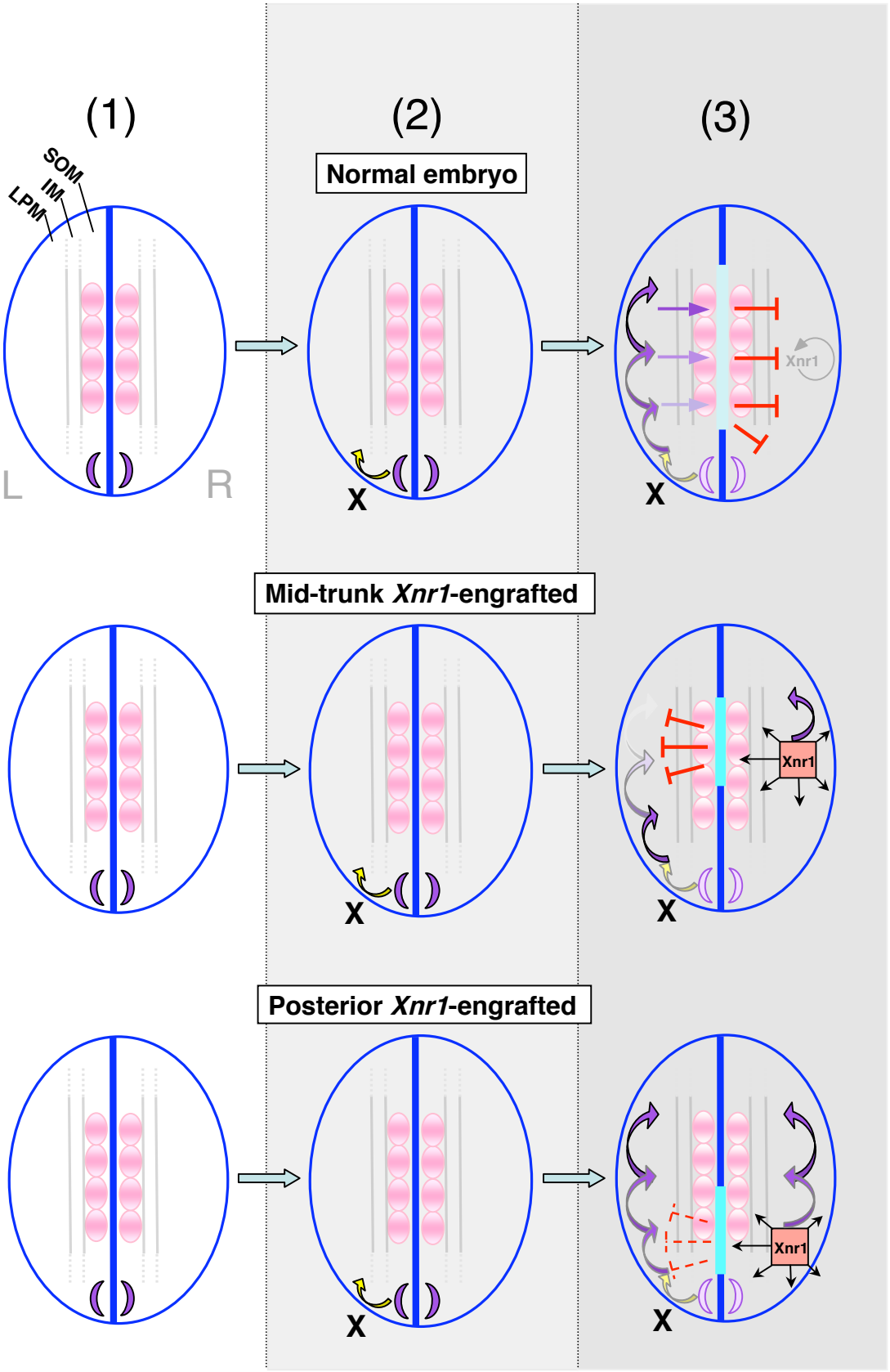
(1)
(2)
(3)
SOM
IM
LPM
Normal embryo
L
R
X
Xnr1
Mid-trunk *Xnr1*-engrafted
Posterior *Xnr1*-engrafted

Orthogonal induction of midline *Xlefty* and contralateral communication in *Xenopus*

Yamamoto *et al*. (2003) demonstrated in mouse embryos that Nodal produced in the LPM could induce midline *Lefty1* expression. Using similar experimental approaches, I have recapitulated these results for the first time in another species, showing conservation in the mechanism that induces midline barrier function. First, embryos without L LPM expression of *Xnr1* lack midline *Xlefty* expression, which is restored by placing *Xnr1*-expressing grafts into the LPM. Second, R side *Xnr1*-engrafted embryos displayed a strong orthogonal induction of *Xlefty* expression in the axial midline, most noticeably in notochord that, although in general proximity to the graft, was relatively extensive along the A-P axis. For unknown reasons, the Nodal/Xnr1 loss- and gain-of-function manipulations of Toyoizumi *et al*. (2005) did not affect the midline expression of *Xlefty*, and we do not know how to explain this discrepancy by differences in our technical and/or experimental approach.

The abnormally high midline expression of *Xlefty* induced by grafts placed in a mid-trunk location, which is proposed by contralateral suppression to give the R-side-induced *Xnr1* expression a significant head-start compared to the endogenous L-side, was associated with a dominant and concordant reversal of cardiac and gut situs (Fig. 4.1C). To our knowledge, this is the most dramatic demonstration of the induction of downstream gene expression, contralateral gene expression responses, and anatomical consequences, of long-range orthogonal Nodal signaling, which was shown by extirpation experiments to require the axial midline.

The observation that the R-sided Xnr1 grafts caused either an anterior truncation of L-sided *Xnr1* and *Xlefty* expression, or caused *Xnr1* expression to be both anteriorly truncated and substantially suppressed, could be related to variability in the precise A-P location of the R-side graft, or how rapidly and efficiently the Xnr1 signal was registered by the host tissue. Both variables may be hard to control with the current experimental

technique. On the other hand, the expression of *XPitx2* showed only an incremental anterior truncation in embryos carrying R-sided Xnr1 grafts. Analyzing stages in addition to those shown here could reveal that *XPitx2* expression does shift forward faster on the R side than on the L. In addition, I have not determined if the L-sided *Xnr1* expression, even when reduced and/or delayed compared to the R side, can still shift anteriorly to induce the anterior domain of L-sided *XPitx2* expression. Another possibility is that the forward diffusion of Xnr1 along the L LPM from a completely stalled L-sided expression wave could induce the anterior *XPitx2* expression.

There is substantial evidence that the L-R symmetry of the *Xenopus* embryo begins to be broken long before gastrulation and this L-R bias eventually becomes converted into the qualitatively different L and R gene expression programs seen during tailbud stages (Bunney et al., 2003; Levin and Mercola, 1998; Levin and Mercola, 1999; Levin et al., 2002; Hyatt et al., 1996; Hyatt and Yost, 1998; Kramer et al., 2002; Kramer and Yost, 2002). The facility with which the normally L-sided expression of *Xnr1* can be activated within R LPM, by my manipulations or those performed by other groups, means that there must be a mechanism(s) that ensure L-R compartmentalization. The importance of maintaining suppression of R-sided activation of the L-sided program during tailbud stages is shown by the fact that the R-sided activation of an *Xnr1* expression wave has a highly significant effect on L-R asymmetry (Fig. 4.1C).

With respect to this issue, previous extirpation studies in *Xenopus* suggested that the midline functions as a regulator of laterality only up until neurula/early tailbud stages. Extirpations were done between stages 15-28, but no effect was noted after stage 20, a time just around the onset of asymmetric gene expression in the LPM (Danos and Yost, 1996; Lohr et al., 1997). I now provide evidence the midline may serve a compartmentalization function during the tailbud-stage period of asymmetric gene expression (stages 20-25), with diffusion of Xlefty from the midline conditioning R LPM against the activation of *Xnr1* expression (Fig. 4.6). My findings are directly in-line with

the SELI model recently proposed from studies in the mouse embryo (Nakamura et al., 2006; Tabin, 2006).

Future hurdles will be to understand how Xnr1, and any other asymmetrically produced factors, generate inducer gradients that change with time, and how the level of intracellular effectors (*e.g.,* Pitx2) established from these activity gradients work to regulate asymmetric morphogenesis. In addition to the active conditioning of the R LPM against initiating the expression of L-sided genes, the long-range regulation of the level of Nodal signaling by Xlefty distributed within the tissues is an integral determinant of the activity gradient. Further challenges will be to understand how such activity gradients in some cases are linked to the emergence of chiral anatomy from tissue sheets or tubes, but in others cause the asymmetric regression of specific tissues, such as is seen for the cardiovascular system primordia.

Movement of Xnr1 and Xlefty during tailbud embryogenesis

My findings in *Xenopus*, as well as the studies in mouse (Nakamura et al., 2006), strongly support a conserved contralateral communication mechanism between the L and R sides of the embryo as a way of ensuring L-R compartmentalization during asymmetry specification. However, the distances that are involved in this type of system for Nodal/Xnr1 to, for example, travel from the LPM to the midline to induce *Lefty/Xlefty* expression and for Lefty/Xlefty to then spread to the contralateral side to suppress *Nodal/Xnr1* expression in R LPM, raise significant issues with regard to how these ligands can move within and/or across the embryo during tailbud/somitogenesis stages. These issues are arguably more relevant in the huge *Xenopus* embryo, as compared to the smaller mouse embryo. Very little is currently known about the movement characteristics of Nodal/Xnr and Lefty/Xlefty proteins, such as how fast and how far they can travel and which routes are taken within the embryo. Although some evidence exists from studies in chicken and mouse that suggests that mouse Nodal and Lefty proteins can

travel quite far from a local source of production, and in keeping with the proposal that Nodal and Lefty comprise a reaction-diffusion system, Lefty has been shown to diffuse faster and farther than Nodal (Sakuma et al., 2002; Nakamura et al., 2006).

As I will describe in Chapter VI in more detail, we plan to investigate the cell biological and/or biochemical mechanisms that could potentially facilitate the movement of Xnr1 and Xlefty proteins during tailbud stage embryogenesis and directly examine how fast and how far these ligands can travel within the LPM. In this section, I will only focus my discussion on the former of these aims and cover the latter in the next chapter (Chapter VI – Summary and Future Perspectives). There are currently no concerted studies being performed in any species on the tissue structure of the LPM around the time of asymmetric gene expression. It is not known, for example, when the LPM becomes epithelialized with distinct apical, basal and lateral compartments. Studies in zebrafish have shown that the LPM is epithelial just before the initiation of gut looping (Horne-Badovinac et al., 2003), although it is unclear when the epithelialization event occurs and how this timing correlates with the asymmetric expression of the *Nodal*-related genes *cyclops* (*cyc*) and *southpaw* (*spaw*) in the L LPM. We hypothesize that the architecture of the LPM before, during and after the L-sided *Xnr1* expression wave may influence how Xnr1 and Xlefty are able to move within this tissue layer. It is possible that inter-tissue space develops either between the two layers of the LPM, the splanchnopleure and the somatopleure, and/or between the LPM and other germ layers that would allow Xnr1 and Xlefty proteins to diffuse more freely. If the LPM is epithelialized during tailbud stages, the presence of gap junctions may also facilitate the rapid transfer of Xnr1/Xlefty ligands between cells. Although our model as well as the SELI model proposed in mouse currently suggest that Nodal/Xnr1 travels along the arc of the LPM to reach the midline to induce *Lefty*/*Xlefty*, that in turn spreads to the contralateral side to suppress Nodal/Xnr1, it is possible that these proteins also travel perpendicularly across the embryo (*e.g.,* from L LPM to endoderm, through the intervening archenteron to the

opposite side). We will investigate alternative routes of movement within and/or across the embryo that would enable these factors to travel over larger distances over shorter time intervals.

Studies from our laboratory have shown that during early blastula/gastrula stages, Xlefty is cleaved from a proprotein into a long ($Xlefty^{L}$) and short ($Xlefty^{S}$) isoform. Although it has been found that during these early stages, only $Xlefty^{L}$ accumulates to detectable levels within the embryo and is the only form that seems capable of blocking Xnr signaling, it is possible that during later tailbud stages, $Xlefty^{S}$ also plays an important role in regulating Xnr1 signaling. We may find that the two forms of Xlefty both play a role during L-R specification stages and that one may be able to travel faster and farther than the other, which could lend further insight into the reaction-diffusion relationship between Xnr1 and Xlefty.

CHAPTER V

PHARMACOLOGICAL INVESTIGATION OF AUTOREGULATORY XNR1 SIGNALING IN THE L LPM DURING L-R SPECIFICATION

Introduction

In chapter III, I described my studies on the mechanism(s) underlying the rapid unidirectional shifting of *Xnr1* expression within the L LPM. Briefly, I showed using explants that the forward propagation of asymmetric *Xnr1* expression occurs LPM-autonomously via planar tissue communication. Moreover, LPM grafts expressing Nodal-specific inhibitors, transplanted into a mid-trunk region of the left side of host embryos, suppressed the dynamic anteriorwards shifting of *Xnr1* expression through the LPM, implicating a rolling wave Xnr1-to-Xnr1 inductive mechanism. The combined data presented in chapters III and IV, gathered concurrently but independently with those of Nakamura *et al.* (2006), led to a Self-Enhancement (contra)Lateral Inhibition (SELI) model that is applicable to both *Xenopus* and mice. The model generally proposes that asymmetric threshold-dependent activation of *Xnr1* expression in the LPM is amplified by positive autoregulatory Xnr1 signaling only in the L LPM. *Xlefty*, directly induced by Xnr1 signaling, functions to both suppress R-sided activation of *Xnr1*, as well as to ensure the transient nature of *Xnr1* expression in the L LPM.

With respect to the mechanism(s) underlying the rapid unidirectional shifting of *Xnr1* expression that occurs in the L LPM during tailbud stages, a number of pertinent issues remain. For example, as mentioned previously, it is uncertain whether the time that is required for the biochemical processes involved in signal receipt, intracellular transduction and ligand production within individual adjacent cells can occur fast enough to be accommodated during the period of observed *Xnr1* expression shifting within the L

LPM. While I have shown evidence strongly supporting the idea that Xnr1 autoinductive signaling is required for the anteriorwards *Xnr1* shift, we cannot rule out the possibility that an additional faster tissue communication process that involves, for example, gap junctional communication, and/or additional signaling pathways (utilizing perhaps smaller ligands that can traverse between cells more easily), acts synergistically with Xnr1 autoactivation to contribute to rapid field-propagation. In this chapter, I describe my preliminary experiments in which I have used a pharmacological approach to inhibit Xnr1 signal transduction specifically at the level of the receptor at different time-points during the *Xnr1* expression wave to further investigate the role that Xnr1 autoregulation plays in maintaining and propagating its own expression within the L LPM.

In comparison to the Xnr1 inhibitor grafting experiments that were described in Chapter III, using a drug-based approach to inhibit Xnr1 signaling provided several advantages. The ease of drug application allowed for much finer temporal control over the timing of inhibitor exposure and therefore allowed examination of the effects of blocking Xnr1 signaling at different time-points throughout development. In contrast, transplantation of the Xnr1 inhibitor-expressing grafts to the left flank of host embryos had to be performed at stage 17 due to such constraints as the time required to perform the actual grafting, as well as embryo healing time. As I will describe in this chapter, novel insight into *Xnr1* and *Xlefty* transcript stability was gained by the ability to block Xnr1 signaling at different intervals during the L LPM *Xnr1* expression wave. This information would have been difficult, if not impossible, to acquire using the grafting approach because of the inability to vary the time of inhibitor production and/or release from the grafts.

Another advantage of using a pharmacological-based approach to investigate asymmetric autoregulatory Xnr1 signaling is the ability to use various concentrations of the drug to alter the level of inhibition. For example, we can use both optimal (defined as the concentration required to completely abolish expression) as well as suboptimal

concentrations of the inhibitor. This will become important in the future (as described in the Discussion of this chapter) as we hope to address the potential interactions of other known signaling pathways (*e.g.,* FGF, Shh, BMP, gap junction communication) that may act synergistically with Xnr1 signaling in promoting or antagonizing the maintenance and anteriorwards shifting of *Xnr1* expression in the L LPM. The general idea would be to expose embryos to suboptimal concentrations of both Xnr1-specific inhibitors, in combination with other signaling pathway inhibitors of tissue communication and analyzing the effects on the maintenance and posterior-to-anterior progression of *Xnr1* expression. The prediction would be that if another pathway, say gap junction communication, works positively with Xnr1 signaling then further suppression of the levels and/or shifting of expression should be observed in the presence of the inhibitor (in this case for example, heptanol or lindane) compared to the situation with Xnr1-specific inhibitors alone. However, if the pathway in question acts antagonistically to Xnr1 signaling, then we should observe increased levels and shifting of *Xnr1* expression.

Nodal/Xnr1 ligands signal through a type I/type II receptor complex, both of which are serine/threonine kinases. Small molecule inhibitors are commercially available that act as competitive ATP binding site kinase inhibitors, two of which are SB-431542 and SB-505124. Both specifically block TGFβ-related signaling by binding to the Alk-4, -5, and -7 type I receptors without affecting Alk-1, -2, -3 or -6 mediated signaling by BMP/GDF1 (Laping et al., 2002; Inman et al., 2002; DaCosta Byfield et al., 2004). Studies in cell lines and zebrafish embryos have indicated that SB-505124 is three to five times more potent of an inhibitor than SB-431542 (DaCosta Byfield et al., 2004; Scott Dougan, University of Georgia, Athens; personal communication**).** However, when I determined the optimal concentration that was required for each SB-drug to block Xnr1 autoregulatory signaling as completely as possible within the L LPM of *Xenopus* embryos, I found that SB-505124 was only about a two-fold more effective inhibitor

(Fig. 5.1; Table 5.1). The discrepancy in these data most likely reflects varying degrees of drug permeability that may differ between species and/or model systems.

I tested the ability of various concentrations of each of the SB-drugs to inhibit Xnr1 signaling, indicated by the loss of asymmetric *Xnr1* expression in the L LPM. I have chosen to step outside of convention and describe these initial experimental findings in the Introduction section of this chapter, as they served to set the stage for the subsequent experiments. The purpose was to determine a single optimal concentration for both SB-431542 and SB-505124 to completely block Xnr1 autoactivation that would be used for the analyses presented herein the main Results section. The drug titration experiments were performed as follows: embryos at various stages during the period of asymmetric *Xnr1* shifting within the L LPM (*e.g.,* stages 19-23) were cultured in medium containing either DMSO alone or 3 different concentrations of each of the SB-inhibitors until stage 24/25, at which point they were analyzed for *Xnr1* and, in some cases, *XKrox-20* expression (see below). The concentrations tested were 50 μM, 100 μM and 150 μM for SB-431542 and 10 μM, 30 μM and 50 μM for SB-505124. In the case of SB-505124, even at the highest concentration tested (*e.g.,* 50 μM), a significant level of *Xnr1* expression was still observed in the L LPM at the time of analysis (Fig. 5.1; Table 5.1). I, therefore, increased the concentration of SB-505124 used in subsequent experiments to 75 μM, which was able to effectively block Xnr1 signaling (Fig. 5.3, 5.4; Table 5.3). Specifically for SB-431542, I found that a concentration of 150 μM was required for completely abolishing L LPM *Xnr1* expression (Fig. 5.1; Table 5.1).

A potential problem to keep in mind when exposing embryos to chemical inhibitors is that the drugs themselves may cause non-specific, global defects due to general toxicity issues. To ensure that the SB-treated embryos were morphologically normal, they were analyzed for *XKrox-20* expression. *XKrox-20* is expressed in rhombomeres 3 and 5 of the developing hindbrain, as well as in populations of migrating neural crest cells that eventually contribute to the pharyngeal arches (Bradley et al.,

1993). *XKrox-20* expression, therefore, served as a powerful internal marker, as it was an indicator for normal anterior development as well as a marker to measure the anteriorward progression of the *Xnr1* expression domain within the L LPM.

Studies in zebrafish have demonstrated that the inhibitory effect of SB-431542 is reversible and the drug can be removed from embryos, as evidenced by the restoration of downstream target gene activation (Ho et al., 2006; Sun et al., 2006). Furthermore, SB-505124 is more aqueous-soluble and therefore can be more effectively washed out of embryos than SB-431542 (Scott Dougan, University of Georgia, Athens; personal communication). These findings are significant as they demonstrate yet another advantage to a drug-based approach for investigating Xnr1 signaling during L-R patterning. The ability to add or remove the signaling inhibitors from the culture medium at any time will allow us in the future to examine the spatial and temporal requirements for Xnr1 autoregulatory signaling in L LPM.

In this chapter, I will describe my preliminary experiments that examine the role of Xnr1 positive autoregulation in maintaining and propagating the P-to-A *Xnr1* expression wave within the L LPM during *Xenopus* tailbud stages. It is important to note, however, that these studies are still in the beginning stages and it will be important to demonstrate reproducibility. Notwithstanding these considerations, I present further supporting evidence that Xnr1-to-Xnr1 autoinduction is required for both maintaining and propagating asymmetric *Xnr1* expression within the L LPM. Moreover, I present novel findings that show that in the absence of active Xnr1 signaling, *Xnr1* and *Xlefty* transcripts are rapidly downregulated within cells of the L LPM. These data suggest that *Xnr1* and *Xlefty* mRNAs are either inherently unstable and/or actively targeted for degradation. These are interesting findings due to the fact that very little is currently known about the longevity of these molecules at both the transcript and protein levels. As I will discuss at the end of this chapter, it will be important in the future to gain a fundamental understanding of these issues as they are directly pertinent and would

greatly impact the dynamics of a reaction-diffusion system, of which Xnr1 and Xlefty are thought to comprise. I will also later discuss what is known about *TGF-β* transcript stability and speculate as to how this information may be relevant to *Xnr1* and *Xlefty* mRNA longevity.

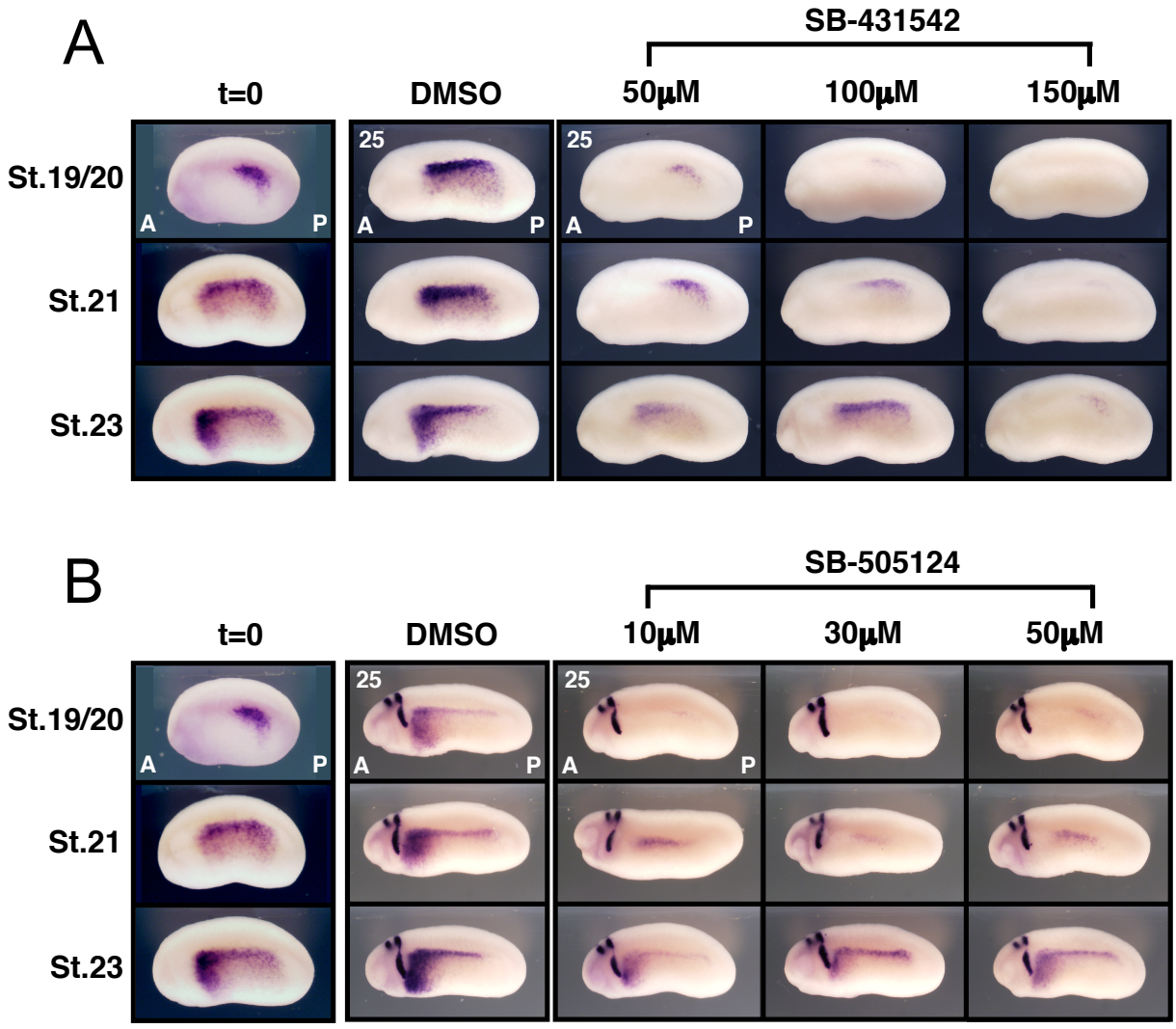

Fig. 5.1 SB-drug titration experiments for determining optimal concentration to block Xnr1 autoregulatory signaling. A,B) Embryos, beginning at the indicated stages (t=0), were cultured in DMSO alone (concentration equivalent to highest SB-concentration) or 3 different concentrations of SB-431542 or SB-505124 until stage 25, when they were analyzed for *Xnr1* expression (and *XKrox-20* expression in the SB-505124 tested subgroup - 2 stripes, hindbrain rhombomeres 3 & 5 and migrating neural crest cells, *see main text*). A, anterior; P, posterior.

Table 5.1. Titration experiments, SB-431542 and SB-505124

A) SB-431542			*n* (%) Robust, forward shifted	*n* (%) Robust, posterior restricted	*n* (%) Weak, forward shifted	*n* (%) Weak, posterior restricted	*n* (%) no signal
Stage (t=0)	Conc. of drug (μM)	*n* embryos (# expts)					
St. 19/20	50	6 (1)	-	1 (17)	-	2 (33)	3 (50)
St. 19/20	100	6 (1)	-	-	-	2 (33)	4 (67)
St. 19/20	150	6 (1)	-	-	-	1 (17)	5 (83)
St. 21	50	6 (1)	2 (33)	1 (17)	-	3 (50)	-
St. 21	100	6 (1)	-	3 (50)	-	3 (50)	-
St. 21	150	6 (1)	-	-	-	2 (33)	4 (67)
St. 23	50	5 (1)	2 (40)	1 (20)	2 (40)	-	-
St. 23	100	6 (1)	3 (50)	-	2 (33)	1 (17)	-
St. 23	150	6 (1)	-	-	-	3 (50)	3 (50)

All DMSO controls showed normal L-side expression and anteriorwards progression of *Xnr1* at St.24/25 regardless of the initial time of drug exposure (comparable number of embryos analyzed for each subgroup).

B) SB-505124			*n* (%) Robust, forward shifted	*n* (%) Robust, posterior restricted	*n* (%) Weak, forward shifted	*n* (%) Weak, posterior restricted	*n* (%) no signal
Stage (t=0)	Conc. of drug (μM)	*n* embryos (# expts)					
St. 19/20	10	6 (1)	-	-	-	2 (33)	4 (67)
St. 19/20	30	6 (1)	-	-	-	2 (33)	4 (67)
St. 19/20	50	6 (1)	-	-	-	1 (17)	5 (83)
St. 21	10	6 (1)	1 (17)	-	1 (17)	-	4 (67)
St. 21	30	7 (1)	-	-	-	3 (43)	4 (57)
St. 21	50	7 (1)	1 (14)	-	-	2 (29)	4 (57)
St. 23	10	5 (1)	2 (40)	-	3 (60)	-	-
St. 23	30	5 (1)	2 (40)	-	3 (60)	-	-
St. 23	50	5 (1)	3 (60)	-	2 (40)	-	-

DMSO controls showed normal *XKrox-20* expression and L-side expression of *Xnr1*, as well as normal anteriorwards progression of *Xnr1* at St.24/25 regardless of the initial time of exposure (comparable number of embryos analyzed for each subgroup).

All SB-treated embryos exhibited normal *XKrox-20* expression at the time of analysis, comparable to control embryos.

Results

Rapid downregulation of *Xnr1* transcripts within L LPM in presence of Alk4 inhibitors

SB-431542 and SB-505124 were used to investigate the role of Xnr1 autoregulation in propagating and maintaining *Xnr1* expression within the L LPM. Although these inhibitors also block other TGFβ-related signaling pathways (*e.g.,* Activin, Derriere and Vg1), in addition to that of Nodal/Xnr1, there is no evidence suggesting that other TGFβ-related ligands are involved in promoting L-R asymmetry specification in normal embryos at this stage of development. We, therefore, infer that any effects on *Xnr1* expression caused by the SB-inhibitors result from a block of Xnr1 signaling.

Embryos were exposed to either DMSO alone (vehicle controls) or SB-431542 at a concentration of 150 μM at various stages during the period of asymmetric *Xnr1* expression within the L LPM, between stages 19 and 23. All embryos were cultured to stage 25 (when *Xnr1* expression has normally shifted far anterior within the L LPM) and then analyzed for *Xnr1* and *XKrox-20* expression. Regardless of the stage at which the embryos were exposed to the signaling inhibitor, *Xnr1* transcripts were rarely detected within L LPM cells by stage 25 (Fig. 5.2; Table 5.2). That is, even embryos exposed to the SB-431542 drug at the latest time-point (stage 23) showed minimal or often no asymmetric *Xnr1* signal at stage 25. When *Xnr1* expression was present in SB-treated embryos, it was at very low levels and restricted to a small mid-trunk region of the L LPM (Fig. 5.2B). Therefore, 2 hours was sufficient for the eventually complete downregulation of *Xnr1* transcripts within the L LPM. *XKrox-20* expression, however, appeared normal in all of the inhibitor-treated embryos (Fig. 5.2; Table 5.2). As expected, DMSO vehicle alone-treated control embryos showed normal *Xnr1* and

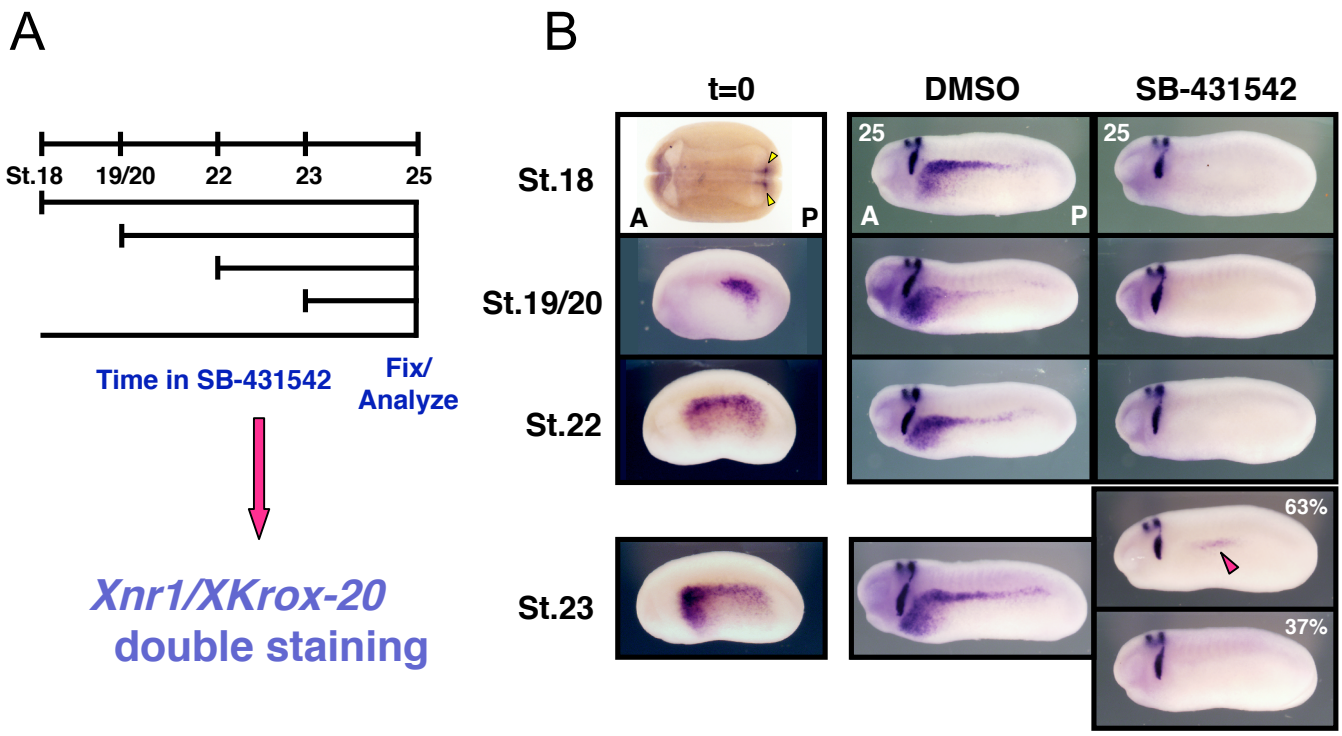

Fig. 5.2 Inhibition of Alk4 signaling causes rapid downregulation of *Xnr1* transcripts. A) Embryos, beginning at the indicated stages, were cultured in DMSO alone or 150μM SB-431542 until stage 25. Embryos were analyzed for both *Xnr1* and *XKrox-20* expression. B) DMSO-controls showed normal anterior progression and levels of *Xnr1* expression at stage 25, whereas *Xnr1* transcripts were rarely detected in SB-treated embryos. Only a subset of embryos exposed to SB-431542 at stage 23 showed weak, mid-trunk restricted *Xnr1* expression (pink arrowhead). *XKrox-20* expression appeared normal. A, anterior; P, posterior.

Table 5.2. *Xnr1* and *Xlefty* transcripts are rapidly downregulated upon exposure to Alk4 receptor inhibitors

Stage (t=0)	Gene	*n* embryos (# expts.)	*n* (%) complete suppression	*n* (%) partial suppression	*n* (%) no suppression
St. 18	Xnr1	7 (1)	7 (100)	-	-
St. 19/20	Xnr1	7 (1)	7 (100)	-	-
St. 22	Xnr1	8 (1)	8 (100)	-	-
St. 23	Xnr1	8 (1)	3 (37)	5 (63)	-
St. 19	Xlefty	6 (1)	6 (100)	-	-
St. 21	Xlefty	6 (1)	6 (100)	-	-
St. 22	Xlefty	6 (1)	6 (100)	-	-
St. 23	Xlefty	8 (1)	5 (63)	3 (37)	-

DMSO controls showed normal *XKrox-20* expression and L-side expression/anteriorwards progression of *Xnr1* and *Xlefty* at St.24/25 regardless of the initial time of drug exposure (comparable numbers were analyzed).

All SB-treated embryos exhibited normal *XKrox-20* expression at the time of analysis, comparable to control embryos.

XKrox-20 expression at the time of analysis, comparable to unmanipulated sibling stage embryos (Fig. 5.2; Table 5.2)**.**

Blocking Alk4 signaling inhibits both maintenance and anteriorward progression of *Xnr1* expression in L LPM

I next wanted to investigate the effect of exposure to the Alk4-specific inhibitors on *Xnr1* transcript levels. Therefore, a time-course analysis was performed in which embryos were exposed to 75 μM SB-505124 beginning at stage 23, when *Xnr1* expression is the most robust and broad within the L LPM, which would allow for a decrease in Xnr1 signal intensity to be the most apparent. Samples were subsequently analyzed every 30 minutes afterwards for a total period of 2.5 hours. Noticeably lower levels of *Xnr1* expression were first observed between 90-120 minutes post-inhibitor exposure as compared to the DMSO-control embryos (Fig. 5.3; Table 5.3a). By two hours, *Xnr1* transcripts were either barely detectable or completely absent from L LPM cells, consistent with our previous results (Fig. 5.2; Table 5.2). From these steady-state analyses, the estimated half-life of *Xnr1* transcripts is approximately 30-60 minutes. In contrast, there was no significant difference in *XKrox-20* expression observed between the SB-treated and DMSO-control embryos, indicating that drug exposure alone did not cause any global embryological defects. These findings indicate that continuous Xnr1 autoactivation is required to maintain asymmetric *Xnr1* expression within the L LPM.

A second time-course analysis was undertaken to examine whether the P-to-A shifting of L-sided *Xnr1* expression within the LPM is regulated by Xnr1-Xnr1 autoregulation. Embryos were therefore exposed to the SB-505124 inhibitor at an earlier time-point during embryogenesis, when *Xnr1* expression is still restricted to a posterior region of the L LPM (*e.g.,* stage 19/20). Embryos were analyzed every 30 minutes after

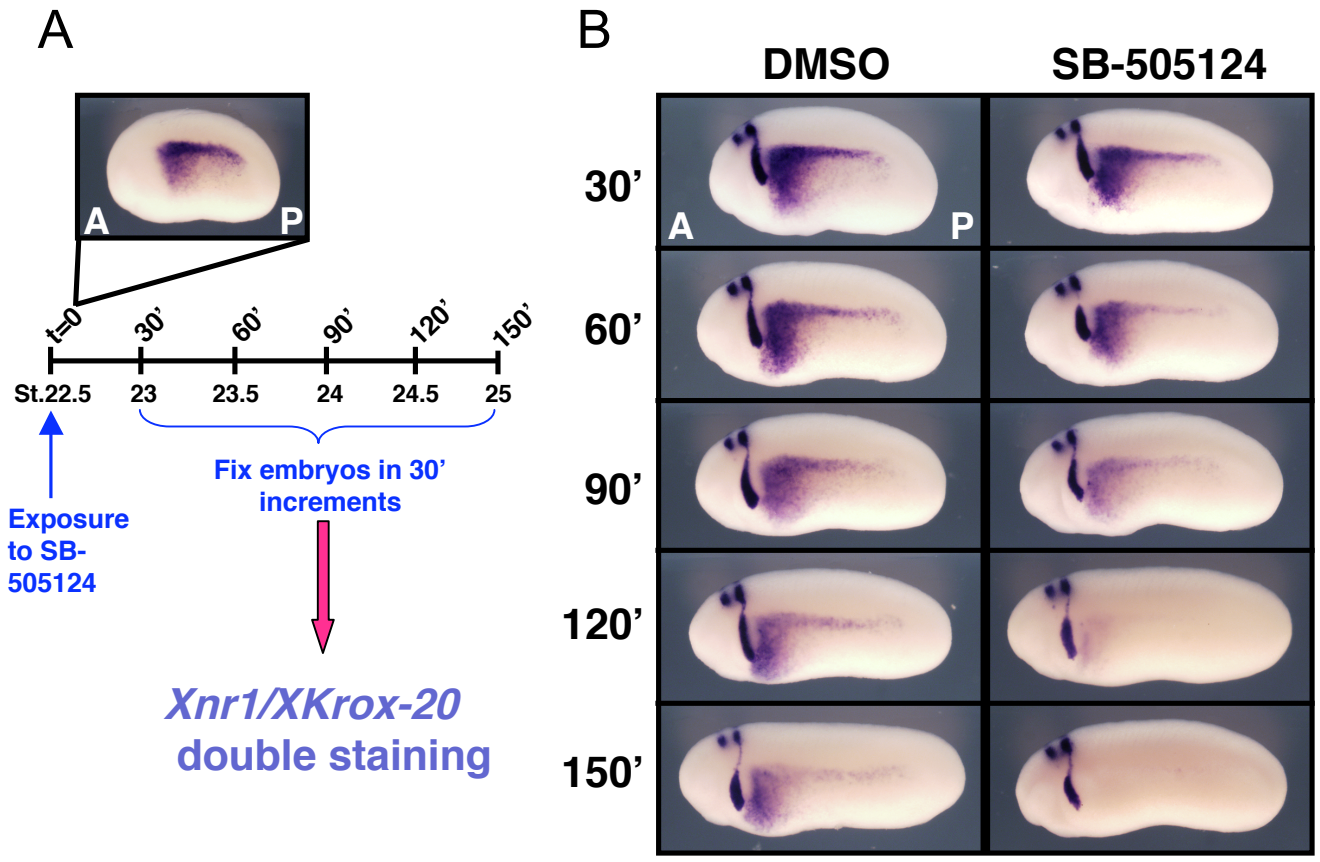

Fig. 5.3 *Xnr1* transcripts are downregulated within 90-120 min. after exposure to SB-inhibitor. A) Embryos were exposed to DMSO alone or 75μM SB-505124 at stage 22.5, when *Xnr1* expression is broad within L LPM (top panel). Groups of embryos were analyzed every 30 min. for 2.5 hrs. for *Xnr1* and *XKrox-20* expression. B) DMSO-controls showed robust *Xnr1/XKrox-20* expression at each timepoint. *Xnr1* transcript levels were noticeably downregulated by 90 min. post-SB-drug exposure and were almost absent by 120 min. At all stages analyzed, *XKrox-20* expression appeared normal in SB-treated group. A, anterior; P, posterior.

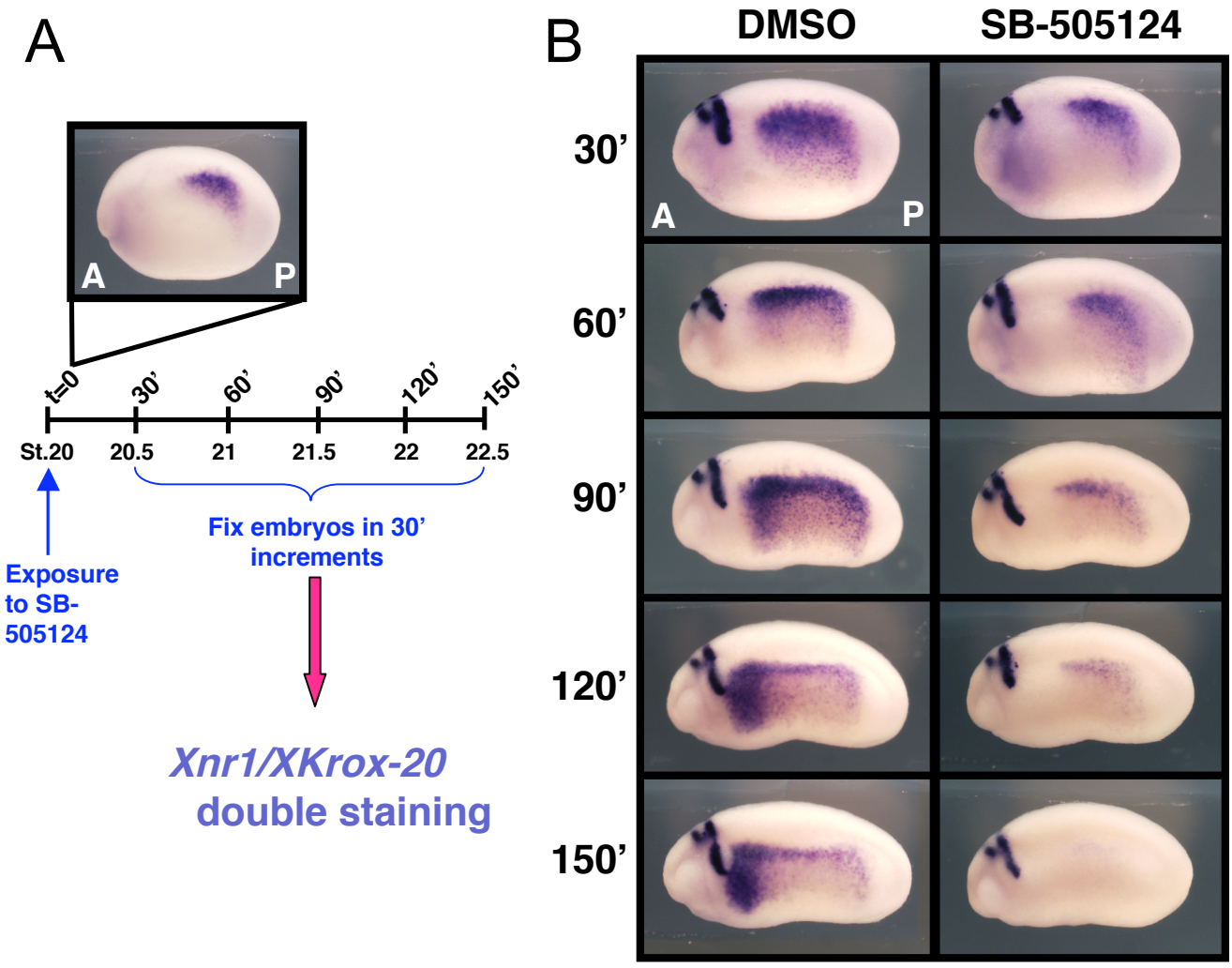

Fig. 5.4 Blocking Alk4 signaling halts anterior progression of *Xnr1* expression wave. A) Embryos were exposed to DMSO alone or 75μM SB-505124 at stage 20, just as *Xnr1* expression initiates within posterior L LPM (top panel). Subsets of embryos were analyzed in 30 min. increments for 2.5 hrs. for *Xnr1* and *XKrox-20* expression. B) DMSO-controls showed robust, anteriorly-shifting *Xnr1* expression, whereas SB-treated embryos showed posteriorly-restricted *Xnr1* expression and rapid loss of transcripts. At all stages analyzed, *XKrox-20* expression was normal in both DMSO- and SB-treated groups. A, anterior; P, posterior.

Table 5.3a. Xnr1 autoregulation is required for the maintenance of *Xnr1* expression within L LPM

Stage (t=0)	Minutes post-exposure	*n* embryos (# expts.)	*n* (%) complete suppression	*n* (%) partial suppression	*n* (%) no suppression
St. 23	30	8 (1)	-	-	8 (100)
St. 23	60	8 (1)	-	-	8 (100)
St. 23	90	8 (1)	-	6 (75)	2 (25)
St. 23	120	8 (1)	4 (50)	4 (50)	-
St. 23	150	9 (1)	9 (100)	-	-

All DMSO controls showed normal *XKrox-20* expression and L-side expression of *Xnr1* at each time-point analyzed, comparable to unmanipulated sibling stage embryos: n=8/8 for each time-point analyzed.

XKrox-20 expression remained unaffected in all SB-treated embryos.

Table 5.3b. Xnr1 autoregulation is required for the anteriorwards propagation of *Xnr1* expression within L LPM

Stage (t=0)	Minutes post-exposure	*n* embryos (# expts.)	*n* (%) Robust, forward shifted	*n* (%) Robust, posterior restricted	*n* (%) Weak, forward shifted	*n* (%) Weak, posterior restricted	*n* (%) no signal
St. 20	30	9 (1)	1 (11)	6 (67)	-	2 (22)	-
St. 20	60	9 (1)	1 (11)	5 (56)	1 (11)	2 (22)	-
St. 20	90	10 (1)	1 (10)	8 (80)	1 (10)	-	-
St. 20	120	10 (1)	-	1 (10)	-	7 (70)	2 (20)
St. 20	150	10 (1)	-	1 (10)	-	2 (20)	7 (70)

All DMSO controls showed normal levels of *XKrox-20* and *Xnr1* expression as well as normal anteriorwards progression of *Xnr1* at each time-point analyzed, comparable to unmanipulated sibling stage embryos: n=8/8 for each time-point analyzed.

XKrox-20 expression was unaffected in all SB-treated embryos.

exposure began for a total of 150 minutes. Consistent with my previous time-course results, *Xnr1* transcripts were almost absent within 90-120 minutes. Moreover, *Xnr1* expression remained restricted to the posterior L LPM at all stages analyzed demonstrating that the anteriorwards progression of the expression domain was suppressed by blocking Xnr1 autoregulation (Fig. 5.4; Table 5.3b). Embryos cultured in DMSO-containing medium alone showed normal P-to-A shifting of *Xnr1* expression, comparable to sibling stage embryos (Fig. 5.4; Table 5.3b). These findings are consistent with my previously described Xnr1-inhibitor grafting experimental results and lend further support to the idea that Xnr1 positive feedback autoactivation is required to both maintain, as well as expand its asymmetric expression within the L LPM during L-R asymmetry patterning.

Rapid downregulation of *Xlefty* transcripts within L LPM in presence of Alk4 inhibitors

As mentioned previously, it is thought that the relationship between Xnr1 and Xlefty resembles a reaction-diffusion system and functions as a built-in, tightly controlled mechanism that acts to limit both the level, as well as spatiotemporal extent of Xnr1 signaling during embryonic patterning. As a complex system, it is conceivable then to think that *Xlefty* may be regulated differently than *Xnr1* at the transcriptional level, such that *Xlefty* mRNA is more stable. An inherent difference in transcript stability may allow for the persistence of Xlefty protein in the L LPM, as compared to Xnr1, and ensure the transient nature of asymmetric *Xnr1* expression during L-R patterning of the embryo by continuous, long-lived suppression of the positive autoregulatory loop.

To test the hypothesis that there may be a difference in transcript stability between *Xnr1* and *Xlefty*, I exposed embryos to 150 μM SB-431542 at various stages during the time of dynamic asymmetric *Xnr1* expression within the LPM. All embryos

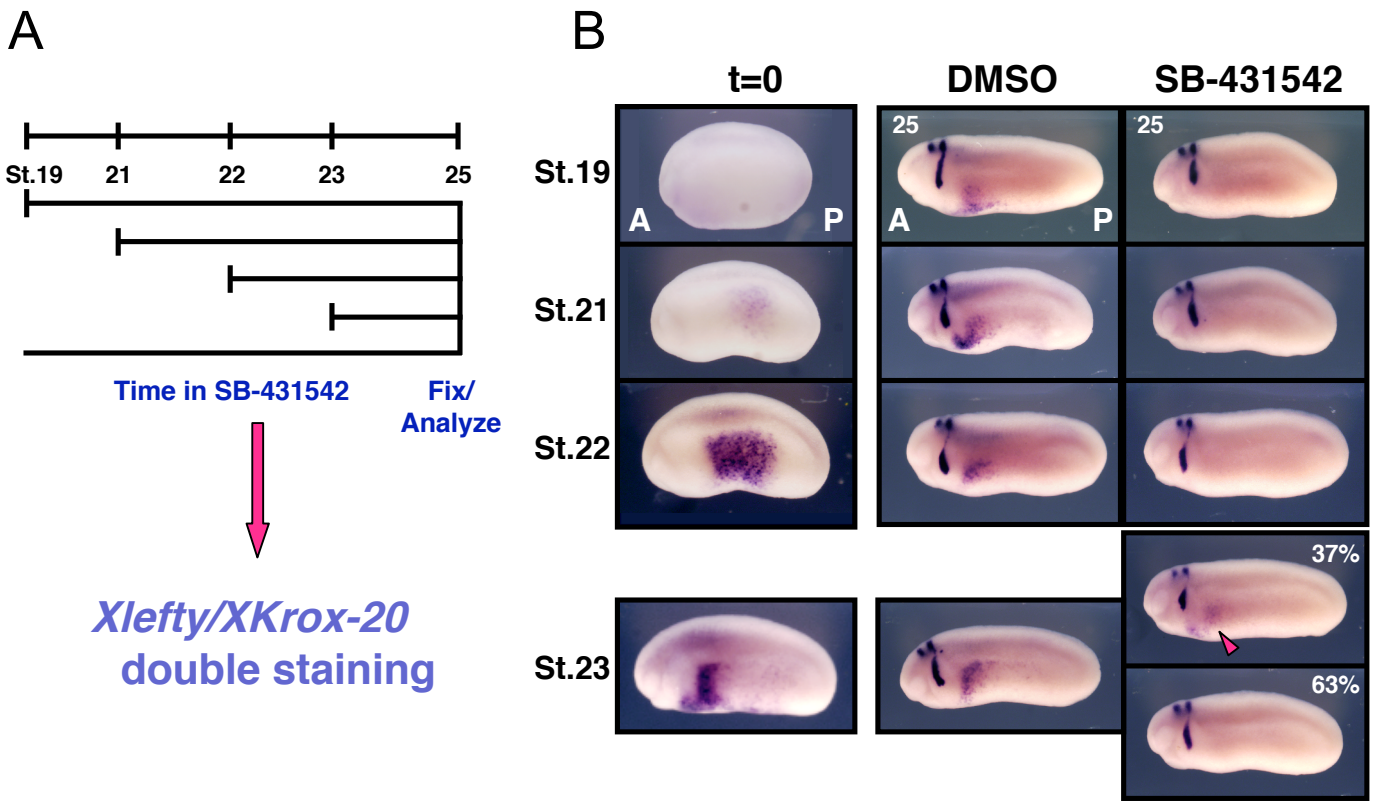

Fig. 5.5 Inhibition of Alk4 signaling causes rapid downregulation of *Xlefty* transcripts. A) Embryos, beginning at the indicated stages, were cultured in DMSO alone or 150μM SB-431542 until stage 25. Embryos were analyzed for *Xlefty*/*XKrox-20* expression. B) DMSO-controls showed normal anterior progression and levels of *Xlefty* expression at stage 25, whereas *Xlefty* transcripts were rarely detected in SB-treated embryos. Only a small percentage of embryos, as indicated, exposed to SB-431542 at the latest timepoint (stage 23) showed weak, *Xlefty* expression (pink arrowhead). *XKrox-20* expression was normal in SB-treated embryos. A, anterior; P, posterior.

were subsequently cultured to stage 25, when they were fixed and analyzed for *Xlefty* and *XKrox-20* expression. Similar to the results for *Xnr1*, *Xlefty* expression was rarely detected in the L LPM by stage 25, regardless of the beginning time-point of exposure (Fig. 5.5; Table 5.2). Only a small population of embryos (n=3/8, 37%) exposed to the inhibitor at the latest time-point (stage 23) showed weak *Xlefty* expression at the time of analysis (Fig. 5.5; Table 5.2). In contrast, *Xlefty* expression appeared robust in DMSO-control embryos and underwent the normal anteriorwards shifting within the L LPM, comparable to unmanipulated sibling stage embryos (Fig. 5.5; Table 5.2). These findings indicate that there is not a significant difference in *Xnr1* and *Xlefty* transcript stability and both mRNAs are rapidly downregulated upon blocking Xnr1 autoregulatory signaling within the L LPM, due to inherent instability and/or active degradation.

Xnr1 expression is not efficiently restored after wash out of Alk4 inhibitors

To address whether the Xnr1 autoregulatory loop can be automatically restarted after *Xnr1* transcripts have been degraded, I transiently exposed embryos to the Alk4-specific inhibitor. The hypothesis under test was whether phospho-Smad2 (P-Smad2, the downstream signal of activated Xnr1 signaling) registration within the nuclei of cells of the L LPM provides a cellular memory of the earlier transient Xnr1 signal (addressed in more detail in the following Discussion section). Embryos were initially cultured for two hours in 75 μM SB-505124 from stage 19/20, when *Xnr1* expression has just initiated in the posterior L LPM, or from stage 21, when *Xnr1* expression has begun to shift anteriorly within the L LPM, followed by washing with normal culture medium. A subset of embryos was analyzed at the 2-hour time-point to allow testing that the inhibitor had effectively abolished *Xnr1* expression. The remainder of embryos that were transferred to fresh medium without the inhibitor was cultured until stage 25 to allow sufficient recovery time. To try to ensure optimal "wash out" of the inhibitor, embryos

were cultured in a relatively large volume with continuous, gentle agitation and the medium was exchanged at least two times during the wash out/recovery period.

As predicted from our previous results, after the 2-hour inhibitor culture period, asymmetric *Xnr1* expression was barely detectable or completely absent in the SB-505124-treated groups, whereas *Xnr1* expression appeared robust in the DMSO-controls (Fig. 5.6; Table 5.4). At stage 25, the majority of SB-treated embryos still lacked *Xnr1* expression in the L LPM (Fig. 5.6; Table 5.4). A small subset of embryos that were initially exposed to the SB-drug at the later stage 21 time-point showed weak *Xnr1* expression, and this was restricted to a small mid-trunk domain of the L LPM (Fig. 5.6; Table 5.4). Preliminarily, these results demonstrate that Xnr1 autoregulatory signaling cannot be automatically reinitiated after *Xnr1* transcript degradation. In future repeat experiments, it will be important to control for the completeness of drug wash out by testing whether *Xnr1*-grafts can reestablish the L-sided *Xnr1* expression wave. The ability to restore asymmetric *Xnr1* expression in the L LPM would also depend upon the longevity of the Xnr1 and Xlefty proteins produced as a result of transient Xnr1 signaling, an issue that will be addressed in the following Discussion section of this chapter.

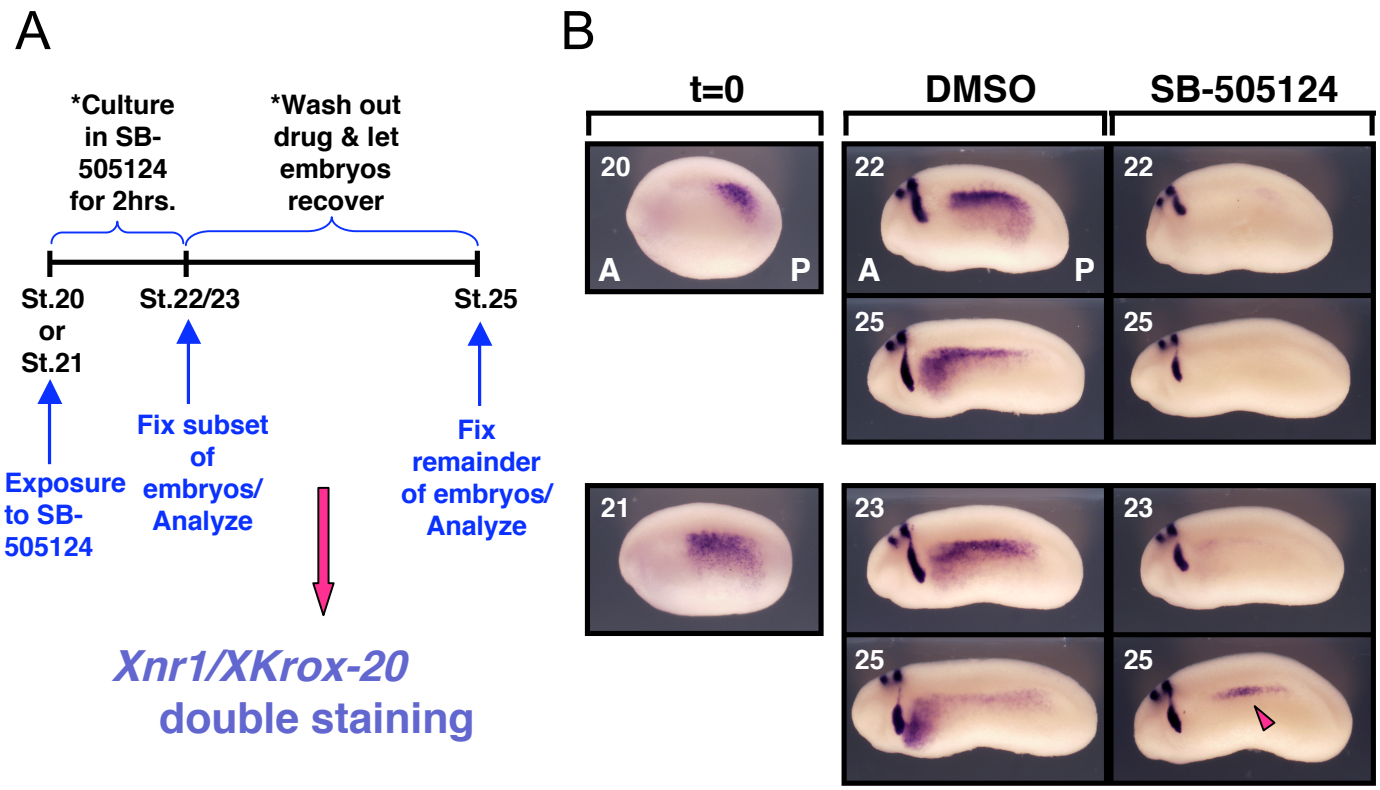

Fig. 5.6 *Xnr1* expression is not efficiently restored after removal of Alk4 inhibitor. A) Embryos, beginning at either stage 20 or 21 were cultured in either DMSO or 75μM SB-505124 for 2 hrs., at which point a subset of embryos were fixed and analyzed for *Xnr1/XKrox-20* expression. Remainder of embryos were transferred to medium lacking inhibitor for rest of culture period until stage 25. Analysis for *Xnr1/XKrox-20* followed. B) Robust *Xnr1* expression was observed in DMSO control embryos. SB-treated embryos showed normal *XKrox-20* expression but lacked *Xnr1.* Only small subset of embryos showed weak, mid-trunk restricted *Xnr1* expression (pink arrowhead). A, anterior; P, posterior.

Table 5.4. *Xnr1* expression within L LPM is not restored after removal of Alk4 receptor-specific inhibitors

Stage (t=0)	Stage of analysis	*n* embryos (# expts. pooled)	*n* (%) complete suppression	*n* (%) partial suppression	*n* (%) no suppression
St. 20	St. 22	16 (2)	10 (63)	6 (38)	-
St. 20	St. 25	16 (2)	16 (100)	-	-
St. 21	St. 23	16 (2)	1 (6)	10 (63)	5 (31)
St. 21	St. 25	17 (2)	12 (71)	5 (29)	-

All DMSO controls showed normal levels of *XKrox-20* and *Xnr1* expression as well as normal anteriorwards progression of *Xnr1* at all stages analyzed: n=8/8 for each subgroup (*e.g.*, analyzed 2 hrs. post-drug exposure and at stage 25).

XKrox-20 expression was unaffected in all SB-treated embryos.

Discussion

Xnr1 and Xlefty are thought to comprise a "reaction-diffusion" system, in which Xnr1 (the activator) controls both its own production, as well as that of its negative feedback inhibitor, Xlefty. Xlefty, in turn, is thought to then travel farther than Xnr1 and act at a long range to limit both the levels and spatial extent of self-amplifying *Xnr1* expression during the processes of mesendoderm induction and L-R axis formation, as recently illustrated by the SELI model (Nakamura et al., 2006). In a reaction-diffusion system, the intimate relationship between the activator and inhibitor establishes a tightly regulated, self-controlled system that is able to achieve precise pattern formation during embryogenesis (for review – see Meinhardt, 2001). However, as an extremely sensitive system that is highly dependent upon the levels and/or activities of the activator versus the inhibitor, even seemingly minute changes in either of these factors can cause a "chain reaction" of events to occur, due to the self-amplifying nature of the activator and the long range inhibitory function of the inhibitor. For example, the SELI model demonstrates that an initial L-R bias that allows for slightly higher levels of *Nodal* to be induced on the L versus the R side enables L-sided only expression because *Nodal* self-amplification is stronger on the left. Due to the principles of a reaction-diffusion system, *Lefty* that is induced in the midline by Nodal is then able to swamp out low levels of *Nodal* on the right side, but is unable to do so on the left because the Nodal autoregulatory loop is stronger than the inhibitory action of Lefty. Asymmetry in *Nodal* expression is then maintained by long range inhibition by Lefty produced in the L LPM and midline that suppresses any *Nodal* self-amplification which could occur on the right side of the embryo.

Due to the inherent sensitivity of Xnr1 and Xlefty as a reaction-diffusion system, it is therefore important to have a fundamental understanding of how these molecules are regulated at both the post-transcriptional, as well as post-translational level, which would directly influence the dynamics of this system. In this chapter, I have presented my

preliminary evidence demonstrating that *Xnr1* and *Xlefty* transcripts are quickly downregulated after blocking Xnr1 autoregulatory signaling, suggesting that continuous reinforcement via Xnr1 signaling is required to maintain *Xnr1* expression within the L LPM during tailbud stages. In the following sections, I will discuss the potential mechanisms and/or factors that may contribute to this rapid clearance, in relation to what is known about *TGF-β* mRNA stability. I will also describe our plans for future experiments that will address the stability of Xnr1 and Xlefty at the protein level. Finally, I will discuss our additional future goals that include investigating how transient asymmetric Xnr1 signaling is translated into long-lasting L-R patterning information upon which asymmetric morphogenetic programs are instructed.

Rapid downregulation of *Xnr1* and *Xlefty* transcripts within L LPM

Exposing embryos to the Alk4 receptor-specific small molecule inhibitors, SB-431542 or SB-505124, caused rapid turnover of *Xnr1* and *Xlefty* transcripts within 90-120 minutes after addition of the inhibitors when compared to transcript levels in the DMSO-vehicle alone controls. Furthermore, *Xnr1* and *Xlefty* expression was rarely detected within the L LPM by 150 minutes. These data suggest that the half-life for both of these mRNAs is approximately 30-60 minutes and fits well with the time required for *Xnr1* and *Xlefty* expression downregulation within posterior L LPM during the anteriorwards shifting in untreated embryos. These findings are also consistent with the observation that mRNAs that encode growth factors, such as FGF or TGF-β, generally have a short half-life of about 30 minutes. In comparison, mRNAs that encode structural proteins, for example β-globin, are quite stable and can have a half-life of 10+ hours. It is thought that the rapid degradation of growth factor mRNAs allows for quick changes in their concentration in response to extracellular signals (Alberts et al., Molecular Biology of the Cell, 3rd edition, 1994). Although my findings are perhaps not surprising in light of what is already known about growth factor mRNA stability, they are nonetheless significant

due to the fact that nothing is known about the transcript or protein stability of Nodal/Xnr1 and Lefty/Xlefty molecules. As I will discuss below, one of our future aims is to investigate the longevity and/or stability of Xnr1 and Xlefty proteins within the LPM during L-R asymmetry specification.

Transcript stability can be altered by the binding of trans-acting factors to cis-elements in the message. The trans-acting factors can act to either protect from or promote cleavage by RNAses. A number of studies have implicated TGF-β in promoting mRNA stability (Dibrov et al., 2006). In many cases, the TGF-β-mediated stabilization of mRNAs is indirect in that TGF-β signaling leads to the downstream activation of genes that encode trans-acting factors that bind to mRNA cis-elements. The *receptor for hyaluronan mediated motility* (*RHAMM*) mRNA is an example of a transcript that is stabilized indirectly by TGF-β signaling. A 30-nucleotide region within the *RHAMM* 3'-UTR was identified as the TGF-β responsive element and this region was shown to interact with cytoplasmic trans-acting factors upon TGF-β stimulation, forming RNA-protein complexes (Dibrov et al., 2006; Amara et al., 1996).

TGF-β1-mediated signaling has also been shown to increase the levels of its own expression in an autoregulatory fashion during the process of wound healing by stabilizing *TGF-β1* transcripts. Studies have demonstrated that cells incubated in the presence of DRB (an inhibitor of new gene transcription) and TGF-β1 resulted in an increase of the half-life of *TGF-β1* mRNA from 45 to 90 minutes compared with untreated cultures (Song et al., 2002). However, the precise mechanism underlying TGF-β autoregulation is still unclear, *i.e.,* whether auto-activation and transcript stabilization are achieved directly or indirectly. It is interesting to speculate then, that *Xnr1* and *Xlefty* transcripts may be stabilized in a similar manner to *TGF-β*, in that active Xnr1 signaling enables the longer perdurance of both of these mRNAs. It may be necessary in the future to address this issue with additional investigation.

Further experiments

Although my preliminary data suggest that *Xnr1* and *Xlefty* transcripts are relatively unstable, it is possible that at the protein level these molecules persist for much longer within the L LPM; an issue that we plan to address in the near future. Unfortunately, due to the lack of high quality, specific antibodies, it is difficult to nearly impossible to detect endogenous TGF-β related proteins in embryonic tissues. To counteract this problem, we will detect exogenously introduced Xnr1 and Xlefty that have been epitope-tagged to investigate the longevity and/or stability of these proteins within L LPM tissue. It is significant to mention, however, that JJ Westmoreland in our laboratory has generated antibodies specific for Xlefty, some of which can detect the normal (untagged) form. Therefore, it may be possible to utilize these antibodies to detect Xlefty protein in tailbud stage tissues, at the very least, using western blot analyses. We also hope to generate Xnr1-specific antibodies that will be able to detect endogenous Xnr1 protein, as well. The basic principle of our epitope-tagged strategy is to introduce tagged forms of these molecules (for example, myc- or HA-tagged), which are known to be functional, produced from plasmid sources into lineage-labeled tissue grafts. These grafts will be transplanted into the LPM of host embryos, similar to the approach outlined in Chapters III and IV of this thesis. The protein levels of Xnr1 and Xlefty produced from the graft will be indirectly examined at various stages after grafting by, for example Myc immunostaining and/or Myc detection by western blot analysis of the adjacent tissues. JJ and a previous postdoctoral fellow in the lab, Shuji Takahashi, have already demonstrated that this approach is successful for detecting Xnr and Xlefty proteins during gastrula stages (as described in more detail in Chapter VI with regard to detecting the movement characteristics of these proteins during tailbud embryogenesis), providing precedent for the success in analyzing Xnr1 and Xlefty protein levels in tailbud stage tissues. Lindsay Bramson has already constructed epitope-tagged versions of both Xnr1 and Xlefty and has preliminary evidence suggesting that both constructs are

functional. We plan to rapidly move forward with these studies with the hopes that they will provide new information for how these proteins are regulated during tailbud stages.

Related to the perdurance of active Xnr1 and Xlefty signaling within the L LPM during L-R specification, it is also of interest in the future to investigate the mechanism(s) underlying ligand clearance and the rapidity by which this occurs. Previous studies on activin signaling have demonstrated that activin remains bound to its receptor and continues signaling within the endolysosomal pathway for many hours before being degraded (Dyson and Gurdon, 1998; Jullien and Gurdon, 2005). These findings demonstrate that morphogen gradient formation and interpretation can therefore be achieved by prolonged downstream signaling after ligand exposure. Examining whether Xnr1 and Xlefty are internalized and cleared in a similar manner will lead to mechanistic insight into how cells of the L LPM receive and respond to these signals during the L-R determination process.

Downstream of Nodal/Xnr1 signaling

A central issue in the L-R field that remains unclear is how transient *Nodal/Xnr1* expression translates into long-lasting information that leads up to asymmetric morphogenesis. Nodal/Xnr1 signaling results in the nuclear accumulation of P-Smad2 in responsive cells, where in conjunction with other co-factors it leads to transcriptional activation of target genes. We hypothesize that cells of the L LPM may "remember" the transient exposure to Xnr1 signaling at later stages by the long-lasting presence of nuclear-localized P-Smad2. We have recently obtained affinity-purified P-Smad2 antibodies from Peter ten Dijke in the Netherlands that we will use to carry out studies to test this hypothesis. We will examine the levels of P-Smad2 during and after the period of asymmetric *Xnr1* expression within the LPM. It is possible that P-Smad2 remains localized within the nuclei of L LPM cells and persists until the time when asymmetric morphogenetic events begin to occur. We plan to establish a spatiotemporal map of

nuclear P-Smad2 relative to the asymmetric *Xnr1* expression wave to examine whether gradients of P-Smad2 form along the anterior-posterior (A-P), as well as dorsal-ventral (D-V) axes. If this is the case, we will analyze whether the areas of strongest *Xnr1* expression correspond spatially with the highest levels of P-Smad2 nuclear localization in the L LPM. Related to this latter point, previous studies in *Xenopus* have shown that the level of nuclear P-Smad2 is dependent upon the level of Nodal signaling registered by the cells, such that high levels of Nodal cause more accumulation of P-Smad2 in the nucleus of cells (Shimizu and Gurdon, 1999). It is possible that if maxima of P-Smad2 exist along the LPM that cells within the vicinity may act as "organizing centers" and influence and/or direct asymmetric morphogenetic events to initiate at these locations. Lastly, it will be important to examine whether a nuclear P-Smad2 signal is only detected within the LPM tissue layer or if regional P-Smad2 is observed in other germ layers, such as endoderm. If the P-Smad2 signal is only observed within the LPM, this would imply that this tissue layer is primarily responsible for directing asymmetric morphogenesis at later stages. On the other hand, nuclear localized P-Smad2 within the endoderm would indicate that this tissue also has a direct influence in morphogenesis. Alternatively, the endoderm could have an indirect role in controlling asymmetric morphogenesis if signals from the LPM, as a response to P-Smad2, are secreted to induce genetic programs and morphogenetic movements within the endoderm, which may then signal back to the LPM.

CHAPTER VI

SUMMARY AND FUTURE PERSPECTIVES

Members of the TGF-β superfamily play an important role in a variety of processes that are critical for cell fate specification and patterning of the vertebrate embryo. Studies on one particular member, Nodal, have demonstrated that this protein is functionally conserved between vertebrates and perhaps some invertebrates, and is critical for mesendoderm induction and patterning, as well as L-R axis determination. During my thesis research, I have investigated how Nodal signals are transmitted within sheets of cells and between different germ layers and how asymmetric signals are L-R compartmentalized, as well as integrated across the *Xenopus* embryo.

Altogether, my findings in *Xenopus*, gathered concurrently but independently, largely support the SELI model recently proposed from studies in the mouse embryo (Nakamura et al., 2006; Tabin, 2006) and therefore provide strong evidence for mechanistic conservation between species. My studies demonstrate that asymmetric threshold-dependent activation of *Xnr1* in the LPM of *Xenopus* embryos leads to the same situation as described in the mouse. In the SELI model, the mouse node is equivalent to the *Xenopus* posterior tailbud region with bilateral *Xnr1* expression and proposes the following: **1)** a L-R biasing mechanism (in the mouse embryo, this may be leftward nodal flow – see Tabin, 2006 review) causes unequal activation of *Nodal* expression adjacent to the node such that expression is stronger on the left side. In *Xenopus*, this L-R biasing event may occur very early during embryogenesis (see general introduction). **2)** *Nodal* positively autoregulates its own expression, as well as induces *Lefty* expression in the midline. Specifically in the *Xenopus* embryo, this induction of midline *Xlefty* may add to the low level of residual expression that is already present, due

to earlier signaling from the Organizer during early gastrula stages (as described in the Introduction of Chapter IV). **3)** Nodal adjacent to the node induces *Nodal* and *Lefty* expression only in the L LPM because according to the principles of a reaction-diffusion system, Lefty inhibition from the midline is relatively stronger than the inductive signal on the R side but weaker than the L-side autoregulatory signal. **4)** Nodal self-amplification expands the expression domains of itself, as well as that of *Lefty*. **5)** Lefty from the midline and L LPM functions contralaterally to suppress R-sided activation of *Nodal* expression. **6)** Lefty in the L LPM ensures that *Nodal* expression is transient by negative feedback regulation of the Nodal autoregulatory loop. In the following sections, I will outline my pertinent findings in relation to a SELI mechanism for L-R patterning during embryogenesis, raise issues that still remain and propose studies that will hopefully provide insight into these issues.

Induction of asymmetric *Xnr1* expression within the L LPM

When I began my graduate training in the Wright laboratory, previous students had characterized the left-specific expression of *Xnr1* (Lowe et al., 1996) and subsequently demonstrated that misexpression of *Xnr1* within the LPM was sufficient to randomize anatomical situs (Sampath et al., 1997), thereby highlighting the importance of Xnr1 in establishing proper L-R asymmetry pattern. A central issue that we wanted to address with my thesis research was to determine the tissue interactions that are required to generate and transmit L-R specifying signals towards the LPM. I took advantage of the attributes of *Xenopus* embryos, including their large size, resilience to manipulation, and ease of developmental staging. I found that L and R LPM explants expressed *Xnr1* only if the explants encompassed tissue that approached the posterior tailbud region where *Xnr1* is expressed bilaterally. My results are consistent with previous studies in chicken and frog, as well as more recent studies in the mouse embryo, which showed that initial induction of *Nodal* in explanted LPM was only observed in the presence of node

tissue (Levin and Mercola, 1998; Nakamura et al., 2006). A second significant finding from these studies was that the expression of *Xnr1* in L and R explants occurred substantially earlier than in intact embryos. We hypothesize that the precociousness reflects an inhibitory influence on both the L and R sides by the midline in whole embryos, which is absent when LPM is explanted. In support of this hypothesis, I found that when embryos were bisected longitudinally (along the A-P axis) prior to asymmetric *Xnr1* induction (*e.g.,* stage 15/16), with each embryo-half including its posterior perinotochordal domain of *Xnr1* expression, asymmetric *Xnr1* expression occurred normally only in the left-half embryo with the correct timing of activation. This finding is consistent with the SELI model's proposal that the R side initially attempts to mount a *Nodal*/*Xnr1* expression response, which is suppressed by signaling from the midline in normal embryos. Additional data from our laboratory provides direct evidence for an initial R-sided activation of *Xnr1*. RT-PCR and *in situ* hybridization analyses have shown that low levels of *Xnr1* expression can be detected in R LPM, confirming the data in mouse (Nakamura et al., 2006).

I also showed that removing the posterior tailbud prior to the initiation of asymmetric *Xnr1* expression (*e.g.,* stage 17) resulted in the absence of expression of the left-side gene cassette (*Xnr1*/*Xlefty*/*XPitx2*) within the L LPM at later stages, demonstrating the requirement for inductive signaling from this region. In contrast, control posterior-cropped embryos, in which the posterior tailbud was removed after initiation of L-sided *Xnr1* expression (stage 19/20), exhibited normal asymmetric gene expression in L LPM that underwent anteriorwards shifting, comparable to that observed in unmanipulated embryos. Anatomical analysis at later stages showed that stage 17-cropped embryos developed randomized cardiac situs across the population, consistent with the idea that in the absence of *Xnr1* expression, the side that becomes dominant is a stochastic choice. All control embryos cropped at stage 20 developed normal situs. As the posterior tailbud in *Xenopus* with its bilateral domains of *Xnr1* expression is

equivalent to the early somitogenesis stage node of the mouse embryo, my results taken together support the findings in mouse that show the transference of a L-instructive *Nodal*/*Xnr1*-inducing signal from the node to the LPM (Lowe et al., 2001; Brennan et al., 2002; Saijoh et al., 2003; Nakamura et al., 2006).

My findings are, however, in disagreement with a previous model that was proposed from studies in *Xenopus* that suggested the LPM (both L and R) expresses *Xnr1* by default, and that a repressive signal(s) produced from the midline is responsible for suppressing the R-sided expression (Lohr et al., 1997; Lohr et al., 1998). These investigators argued against a midline/node inductive role for initiating *Xnr1* expression in the L LPM. This discrepancy is most likely due to differences in experimental technique. The authors showed that L and R lateral explants isolated at stage 15/16 (the same stage that I performed the isolation) went on to express bilateral *Xnr1* expression (Lohr et al., 1997), which could very well be explained by the presence of posterior tissues. In contrast, explants isolated at stage 19/20 only developed L-sided expression (Lohr et al., 1997). Furthermore, stage 15/16 explants recombined with stage 19/20 isolated notochord led to suppression of *Xnr1* expression (Lohr et al., 1998), leading to the above-mentioned hypothesis that the midline has an inhibitory rather than an inductive role in initiating L-sided *Xnr1* expression in LPM. These results can easily be explained by the stage of midline and LPM used in these experiments, as my findings as well as those in mouse have demonstrated that the relationship between these tissues differs depending on the time of tailbud-stage embryogenesis. My data, in combination with the Nakamura *et al*. (2006) findings strongly support the notion that the initiation and maintenance of L-sided *Nodal*/*Xnr1* expression is a result of a constant competition between inductive and repressive signals derived from the midline, as well as lateral tissues, and that L-R asymmetric signals need to reach particular thresholds in order to elicit proper asymmetric gene expression in the L LPM.

Several lines of evidence, primarily from studies in the mouse embryo, point to the hypothesis that Nodal itself, secreted from the node or its functional equivalent, initiates LPM *Nodal* expression. In support of this hypothesis, in some assays, Nodal exhibits long-range movement (Chen and Schier, 2001; Sakuma et al., 2002; Williams et al., 2004). It is conceivable, then, that Nodal is concentrated at the left edge of the node, under the influence of nodal fluid flow or some other L-R biasing event, and moves from there to initiate *Nodal* expression in the L LPM. This notion is supported by several observations. There is no or minimal L-sided *Nodal* or *Lefty* expression in mouse embryos that are null for cryptic (encoding an EGF-CFC factor required for Nodal signaling; Yan et al., 1999), carrying a hypomorphic *Nodal* allele (Lowe et al., 2001), lacking node *Nodal* expression because of a deletion of cis-regulatory regions (Brennan et al., 2002; Saijoh et al., 2003), or in which the Nodal autoregulatory loop component *FoxH1* gene is inactivated (Saijoh et al., 2000). Consistent with these previous findings in the mouse, I found that exposing stage 17 embryos, before *Xnr1* is asymmetrically expressed, to small molecule inhibitors that specifically block the Nodal/Xnr1 Alk4 receptor abolished L LPM *Xnr1* expression, suggesting that an Alk4-mediated signaling mechanism is required to initiate asymmetric expression.

Dynamics of asymmetric *Xnr1* expression during L-R specification

At the time when *Xnr1* was originally isolated and its expression characterized, it had been noted that during tailbud stages, the asymmetric *Xnr1* expression domain undergoes a rapid, dynamic posterior-to-anterior (P-to-A) shifting within the L LPM before being shut down in the same directional fashion (Lowe et al., 1996; Lustig et al., 1996). Although a general anteriorwards shifting of *Nodal* expression within the L LPM had been observed in other species such as mouse and more recently in zebrafish and medaka (Lowe et al., 1996; Murray and Gridley, 2006; Long et al., 2003; Soroldoni et al., 2006; Ito et al., 2006), the mechanism(s) underlying this dynamic unidirectional shifting

was unclear and had not been studied. Therefore, as the second part of my thesis research project I investigated how *Xnr1* expression is propagated anteriorwards within the L LPM and whether this process occurs L LPM-autonomously.

Using a combination of tissue explantation, overexpression and grafting techniques I demonstrated that the progression of asymmetric *Xnr1* expression within the L LPM is dependent upon planar tissue communication and requires Xnr1 autoinduction between adjacent cell fields. I found that disrupting P-to-A communication within the L LPM by bisecting either whole embryos, or LPM explants alone was sufficient to prevent the anteriorwards progression of asymmetric *Xnr1* expression. I also observed that the posterior expression of *Xnr1* in these explants was prolonged compared to the situation in normal embryos, suggesting that A-to-P feedback communication within the L LPM may also be necessary for proper temporal expression. By performing a time-course analysis of *Xnr1* expression in anteriorly-marked L LPM explants, I demonstrated that the forward propagation of asymmetric *Xnr1* occurs L LPM-autonomously. Moreover, I found that small LPM grafts expressing Xnr1 signaling specific inhibitors (*e.g.*, Cer-S and Xlefty) suppressed the forward movement of the L-side expression wave within the LPM.

Further supporting the idea that Xnr1 autoregulation is necessary for the maintenance and progression of the L LPM *Xnr1* expression domain, as discussed in Chapter V, Alk4 receptor-specific inhibitors were sufficient to block both the maintenance and anteriorwards shifting of asymmetric *Xnr1* expression. A significant issue that remains however is whether other mechanisms contribute to Xnr1 autoregulatory signaling to promote the rapid shifting of *Xnr1* expression within the L LPM. Lindsay Bramson in the laboratory plans to carry out a pharmacological screen to look for other signaling pathways that may work in synergy with Xnr1 signaling to contribute to the rate of anterior shifting within the L LPM (as described in the Introduction of Chapter V). The commercial availability of inhibitors that are known to block a number of signaling systems will facilitate the testing of a potential interaction.

For example, Noggin, CUR61414 or cyclopamine, SU5402, heptanol or lindane can be used to block BMP, Sonic hedgehog (Shh), FGF, or gap junctional communication pathways, respectively. The general idea for examining a synergistic interaction would involve exposing embryos to these inhibitors in combination with suboptimal doses of the SB-type Alk4 inhibitors that cause a reduction of *Xnr1* expression in a spatiotemporal manner. A positive relationship between Xnr1 signaling and another pathway would result in further suppression of the levels and/or shifting of L LPM *Xnr1* expression, whereas an antagonistic interaction would cause an increase.

High-resolution analysis of *Xlefty* expression in the L LPM, in relation to the asymmetric expression of *Xnr1* demonstrated that *Xlefty* expression spatially mimics that of *Xnr1* but with a temporal delay, consistent with the idea that *Xlefty* is a direct target of Xnr1 signaling (Tanegashima et al., 2000; Cheng et al., 2000). I, therefore, proposed the hypothesis that transient L-sided *Xnr1* expression is ensured by the delayed expression of its target gene and feedback inhibitor, *Xlefty*. It will be of interest in the future to investigate whether a second wave of *Xnr1* expression can be initiated in the L LPM. Directly related to the longevity and/or stability of Xlefty protein discussed in Chapter V, it is possible that if Xlefty is relatively long-lived within the L LPM, it could create a suppressive environment against re-initiation of *Xnr1* expression. Such a mechanism would ensure that the L LPM only receives a single exposure to L-specifying information.

Movement of Xnr1 and Xlefty ligands during tailbud embryogenesis

Very little is currently known about the characteristic movement of Nodal/Xnr1 and Lefty/Xlefty ligands within the LPM or throughout the embryo, although some evidence from studies of mouse Nodal and Lefty suggest that these proteins can move quite far (Sakuma et al., 2002; Nakamura et al., 2006). The speed and direction of movement of Xnr1 and Xlefty within the LPM from a localized source will be important

to determine as a fundamental underlying parameter of the *Xnr1* expression shift. It is also of significance to understand whether these ligands move in a preferential direction through the LPM. It is likely that the architecture of L LPM tissue at the time of the asymmetric *Xnr1* expression shifting influences the directionality of movement of the Xnr1 and Xlefty proteins, as addressed below. Another hypothesis that we plan to test is that after activation of *Xnr1* in the L LPM, Xlefty produced initially from the posterior midline of the early tailbud stage embryo as a result of Xnr1 induction, conditions the posterior region against re-expressing *Xnr1*, thereby directing the autoregulatory expression wave only anteriorwards. If this hypothesis is correct, we can predict that removing this posterior influence (*e.g.,* by posterior cropping, that I have shown abolishes midline and LPM *Xlefty* expression) should allow *Xnr1* expression shifting to occur bidirectionally from say, an *Xnr1*-graft.

The *Xenopus* embryo is an advantageous system to investigate ligand movement due to, for example, the ability to employ localized grafting strategies as I have described previously. Due to the large size of the embryo and ease of manipulation, this technique allows us to vary the graft location and assess the direction and speed of movement from various locations and at various easily accessed developmental stages. We will use a similar epitope-tagging and overexpression grafting strategy as described in the Discussion of Chapter V with regard to analyzing protein stability during tailbud stages. Briefly, epitope-tagged versions of Xnr1 and Xlefty will be overexpressed in donor LPM tissue, followed by transplantation of LPM tissue grafts to wild-type host embryos. We will indirectly examine Xnr1 and Xlefty movement from the graft by immuno-histochemical analysis of whole embryos and LPM tissue sections, as well as by western blot analysis of tissues adjacent to the graft. Previous and current members of the lab have shown that they can visualize Xnr and Xlefty protein movement away from a local source of production in gastrula stage embryos by indirect immunohistochemical detection (Takahashi et al., 2006; manuscript in preparation), providing a precedent that

this type of strategy should also work for detecting the movement of Xnr1 and Xlefty within tailbud stage tissues. Additionally, we will attempt to use green fluorescent protein (GFP) tagging to visualize ligand movement in live embryonic tissues.

Studies from our laboratory have shown that during early blastula/gastrula stages, Xlefty is cleaved from a proprotein into a long ($Xlefty^{L}$) and short ($Xlefty^{S}$) isoform. Although it has been found that during these early stages, only $Xlefty^{L}$ accumulates to detectable levels within the embryo and is the only form that seems capable of blocking Xnr signaling, it is possible that during later tailbud stages, $Xlefty^{S}$ also plays an important role in regulating Xnr1 signaling. We may find that the two forms of Xlefty both play a role during L-R specification stages and that one may be able to travel faster and farther than the other, which could lend further insight into the reaction-diffusion relationship between Xnr1 and Xlefty.

As mentioned above, we hypothesize that the architecture of the L LPM may directly influence how Xnr1 and Xlefty move within and through this tissue. It is therefore important to gain a fundamental knowledge of how the LPM is organized before, during and after the L-sided *Xnr1* expression wave. It is possible, for example, that inter-tissue space develops prior to or during L LPM *Xnr1* expression that would provide for freer movement/diffusion of the Xnr1 and Xlefty ligands, thereby facilitating the rapid transfer of signals between cells. The rapid expression shifting of *Xnr1* expression in L LPM may also be facilitated by some form of planar cell polarity mechanism (similar to the PCP pathway involved in ommatidia development in the *Drosophila* eye), in which the Xnr1 ligand becomes preferentially localized on anterior surfaces of L LPM cells, affecting its transport characteristics (as proposed in the Discussion of Chapter III).

We will also investigate when the LPM becomes epithelialized with distinct apical, basal and lateral compartments. If we find that the L LPM becomes epithelial prior to or during the asymmetric *Xnr1* expression wave, it is possible that Xnr1 and

Xlefty proteins (in addition to a potential A-P preferential cellular localization) are deployed only on apical or basal cell surfaces, which could again affect the rate of signal transfer through the LPM. The presence of gap junctions could also facilitate the movement of Xnr1 and Xlefty between cells. When the LPM becomes epithelialized during embryogenesis is also of significance in attempting to understand the cellular and/or tissue changes that occur in response to Xnr1 signaling and leading up to asymmetric morphogenesis. Studies in zebrafish demonstrated that directional movement of the L and R LPM resulted in asymmetric "deformation" of the linear gut tube. These studies also showed that the LPM is epithelial just before gut looping is initiated, with distinct apical marker localization (Horne-Badovinac et al., 2003); however, the relationship with timing of L-sided *cyclops* (*cyc*) and *southpaw* (*spaw*) expression is vague. Studies in the chicken have also shown by scanning electron microscopic (SEM) and histological analysis that the LPM has separated into the two splanchnic and somatic layers at the 10-somite stage and each of these layers appears to be epithelial with proper apical-basal polarity (Meier, 1979; Funayama et al., 1999). Again, however, how this event relates to the timing of asymmetric L-sided *Nodal* expression is not clear. We will use established apical and basal markers to examine when the LPM becomes epithelialized in the *Xenopus* embryo and analyze how the timing of this event relates to the *Xnr1* expression wave.

Overall, we plan to investigate in *Xenopus* whether there is an intrinsic polarity in the LPM, and if so, when during embryogenesis it occurs, and how this tissue organization may facilitate the rapid anteriorward shifting of *Xnr1* expression and lead up to asymmetric morphogenetic events much later.

Orthogonal induction of midline Xlefty and contralateral communication in *Xenopus*

Although a long standing role for the midline in regulating L-R asymmetry patterning has been established, primarily from studies in the mouse, *Xenopus*, and zebrafish embryo (see Chapter I – general introduction), precisely how it functions has remained vague. It is also largely unknown when during embryogenesis the midline functions to affect the L-R specification program, although some evidence suggests that the midline acts during the early phase of asymmetry setting (Danos and Yost, 1996; Lohr et al., 1997; Meno et al., 1998). Previous studies in the mouse embryo have demonstrated the importance of Lefty1 in the midline for the proper development of asymmetric gene expression, as well as anatomical situs (Meno et al., 1998). During my studies, it was shown in mouse that Nodal signaling from the LPM could induce expression of *Lefty1* in the midline (Yamamoto et al., 2003). Around this time, I was finding that mid-trunk *Xnr1*-expressing LPM grafts induced *Xnr1* expression within the R LPM of host embryos, and also that the ectopic strong R-sided expression was associated with a reduced level and/or anterior extent of endogenous L-sided *Xnr1* expression. Analysis of *Xlefty* expression in the engrafted hosts showed a robust enhancement of expression in the midline orthogonal to the grafts, consistent with the Yamamoto *et al.* (2003) findings in mouse. These results demonstrated that in both the mouse and *Xenopus* embryo, Nodal/Xnr1 signaling from the LPM could induce *Lefty*/*Xlefty* in the midline.

Mid-trunk R-side *Xnr1*-engraftment resulted in a concordant reversal of cardiac and gut situs across the entire population, suggesting that the engrafted R-side had been converted to the new, dominant left. These results, taken together, led to the working hypothesis that in R-side *Xnr1*-engrafted embryos, the ectopic induction of *Xlefty* in the midline by orthogonal Xnr1 signaling from the graft/host R LPM, resulted in the contralateral spreading of Xlefty and subsequent inhibition of the L-sided Xnr1 autoregulatory loop causing both the suppression of asymmetric gene expression, as well

as dominant reversal of anatomical situs at later stages. Similar to my findings in frog, studies from Hiroshi Hamada's group concurrently but independently found that ectopically expressing *Nodal* on the R side led to the suppression of endogenous L-sided *Nodal* expression in the mouse embryo (Nakamura et al., 2006). We hypothesized that two factors could explain why the R-engrafted side could be converted to a dominant left in these embryos. First, the mid-trunk placement of *Xnr1*-grafts in the R LPM of hosts would give the R-side graft-induced *Xnr1* expression a "head-start" in anteriorward shifting, as compared to the L-side endogenous expression, which is initiated more posteriorly in the L LPM. Therefore, the L-specifying Xnr1 signal would inevitably reach the organ/cardiac anlagen earlier on the R side. Second, the induction of midline *Xlefty* by orthogonal Xnr1 signaling from the engrafted right side represses L-sided *Xnr1* expression, reducing the levels and anterior shifting within the L LPM. Our current hypothesis is the following: it is the level of Xnr1 and/or the integrated time of receipt of this signal that determines how "leftness" information is received and registered by the LPM.

In support of our hypotheses, I showed that either altering the placement of the R-sided *Xnr1*-graft to a more posterior position or removing the region of the midline that encompassed the ectopic domain of *Xlefty* abolished the R-sided dominance in the engrafted embryos (for more detail – see Chapter IV). For example, posterior engraftment of *Xnr1*-grafts on the R side resulted in equivalent levels and anterior shifting of L and R LPM *Xnr1* expression and randomization of cardiac and gut situs across the population (although heart and gut situs was concordant within each individual embryo). These findings support the idea that in embryos with equal, bilateral *Nodal*/*Xnr1* expression, which side becomes dominant is determined stochastically. Altogether, my R-side *Xnr1*-engraftment data led us to propose an integrated model for L-R asymmetry specification during *Xenopus* tailbud embryogenesis, in that orthogonal Xnr1 signaling from the L LPM induces *Xlefty*, that in turn, spreads to the contralateral

side and suppresses R-sided activation of *Xnr1* expression. My findings on the induction and dynamics of asymmetric *Xnr1* expression in the LPM (described in Chapter III) combined with our contralateral communication model just described, fits nicely and is consistent with a SELI mechanism for ensuring L-R compartmentalization of the embryo during asymmetry determination and transient L-sided Xnr1 signaling.

As discussed above, we are interested in investigating how Xnr1 and Xlefty ligands move within the L LPM. The speed at which these proteins move through LPM tissue, as well as whether they move with an inherent directionality are certainly relevant issues to understand with regard to a SELI system. Additionally, we hope to address how Xnr1 and Xlefty move within and/or across the embryo. In relation to the contralateral spreading of Xlefty from the L LPM and midline to the R side to suppress *Xnr1* expression in the R LPM as proposed from our findings and the SELI model, it is important to know whether these secreted ligands can travel only around the arc of the embryo (*e.g.,* from L LPM to the midline, then over to R LPM – Route 1 in Fig. 6.1), or if they can travel perpendicularly from the L LPM to endoderm, through the archenteron to the R LPM on the other side (Route 2 in Fig. 6.1). This is perhaps a more significant issue in the large *Xenopus* embryo, due to the long distances of travel that are involved as compared to the smaller mouse embryo. We can differentiate between these two routes of transport, for example, by examining whether Xnr1 and Xlefty proteins can be detected in tissues other than the LPM at various times of tailbud stage embryogenesis. We will use the aforementioned strategy in which LPM grafts overexpressing epitope-tagged versions of Xnr1 and Xlefty are transplanted to the L flank of host embryos. Western blot analysis of dissected tissues will be attempted to test for perpendicular movement across the embryo. As I have described, this grafting technique allows the flexibility of changing the location of the local producing source with respect to specific anatomical landmarks (for example, moving the graft closer or away from the paraxial mesoderm adjacent to the midline). We will detect tagged Xnr1 and Xlefty at stages that

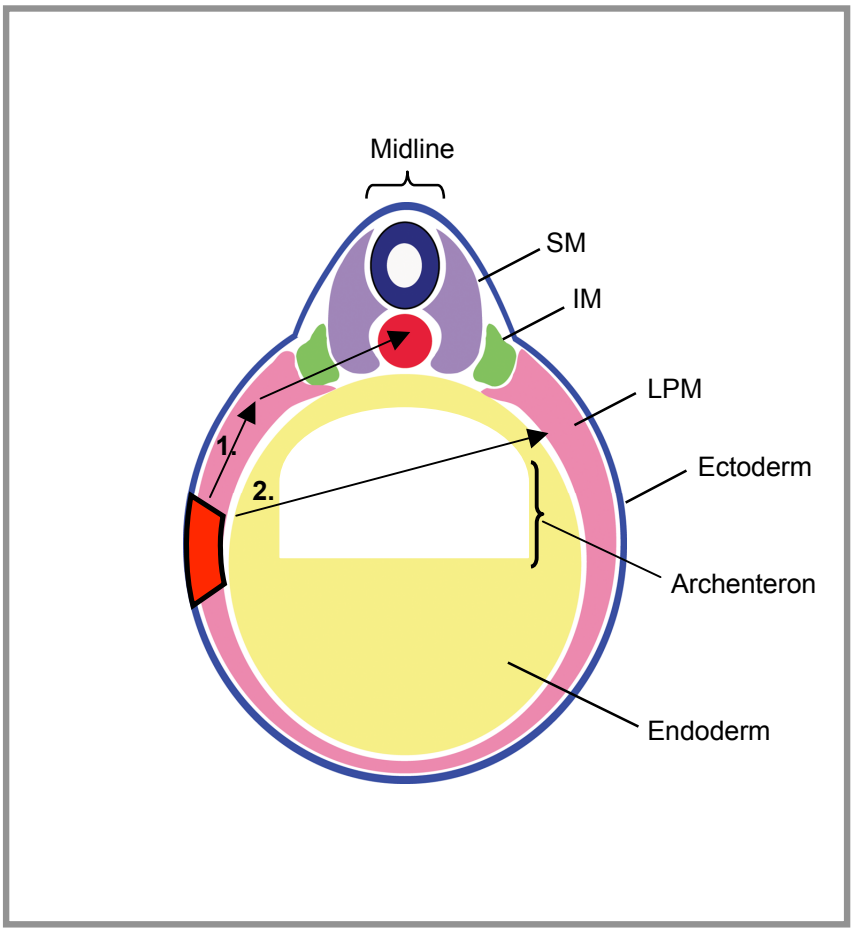

Fig. 6.1 Possible routes of Xnr1 and Xlefty movement from LPM associated with L-R contralateral communication. Route 1: Xnr1 may only travel around the LPM arc to reach the midline. **Route 2:** Perpendicular transport of Xnr1 from LPM to endoderm, or through the archenteron to the contralateral side. SM, somitic mesoderm; IM, intermediate mesoderm; LPM, lateral plate mesoderm.

correlate with the time of say, midline *Xlefty* induction. Finally, we will be able to assess the potential presence in the archenteron by employing techniques that involve extracting the fluid from this cavity and checking for Xnr1 and Xlefty over time.

My findings, as well as those of Nakamura *et al*. (2006) lend strong support to the idea that L-R compartmentalization of the embryo is greatly ensured by a contralateral inhibitory role of the dorsal axial midline. To maintain distinct L and R compartments, it is conceivable to think that an analogous "inhibitory zone" also exists ventrally to prevent the spreading of Xnr1 signals to the R-side. It is of interest that *Xnr1* appears to be expressed in a dorsal-to-ventral gradient within the L LPM, such that the strongest regions of expression are more dorsal, just adjacent to the paraxial mesoderm, with decreasing levels of signal more ventral. Analysis of *BMP4* during tailbud stages demonstrated that its expression was highly enriched and restricted along a ventral domain and comparison with *Xnr1* during similar stages showed very little if any overlap with the more ventral-lateral *Xnr1* expression in the L LPM (Fig. 6.2A). My preliminary findings have shown that *Xnr1*-expressing LPM grafts placed within the "belly" region (*e.g*., ventral midline) of host embryos failed to induce a self-propagating *Xnr1* expression wave (Fig. 6.2B). Additionally, I observed minimal induction of host *Xnr1* expression outside of the *Xnr1*-graft, even under conditions where a majority of the graft cells were expressing *Xnr1* from the pCSKA plasmid promoter. In contrast, mid-trunk-engrafted controls induced robust, anteriorly-shifting *Xnr1* expression, consistent with my previous results (Fig. 6.2B). We hypothesize that a ventral "inhibitory zone" generated by BMP signaling may act to prevent contralateral crossing of Xnr1 from the L to R side, thereby reinforcing embryo compartmentalization. We will test this hypothesis by introducing either *Noggin*-expressing grafts or Noggin-impregnated beads adjacent to ventrally-placed *Xnr1*-grafts to examine whether this allows for the ectopic induction of *Xnr1*. Alternatively, we can attempt to precondition the ventral region of host embryos against BMP inhibition by placing the *Noggin*-grafts and/or beads at a time prior to *Xnr1*-

engraftment. We will also try to simply increase the dose of *Xnr1* expressed in the ventral graft by either using a larger graft or by increasing the concentration of plasmid injected into donor embryos and test whether this approach is able to counteract the potential inhibitory effect of BMP.

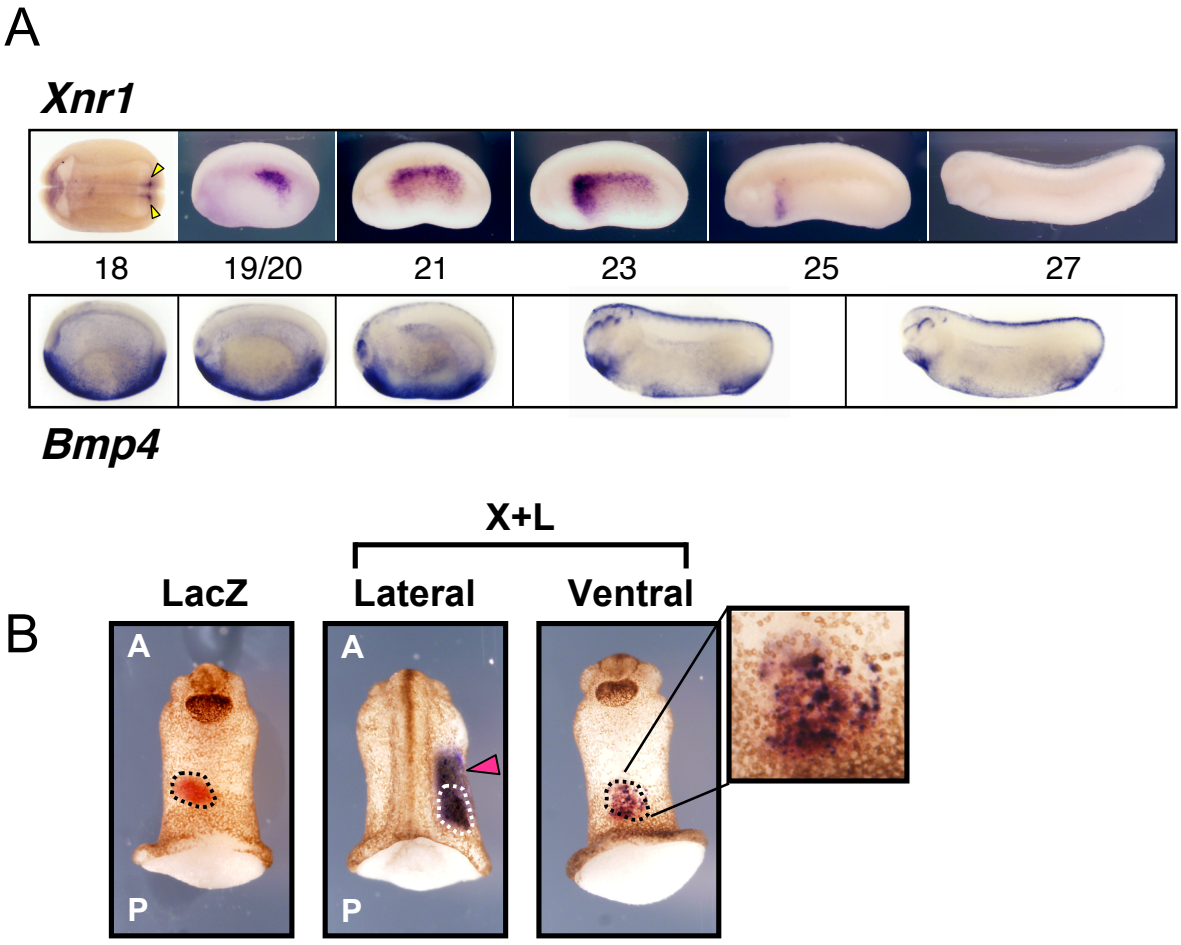

Fig. 6.2 Complementary expression domains of *Xnr1* and *BMP4* and differential regions of competence to express *Xnr1*. A) *Xnr1* expression is excluded from ventral *BMP4* expression domain during tailbud stages. Left-most panel in top row, dorsal view; all other panels, lateral view. Embryos in bottom row are cleared. Anterior left. B) *Xnr1* expression was not induced from both LacZ and Xnr1+LacZ (X+L) ventral grafts (left- and right-most panels, ventral views) but was robustly induced from mid-trunk placed X+L grafts (pink arrowhead, middle panel, dorsal view). Note *Xnr1*-expressing cells within ventral graft in right-most panel (inset). Dotted lines demarcate lineage labeled graft. A, anterior; P, posterior.

REFERENCES

Alberts, B., Bray, D., Lewis, J., Raff, M., Roberts, K., and Watson, J. D. (1994). Molecular Biology of the Cell, 3rd edition. Garland Publishing, New York.

Agathon, A., Thisse, B., and Thisse, C. (2001). Morpholino knock-down of antivin1 and antivin2 upregulates nodal signaling. *Genesis* **30,** 178-82.

Agius, E., Oelgeschlager, M., Wessely, O., Kemp, C., and De Robertis, E. M. (2000). Endodermal Nodal-related signals and mesoderm induction in Xenopus. *Development* **127,** 1173-83.

Altmann, C. R., Chang, C., Munoz-Sanjuan, I., Bell, E., Heke, M., Rifkin, D. B., and Brivanlou, A. H. (2002). The latent-TGFbeta-binding-protein-1 (LTBP-1) is expressed in the organizer and regulates nodal and activin signaling. *Dev Biol* **248,** 118-27.

Amara, F. M., Entwistle, J., Kuschak, T. I., Turley, E. A., and Wright, J. A. (1996). Transforming growth factor-beta1 stimulates multiple protein interactions at a unique cis-element in the 3'-untranslated region of the hyaluronan receptor RHAMM mRNA. *J Biol Chem* **271,** 15279-84.

Ashe, H. L., and Briscoe, J. (2006). The interpretation of morphogen gradients. *Development* **133,** 385-94.

Bader, D., Masaki, T., and Fischman, D. A. (1982). Immunochemical analysis of myosin heavy chain during avian myogenesis in vivo and in vitro. J Cell Biol **95**, 763-70.

Beck, S., Le Good, J. A., Guzman, M., Ben Haim, N., Roy, K., Beermann, F., and Constam, D. B. (2002). Extraembryonic proteases regulate Nodal signalling during gastrulation. *Nat Cell Biol* **4,** 981-5.

Bianco, C., Adkins, H. B., Wechselberger, C., Seno, M., Normanno, N., De Luca, A., Sun, Y., Khan, N., Kenney, N., Ebert, A., Williams, K. P., Sanicola, M., and Salomon, D. S. (2002). Cripto-1 activates nodal- and ALK4-dependent and -independent signaling pathways in mammary epithelial Cells. *Mol Cell Biol* **22,** 2586-97.

Bisgrove, B. W., Essner, J. J., and Yost, H. J. (1999). Regulation of midline development by antagonism of lefty and nodal signaling. *Development* **126,** 3253-62.

Boggetti, B., Argenton, F., Haffter, P., Bianchi, M. E., Cotelli, F., and Beltrame, M. (2000). Cloning and expression pattern of a zebrafish homolog of forkhead activin signal transducer (FAST), a transcription factor mediating Nodal-related signals. *Mech Dev* **99,** 187-90.

Boorman, C. J., and Shimeld, S. M. (2002). The evolution of left-right asymmetry in chordates. *Bioessays* **24,** 1004-11.

Bradley, L. C., Snape, A., Bhatt, S., and Wilkinson, D. G. (1993). The structure and expression of the Xenopus Krox-20 gene: conserved and divergent patterns of expression in rhombomeres and neural crest. *Mech Dev* **40,** 73-84.

Branford, W. W., Essner, J. J., and Yost, H. J. (2000). Regulation of gut and heart left-right asymmetry by context-dependent interactions between xenopus lefty and BMP4 signaling. *Dev Biol* **223,** 291-306.

Branford, W. W., and Yost, H. J. (2002). Lefty-dependent inhibition of Nodal- and Wnt-responsive organizer gene expression is essential for normal gastrulation. *Curr Biol* **12,** 2136-41.

Brennan, J., Norris, D. P., and Robertson, E. J. (2002). Nodal activity in the node governs left-right asymmetry. *Genes Dev* **16,** 2339-44.

Brown, C. B., Boyer, A. S., Runyan, R. B., and Barnett, J. V. (1999). Requirement of type III TGF-beta receptor for endocardial cell transformation in the heart. *Science* **283,** 2080-2.

Bunney, T. D., De Boer, A. H., and Levin, M. (2003). Fusicoccin signaling reveals 14-3-3 protein function as a novel step in left-right patterning during amphibian embryogenesis. *Development* **130,** 4847-58.

Burdine, R. D., and Schier, A. F. (2000). Conserved and divergent mechanisms in left-right axis formation. *Genes Dev* **14,** 763-76.

Capdevila, J., Vogan, K. J., Tabin, C. J., and Izpisua Belmonte, J. C. (2000). Mechanisms of left-right determination in vertebrates. *Cell* **101,** 9-21.

Casey, B. (1998). Two rights make a wrong: human left-right malformations. *Hum Mol Genet* **7,** 1565-71.

Casey, B., Devoto, M., Jones, K. L., and Ballabio, A. (1993). Mapping a gene for familial situs abnormalities to human chromosome Xq24-q27.1. *Nat Genet* **5**, 403-7.

Cha, Y. R., Takahashi, S., and Wright, C. V. (2006). Cooperative non-cell and cell autonomous regulation of Nodal gene expression and signaling by Lefty/Antivin and Brachyury in Xenopus. *Dev Biol* **290,** 246-64.

Chalmers, A. D., and Slack, J. M. (2000). The Xenopus tadpole gut: fate maps and morphogenetic movements. *Development* **127,** 381-92.

Chang, H., Zwijsen, A., Vogel, H., Huylebroeck, D., and Matzuk, M. M. (2000). Smad5 is essential for left-right asymmetry in mice. *Dev Biol* **219,** 71-8.

Chea, H. K., Wright, C. V., and Swalla, B. J. (2005). Nodal signaling and the evolution of deuterostome gastrulation. *Dev Dyn* **234,** 269-78.

Chen, X., Rubock, M. J., and Whitman, M. (1996). A transcriptional partner for MAD proteins in TGF-beta signalling. *Nature* **383,** 691-6.

Chen, Y., and Schier, A. F. (2001). The zebrafish Nodal signal Squint functions as a morphogen. *Nature* **411,** 607-10.

Chen, Y., and Schier, A. F. (2002). Lefty proteins are long-range inhibitors of squint-mediated nodal signaling. *Curr Biol* **12,** 2124-8.

Cheng, A. M., Thisse, B., Thisse, C., and Wright, C. V. (2000). The lefty-related factor Xatv acts as a feedback inhibitor of nodal signaling in mesoderm induction and L-R axis development in Xenopus. *Development* **127,** 1049-61.

Cheng, S. K., Olale, F., Bennett, J. T., Brivanlou, A. H., and Schier, A. F. (2003). EGF-CFC proteins are essential coreceptors for the TGF-beta signals Vg1 and GDF1. *Genes Dev* **17,** 31-6.

Collignon, J., Varlet, I., and Robertson, E. J. (1996). Relationship between asymmetric nodal expression and the direction of embryonic turning. *Nature* **381,** 155-8.

Condie, B. G., Brivanlou, A. H., and Harland, R. M. (1990). Most of the homeobox-containing Xhox 36 transcripts in early Xenopus embryos cannot encode a homeodomain protein. *Mol Cell Biol* **10,** 3376-85.

Conlon, F. L., Lyons, K. M., Takaesu, N., Barth, K. S., Kispert, A., Herrmann, B., and Robertson, E. J. (1994). A primary requirement for nodal in the formation and maintenance of the primitive streak in the mouse. *Development* **120,** 1919-28.

Constam, D. B., and Robertson, E. J. (2000). SPC4/PACE4 regulates a TGFbeta signaling network during axis formation. *Genes Dev* **14,** 1146-55.

Constam, D. B., and Robertson, E. J. (2000). Tissue-specific requirements for the proprotein convertase furin/SPC1 during embryonic turning and heart looping. *Development* **127,** 245-54.

DaCosta Byfield, S., Major, C., Laping, N. J., and Roberts, A. B. (2004). SB-505124 is a selective inhibitor of transforming growth factor-beta type I receptors ALK4, ALK5, and ALK7. *Mol Pharmacol* **65,** 744-52.

Danos, M. C., and Yost, H. J. (1995). Linkage of cardiac left-right asymmetry and dorsal-anterior development in Xenopus. *Development* **121,** 1467-74.

Danos, M. C., and Yost, H. J. (1996). Role of notochord in specification of cardiac left-right orientation in zebrafish and Xenopus. *Dev Biol* **177,** 96-103.

De Robertis, E. M., Larrain, J., Oelgeschlager, M., and Wessely, O. (2000). The establishment of Spemann's organizer and patterning of the vertebrate embryo. *Nat Rev Genet* **1,** 171-81.

Di Guglielmo, G. M., Le Roy, C., Goodfellow, A. F., and Wrana, J. L. (2003). Distinct endocytic pathways regulate TGF-beta receptor signalling and turnover. *Nat Cell Biol* **5,** 410-21.

Dibrov, A., Kashour, T., and Amara, F. M. (2006). The role of transforming growth factor beta signaling in messenger RNA stability. *Growth Factors* **24,** 1-11.

Ding, J., Yang, L., Yan, Y. T., Chen, A., Desai, N., Wynshaw-Boris, A., and Shen, M. M. (1998). Cripto is required for correct orientation of the anterior-posterior axis in the mouse embryo. *Nature* **395,** 702-7.

Duboc, V., Rottinger, E., Lapraz, F., Besnardeau, L., and Lepage, T. (2005). Left-right asymmetry in the sea urchin embryo is regulated by nodal signaling on the right side. *Dev Cell* **9,** 147-58.

Dupont, S., Zacchigna, L., Cordenonsi, M., Soligo, S., Adorno, M., Rugge, M., and Piccolo, S. (2005). Germ-layer specification and control of cell growth by Ectodermin, a Smad4 ubiquitin ligase. *Cell* **121,** 87-99.

Dyson, S., and Gurdon, J. B. (1998). The interpretation of position in a morphogen gradient as revealed by occupancy of activin receptors. *Cell* **93,** 557-68.

Ebisawa, T., Fukuchi, M., Murakami, G., Chiba, T., Tanaka, K., Imamura, T., and Miyazono, K. (2001). Smurf1 interacts with transforming growth factor-beta type I receptor through Smad7 and induces receptor degradation. *J Biol Chem* **276,** 12477-80.

Erter, C. E., Solnica-Krezel, L., and Wright, C. V. (1998). Zebrafish nodal-related 2 encodes an early mesendodermal inducer signaling from the extraembryonic yolk syncytial layer. *Dev Biol* **204,** 361-72.

Essner, J. J., Branford, W. W., Zhang, J., and Yost, H. J. (2000). Mesendoderm and left-right brain, heart and gut development are differentially regulated by pitx2 isoforms. *Development* **127,** 1081-93.

Essner, J. J., Vogan, K. J., Wagner, M. K., Tabin, C. J., Yost, H. J., and Brueckner, M. (2002). Conserved function for embryonic nodal cilia. *Nature* **418,** 37-8.

Ewart, J. L., Cohen, M. F., Meyer, R. A., Huang, G. Y., Wessels, A., Gourdie, R. G., Chin, A. J., Park, S. M., Lazatin, B. O., Villabon, S., and Lo, C. W. (1997). Heart and neural tube defects in transgenic mice overexpressing the Cx43 gap junction gene. *Development* **124,** 1281-92.

Faure, S., Lee, M. A., Keller, T., ten Dijke, P., and Whitman, M. (2000). Endogenous patterns of TGFbeta superfamily signaling during early Xenopus development. *Development* **127,** 2917-31.

Feldman, B., Gates, M. A., Egan, E. S., Dougan, S. T., Rennebeck, G., Sirotkin, H. I., Schier, A. F., and Talbot, W. S. (1998). Zebrafish organizer development and germ-layer formation require nodal-related signals. *Nature* **395,** 181-5.

Fujiwara, T., Dehart, D. B., Sulik, K. K., and Hogan, B. L. (2002). Distinct requirements for extra-embryonic and embryonic bone morphogenetic protein 4 in the formation of the node and primitive streak and coordination of left-right asymmetry in the mouse. *Development* **129,** 4685-96.

Funayama, N., Sato, Y., Matsumoto, K., Ogura, T., and Takahashi, Y. (1999). Coelom formation: binary decision of the lateral plate mesoderm is controlled by the ectoderm. *Development* **126,** 4129-38.

Furuhashi, M., Yagi, K., Yamamoto, H., Furukawa, Y., Shimada, S., Nakamura, Y., Kikuchi, A., Miyazono, K., and Kato, M. (2001). Axin facilitates Smad3 activation in the transforming growth factor beta signaling pathway. *Mol Cell Biol* **21,** 5132-41.

Gage, P. J., Suh, H., and Camper, S. A. (1999). Dosage requirement of Pitx2 for development of multiple organs. *Development* **126,** 4643-51.

Gebbia, M., Ferrero, G. B., Pilia, G., Bassi, M. T., Aylsworth, A. S., Penman-Splitt, M., Bird, L. M., Bamforth, J. S., Burn, J., Schlessinger, D., Nelson, D. L., and Casey, B. (1997). X-linked situs abnormalities result from mutations in ZIC3. *Nat Genet* **17**, 305-8.

Giltay, R., Kostka, G., and Timpl, R. (1997). Sequence and expression of a novel member (LTBP-4) of the family of latent transforming growth factor-beta binding proteins. *FEBS Lett* **411,** 164-8.

Gritsman, K., Zhang, J., Cheng, S., Heckscher, E., Talbot, W. S., and Schier, A. F. (1999). The EGF-CFC protein one-eyed pinhead is essential for nodal signaling. *Cell* **97,** 121-32.

Harland, R. M. (1991). In situ hybridization: an improved whole-mount method for Xenopus embryos. Methods in Cell Biology 36, 685-695.

Henry, G. L., and Melton, D. A. (1998). Mixer, a homeobox gene required for endoderm development. *Science* **281,** 91-6.

Ho, D. M., Chan, J., Bayliss, P., and Whitman, M. (2006). Inhibitor-resistant type I receptors reveal specific requirements for TGF-beta signaling in vivo. *Dev Biol* **295,** 730-42.

Hocevar, B. A., Smine, A., Xu, X. X., and Howe, P. H. (2001). The adaptor molecule Disabled-2 links the transforming growth factor beta receptors to the Smad pathway. *Embo J* **20,** 2789-801.

Horne-Badovinac, S., Rebagliati, M., and Stainier, D. Y. (2003). A cellular framework for gut-looping morphogenesis in zebrafish. *Science* **302,** 662-5.

Hudson, C., and Yasuo, H. (2005). Patterning across the ascidian neural plate by lateral Nodal signalling sources. *Development* **132,** 1199-210.

Hyatt, B. A., Lohr, J. L., and Yost, H. J. (1996). Initiation of vertebrate left-right axis formation by maternal Vg1. *Nature* **384,** 62-5.

Hyatt, B. A., and Yost, H. J. (1998). The left-right coordinator: the role of Vg1 in organizing left-right axis formation. *Cell* **93,** 37-46.

Inman, G. J., Nicolas, F. J., Callahan, J. F., Harling, J. D., Gaster, L. M., Reith, A. D., Laping, N. J., and Hill, C. S. (2002). SB-431542 is a potent and specific inhibitor of transforming growth factor-beta superfamily type I activin receptor-like kinase (ALK) receptors ALK4, ALK5, and ALK7. *Mol Pharmacol* **62,** 65-74.

Iratni, R., Yan, Y. T., Chen, C., Ding, J., Zhang, Y., Price, S. M., Reinberg, D., and Shen, M. M. (2002). Inhibition of excess nodal signaling during mouse gastrulation by the transcriptional corepressor DRAP1. *Science* **298,** 1996-9.

Isaac, A., Sargent, M. G., and Cooke, J. (1997). Control of vertebrate left-right asymmetry by a snail-related zinc finger gene. *Science* **275,** 1301-4.

Ito, Y., Oinuma, T., Takano, K., Komazaki, S., Obata, S., and Asashima, M. (2006). CyNodal, the Japanese newt nodal-related gene, is expressed in the left side of the lateral plate mesoderm and diencephalon. *Gene Expr Patterns* **6,** 294-8.

Izraeli, S., Lowe, L. A., Bertness, V. L., Good, D. J., Dorward, D. W., Kirsch, I. R., and Kuehn, M. R. (1999). The SIL gene is required for mouse embryonic axial development and left-right specification. *Nature* **399,** 691-4.

Jones, C. M., Kuehn, M. R., Hogan, B. L., Smith, J. C., and Wright, C. V. (1995). Nodal-related signals induce axial mesoderm and dorsalize mesoderm during gastrulation. *Development* **121,** 3651-62.

Joseph, E. M., and Melton, D. A. (1997). Xnr4: a Xenopus nodal-related gene expressed in the Spemann organizer. *Dev Biol* **184,** 367-72.

Juan, H., and Hamada, H. (2001). Roles of nodal-lefty regulatory loops in embryonic patterning of vertebrates. *Genes Cells* **6,** 923-30.

Jullien, J., and Gurdon, J. (2005). Morphogen gradient interpretation by a regulated trafficking step during ligand-receptor transduction. *Genes Dev* **19,** 2682-94.

Kaestner, K. H., Knochel, W., and Martinez, D. E. (2000). Unified nomenclature for the winged helix/forkhead transcription factors. *Genes Dev* **14,** 142-6.

Kavsak, P., Rasmussen, R. K., Causing, C. G., Bonni, S., Zhu, H., Thomsen, G. H., and Wrana, J. L. (2000). Smad7 binds to Smurf2 to form an E3 ubiquitin ligase that targets the TGF beta receptor for degradation. *Mol Cell* **6,** 1365-75.

Kay, B. K., Peng, H.B. (1991). "Xenopus laevis: Practical uses in cell and molecular biology." Academic Press., San Diego.

Kitamura, K., Miura, H., Miyagawa-Tomita, S., Yanazawa, M., Katoh-Fukui, Y., Suzuki, R., Ohuchi, H., Suehiro, A., Motegi, Y., Nakahara, Y., Kondo, S., and Yokoyama, M. (1999). Mouse Pitx2 deficiency leads to anomalies of the ventral body wall, heart, extra- and periocular mesoderm and right pulmonary isomerism. *Development* **126,** 5749-58.

Kofron, M., Demel, T., Xanthos, J., Lohr, J., Sun, B., Sive, H., Osada, S., Wright, C., Wylie, C., and Heasman, J. (1999). Mesoderm induction in Xenopus is a zygotic event regulated by maternal VegT via TGFbeta growth factors. *Development* **126,** 5759-70.

Kramer, K. L., Barnette, J. E., and Yost, H. J. (2002). PKCgamma regulates syndecan-2 inside-out signaling during xenopus left-right development. *Cell* **111,** 981-90.

Kramer, K. L., and Yost, H. J. (2002). Ectodermal syndecan-2 mediates left-right axis formation in migrating mesoderm as a cell-nonautonomous Vg1 cofactor. *Dev Cell* **2,** 115-24.

Krebs, L. T., Iwai, N., Nonaka, S., Welsh, I. C., Lan, Y., Jiang, R., Saijoh, Y., O'Brien, T. P., Hamada, H., and Gridley, T. (2003). Notch signaling regulates left-right asymmetry determination by inducing Nodal expression. *Genes Dev* **17,** 1207-12.

Laping, N. J., Grygielko, E., Mathur, A., Butter, S., Bomberger, J., Tweed, C., Martin, W., Fornwald, J., Lehr, R., Harling, J., Gaster, L., Callahan, J. F., and Olson, B. A. (2002). Inhibition of transforming growth factor (TGF)-beta1-induced extracellular matrix with a novel inhibitor of the TGF-beta type I receptor kinase activity: SB-431542. *Mol Pharmacol* **62,** 58-64.

Levin, M. (2005). Left-right asymmetry in embryonic development: a comprehensive review. *Mech Dev* **122,** 3-25.

Levin, M., Johnson, R. L., Stern, C. D., Kuehn, M., and Tabin, C. (1995). A molecular pathway determining left-right asymmetry in chick embryogenesis. *Cell* **82,** 803-14.

Levin, M., and Mercola, M. (1998). Evolutionary conservation of mechanisms upstream of asymmetric Nodal expression: reconciling chick and Xenopus. *Dev Genet* **23,** 185-93.

Levin, M., and Mercola, M. (1998). Gap junctions are involved in the early generation of left-right asymmetry. *Dev Biol* **203,** 90-105.

Levin, M., and Mercola, M. (1999). Gap junction-mediated transfer of left-right patterning signals in the early chick blastoderm is upstream of Shh asymmetry in the node. *Development* **126,** 4703-14.

Levin, M., Pagan, S., Roberts, D. J., Cooke, J., Kuehn, M. R., and Tabin, C. J. (1997). Left/right patterning signals and the independent regulation of different aspects of situs in the chick embryo. *Dev Biol* **189,** 57-67.

Levin, M., Roberts, D. J., Holmes, L. B., and Tabin, C. (1996). Laterality defects in conjoined twins. *Nature* **384,** 321.

Levin, M., Thorlin, T., Robinson, K. R., Nogi, T., and Mercola, M. (2002). Asymmetries in H+/K+-ATPase and cell membrane potentials comprise a very early step in left-right patterning. *Cell* **111,** 77-89.

Lin, C. R., Kioussi, C., O'Connell, S., Briata, P., Szeto, D., Liu, F., Izpisua-Belmonte, J. C., and Rosenfeld, M. G. (1999). Pitx2 regulates lung asymmetry, cardiac positioning and pituitary and tooth morphogenesis. *Nature* **401,** 279-82.

Lo, R. S., and Massague, J. (1999). Ubiquitin-dependent degradation of TGF-beta-activated smad2. *Nat Cell Biol* **1,** 472-8.

Logan, M., Pagan-Westphal, S. M., Smith, D. M., Paganessi, L., and Tabin, C. J. (1998). The transcription factor Pitx2 mediates situs-specific morphogenesis in response to left-right asymmetric signals. *Cell* **94,** 307-17.

Lohr, J. L., Danos, M. C., Groth, T. W., and Yost, H. J. (1998). Maintenance of asymmetric nodal expression in Xenopus laevis. *Dev Genet* **23,** 194-202.

Lohr, J. L., Danos, M. C., and Yost, H. J. (1997). Left-right asymmetry of a nodal-related gene is regulated by dorsoanterior midline structures during Xenopus development. *Development* **124,** 1465-72.

Long, S., Ahmad, N., and Rebagliati, M. (2003). The zebrafish nodal-related gene southpaw is required for visceral and diencephalic left-right asymmetry. *Development* **130,** 2303-16.

Lowe, L. A., Supp, D. M., Sampath, K., Yokoyama, T., Wright, C. V., Potter, S. S., Overbeek, P., and Kuehn, M. R. (1996). Conserved left-right asymmetry of nodal expression and alterations in murine situs inversus. *Nature* **381,** 158-61.

Lowe, L. A., Yamada, S., and Kuehn, M. R. (2001). Genetic dissection of nodal function in patterning the mouse embryo. *Development* **128,** 1831-43.

Lu, M. F., Pressman, C., Dyer, R., Johnson, R. L., and Martin, J. F. (1999). Function of Rieger syndrome gene in left-right asymmetry and craniofacial development. *Nature* **401,** 276-8.

Lustig, K. D., Kroll, K., Sun, E., Ramos, R., Elmendorf, H., and Kirschner, M. W. (1996). A Xenopus nodal-related gene that acts in synergy with noggin to induce complete secondary axis and notochord formation. *Development* **122,** 3275-82.

Massague, J. (1998). TGF-beta signal transduction. *Annu Rev Biochem* **67,** 753-91.

Matzuk, M. M., Kumar, T. R., Vassalli, A., Bickenbach, J. R., Roop, D. R., Jaenisch, R., and Bradley, A. (1995). Functional analysis of activins during mammalian development. *Nature* **374,** 354-6.

McGrath, J., and Brueckner, M. (2003). Cilia are at the heart of vertebrate left-right asymmetry. *Curr Opin Genet Dev* **13,** 385-92.

McGrath, J., Somlo, S., Makova, S., Tian, X., and Brueckner, M. (2003). Two populations of node monocilia initiate left-right asymmetry in the mouse. *Cell* **114,** 61-73.

Meier, S. (1979). Development of the chick embryo mesoblast. Formation of the embryonic axis and establishment of the metameric pattern. *Dev Biol* **73,** 24-45.

Meinhardt, H. (2001). Organizer and axes formation as a self-organizing process. *Int J Dev Biol* **45,** 177-88.

Melloy, P. G., Ewart, J. L., Cohen, M. F., Desmond, M. E., Kuehn, M. R., and Lo, C. W. (1998). No turning, a mouse mutation causing left-right and axial patterning defects. *Dev Biol* **193,** 77-89.

Meno, C., Gritsman, K., Ohishi, S., Ohfuji, Y., Heckscher, E., Mochida, K., Shimono, A., Kondoh, H., Talbot, W. S., Robertson, E. J., Schier, A. F., and Hamada, H. (1999). Mouse Lefty2 and zebrafish antivin are feedback inhibitors of nodal signaling during vertebrate gastrulation. *Mol Cell* **4,** 287-98.

Meno, C., Saijoh, Y., Fujii, H., Ikeda, M., Yokoyama, T., Yokoyama, M., Toyoda, Y., and Hamada, H. (1996). Left-right asymmetric expression of the TGF beta-family member lefty in mouse embryos. *Nature* **381,** 151-5.

Meno, C., Shimono, A., Saijoh, Y., Yashiro, K., Mochida, K., Ohishi, S., Noji, S., Kondoh, H., and Hamada, H. (1998). lefty-1 is required for left-right determination as a regulator of lefty-2 and nodal. *Cell* **94,** 287-97.

Meno, C., Takeuchi, J., Sakuma, R., Koshiba-Takeuchi, K., Ohishi, S., Saijoh, Y., Miyazaki, J., ten Dijke, P., Ogura, T., and Hamada, H. (2001). Diffusion of nodal signaling activity in the absence of the feedback inhibitor Lefty2. *Dev Cell* **1,** 127-38.

Mercola, M., and Levin, M. (2001). Left-right asymmetry determination in vertebrates. *Annu Rev Cell Dev Biol* **17,** 779-805.

Meyers, E. N., and Martin, G. R. (1999). Differences in left-right axis pathways in mouse and chick: functions of FGF8 and SHH. *Science* **285,** 403-6.

Mogi, K., Goto, M., Ohno, E., Azumi, Y., Takeuchi, S., and Toyoizumi, R. (2003). Xenopus neurula left-right asymmetry is respeficied by microinjecting TGF-beta5 protein. *Int J Dev Biol* **47,** 15-29.

Morokuma, J., Ueno, M., Kawanishi, H., Saiga, H., and Nishida, H. (2002). HrNodal, the ascidian nodal-related gene, is expressed in the left side of the epidermis, and lies upstream of HrPitx. *Dev Genes Evol* **212,** 439-46.

Murray, S. A., and Gridley, T. (2006). Snail family genes are required for left-right asymmetry determination, but not neural crest formation, in mice. *Proc Natl Acad Sci U S A* **103,** 10300-4.

Nakamura, T., Mine, N., Nakaguchi, E., Mochizuki, A., Yamamoto, M., Yashiro, K., Meno, C., and Hamada, H. (2006). Generation of robust left-right asymmetry in the mouse embryo requires a self-enhancement and lateral-inhibition system. *Dev Cell* **11,** 495-504.

Nascone, N., and Mercola, M. (1997). Organizer induction determines left-right asymmetry in Xenopus. *Dev Biol* **189,** 68-78.

Nieuwkoop, P. D., Faber, J. (1967). "Normal Table of Xenopus laevis (Daudin): a systematical and chronological survey of the development from the fertilized egg till the end of metamorphosis." North-Holland Publishing Company, Amsterdam.

Nonaka, S., Shiratori, H., Saijoh, Y., and Hamada, H. (2002). Determination of left-right patterning of the mouse embryo by artificial nodal flow. *Nature* **418,** 96-9.

Nonaka, S., Tanaka, Y., Okada, Y., Takeda, S., Harada, A., Kanai, Y., Kido, M., and Hirokawa, N. (1998). Randomization of left-right asymmetry due to loss of nodal cilia generating leftward flow of extraembryonic fluid in mice lacking KIF3B motor protein. *Cell* **95,** 829-37.

Okada, Y., Nonaka, S., Tanaka, Y., Saijoh, Y., Hamada, H., and Hirokawa, N. (1999). Abnormal nodal flow precedes situs inversus in iv and inv mice. *Mol Cell* **4,** 459-68.

Osada, S. I., Saijoh, Y., Frisch, A., Yeo, C. Y., Adachi, H., Watanabe, M., Whitman, M., Hamada, H., and Wright, C. V. (2000). Activin/nodal responsiveness and asymmetric expression of a Xenopus nodal-related gene converge on a FAST-regulated module in intron 1. *Development* **127,** 2503-14.

Pagan-Westphal, S. M., and Tabin, C. J. (1998). The transfer of left-right positional information during chick embryogenesis. *Cell* **93,** 25-35.

Patel, K., Isaac, A., and Cooke, J. (1999). Nodal signalling and the roles of the transcription factors SnR and Pitx2 in vertebrate left-right asymmetry. *Curr Biol* **9,** 609-12.

Pennekamp, P., Karcher, C., Fischer, A., Schweickert, A., Skryabin, B., Horst, J., Blum, M., and Dworniczak, B. (2002). The ion channel polycystin-2 is required for left-right axis determination in mice. *Curr Biol* **12,** 938-43.

Piccolo, S., Agius, E., Leyns, L., Bhattacharyya, S., Grunz, H., Bouwmeester, T., and De Robertis, E. M. (1999). The head inducer Cerberus is a multifunctional antagonist of Nodal, BMP and Wnt signals. *Nature* **397,** 707-10.

Piedra, M. E., Icardo, J. M., Albajar, M., Rodriguez-Rey, J. C., and Ros, M. A. (1998). Pitx2 participates in the late phase of the pathway controlling left-right asymmetry. *Cell* **94,** 319-24.

Piedra, M. E., and Ros, M. A. (2002). BMP signaling positively regulates Nodal expression during left right specification in the chick embryo. *Development* **129,** 3431-40.

Pogoda, H. M., Solnica-Krezel, L., Driever, W., and Meyer, D. (2000). The zebrafish forkhead transcription factor FoxH1/Fast1 is a modulator of nodal signaling required for organizer formation. *Curr Biol* **10,** 1041-9.

Pourquie, O. (2001). Vertebrate somitogenesis. *Annu Rev Cell Dev Biol* **17,** 311-50.

Qiu, D., Cheng, S. M., Wozniak, L., McSweeney, M., Perrone, E., and Levin, M. (2005). Localization and loss-of-function implicates ciliary proteins in early, cytoplasmic roles in left-right asymmetry. *Dev Dyn* **234,** 176-89.

Ramsdell, A. F., and Yost, H. J. (1998). Molecular mechanisms of vertebrate left-right development. *Trends Genet* **14,** 459-65.

Ramsdell, A. F., and Yost, H. J. (1999). Cardiac looping and the vertebrate left-right axis: antagonism of left-sided Vg1 activity by a right-sided ALK2-dependent BMP pathway. *Development* **126,** 5195-205.

Randall, R. A., Germain, S., Inman, G. J., Bates, P. A., and Hill, C. S. (2002). Different Smad2 partners bind a common hydrophobic pocket in Smad2 via a defined proline-rich motif. *Embo J* **21,** 145-56.

Raya, A., and Belmonte, J. C. (2006). Left-right asymmetry in the vertebrate embryo: from early information to higher-level integration. *Nat Rev Genet* **7,** 283-93.

Raya, A., Kawakami, Y., Rodriguez-Esteban, C., Buscher, D., Koth, C. M., Itoh, T., Morita, M., Raya, R. M., Dubova, I., Bessa, J. G., de la Pompa, J. L., and Belmonte, J. C. (2003). Notch activity induces Nodal expression and mediates the establishment of left-right asymmetry in vertebrate embryos. *Genes Dev* **17,** 1213-8.

Raya, A., Kawakami, Y., Rodriguez-Esteban, C., Ibanes, M., Rasskin-Gutman, D., Rodriguez-Leon, J., Buscher, D., Feijo, J. A., and Izpisua Belmonte, J. C. (2004). Notch activity acts as a sensor for extracellular calcium during vertebrate left-right determination. *Nature* **427,** 121-8.

Reaume, A. G., de Sousa, P. A., Kulkarni, S., Langille, B. L., Zhu, D., Davies, T. C., Juneja, S. C., Kidder, G. M., and Rossant, J. (1995). Cardiac malformation in neonatal mice lacking connexin43. *Science* **267,** 1831-4.

Rebagliati, M. R., Toyama, R., Fricke, C., Haffter, P., and Dawid, I. B. (1998). Zebrafish nodal-related genes are implicated in axial patterning and establishing left-right asymmetry. *Dev Biol* **199,** 261-72.

Reissmann, E., Jornvall, H., Blokzijl, A., Andersson, O., Chang, C., Minchiotti, G., Persico, M. G., Ibanez, C. F., and Brivanlou, A. H. (2001). The orphan receptor ALK7 and the Activin receptor ALK4 mediate signaling by Nodal proteins during vertebrate development. *Genes Dev* **15,** 2010-22.

Rodriguez Esteban, C., Capdevila, J., Economides, A. N., Pascual, J., Ortiz, A., and Izpisua Belmonte, J. C. (1999). The novel Cer-like protein Caronte mediates the establishment of embryonic left-right asymmetry. *Nature* **401,** 243-51.

Rosa, F. M. (2002). Cripto, a multifunctional partner in signaling: molecular forms and activities. *Sci STKE* **2002,** PE47.

Ryan, A. K., Blumberg, B., Rodriguez-Esteban, C., Yonei-Tamura, S., Tamura, K., Tsukui, T., de la Pena, J., Sabbagh, W., Greenwald, J., Choe, S., Norris, D. P., Robertson, E. J., Evans, R. M., Rosenfeld, M. G., and Izpisua Belmonte, J. C. (1998). Pitx2 determines left-right asymmetry of internal organs in vertebrates. *Nature* **394,** 545-51.

Saijoh, Y., Adachi, H., Sakuma, R., Yeo, C. Y., Yashiro, K., Watanabe, M., Hashiguchi, H., Mochida, K., Ohishi, S., Kawabata, M., Miyazono, K., Whitman, M., and Hamada, H. (2000). Left-right asymmetric expression of lefty2 and nodal is induced by a signaling pathway that includes the transcription factor FAST2. *Mol Cell* **5,** 35-47.

Saijoh, Y., Oki, S., Ohishi, S., and Hamada, H. (2003). Left-right patterning of the mouse lateral plate requires nodal produced in the node. *Dev Biol* **256,** 160-72.

Sakuma, R., Ohnishi Yi, Y., Meno, C., Fujii, H., Juan, H., Takeuchi, J., Ogura, T., Li, E., Miyazono, K., and Hamada, H. (2002). Inhibition of Nodal signalling by Lefty mediated through interaction with common receptors and efficient diffusion. *Genes Cells* **7,** 401-12.

Sampath, K., Cheng, A. M., Frisch, A., and Wright, C. V. (1997). Functional differences among Xenopus nodal-related genes in left-right axis determination. *Development* **124,** 3293-302.

Sampath, K., Rubinstein, A. L., Cheng, A. M., Liang, J. O., Fekany, K., Solnica-Krezel, L., Korzh, V., Halpern, M. E., and Wright, C. V. (1998). Induction of the zebrafish ventral brain and floorplate requires cyclops/nodal signalling. *Nature* **395,** 185-9.

Schier, A. F. (2003). Nodal signaling in vertebrate development. *Annu Rev Cell Dev Biol* **19,** 589-621.

Schlange, T., Arnold, H. H., and Brand, T. (2002). BMP2 is a positive regulator of Nodal signaling during left-right axis formation in the chicken embryo. *Development* **129,** 3421-9.

Schneider, A., Mijalski, T., Schlange, T., Dai, W., Overbeek, P., Arnold, H. H., and Brand, T. (1999). The homeobox gene NKX3.2 is a target of left-right signalling and is expressed on opposite sides in chick and mouse embryos. *Curr Biol* **9,** 911-4.

Schweickert, A., Campione, M., Steinbeisser, H., and Blum, M. (2000). Pitx2 isoforms: involvement of Pitx2c but not Pitx2a or Pitx2b in vertebrate left-right asymmetry. *Mech Dev* **90,** 41-51.

Sefton, M., Sanchez, S., and Nieto, M. A. (1998). Conserved and divergent roles for members of the Snail family of transcription factors in the chick and mouse embryo. *Development* **125,** 3111-21.

Semina, E. V., Reiter, R., Leysens, N. J., Alward, W. L., Small, K. W., Datson, N. A., Siegel-Bartelt, J., Bierke-Nelson, D., Bitoun, P., Zabel, B. U., Carey, J. C., and Murray, J. C. (1996). Cloning and characterization of a novel bicoid-related homeobox transcription factor gene, RIEG, involved in Rieger syndrome. *Nat Genet* **14,** 392-9.

Shen, M. M., and Schier, A. F. (2000). The EGF-CFC gene family in vertebrate development. *Trends Genet* **16,** 303-9.

Shi, Y., and Massague, J. (2003). Mechanisms of TGF-beta signaling from cell membrane to the nucleus. *Cell* **113,** 685-700.

Shimizu, K., and Gurdon, J. B. (1999). A quantitative analysis of signal transduction from activin receptor to nucleus and its relevance to morphogen gradient interpretation. *Proc Natl Acad Sci U S A* **96,** 6791-6.

Shiratori, H., Sakuma, R., Watanabe, M., Hashiguchi, H., Mochida, K., Sakai, Y., Nishino, J., Saijoh, Y., Whitman, M., and Hamada, H. (2001). Two-step regulation of left-right asymmetric expression of Pitx2: initiation by nodal signaling and maintenance by Nkx2. *Mol Cell* **7,** 137-49.

Sirotkin, H. I., Gates, M. A., Kelly, P. D., Schier, A. F., and Talbot, W. S. (2000). Fast1 is required for the development of dorsal axial structures in zebrafish. *Curr Biol* **10,** 1051-4.

Sive, H. L., Grainger, R.M., Harland, R.M. (2000). "Early development of Xenopus laevis: A laboratory manual." Cold Spring Harbor Laboratory Press, Cold Spring Harbor, NY.

Smith, W. C., McKendry, R., Ribisi, S., Jr., and Harland, R. M. (1995). A nodal-related gene defines a physical and functional domain within the Spemann organizer. *Cell* **82,** 37-46.

Solnica-Krezel, L. (2003). Vertebrate development: taming the nodal waves. *Curr Biol* **13,** R7-9.

Song, Q. H., Klepeis, V. E., Nugent, M. A., and Trinkaus-Randall, V. (2002). TGF-beta1 regulates TGF-beta1 and FGF-2 mRNA expression during fibroblast wound healing. *Mol Pathol* **55,** 164-76.

Soroldoni, D., Bajoghli, B., Aghaallaei, N., and Czerny, T. (2006). Dynamic expression pattern of Nodal-related genes during left-right development in medaka. *Gene Expr Patterns* **7,** 93-101.

St Amand, T. R., Ra, J., Zhang, Y., Hu, Y., Baber, S. I., Qiu, M., and Chen, Y. (1998). Cloning and expression pattern of chicken Pitx2: a new component in the SHH signaling pathway controlling embryonic heart looping. *Biochem Biophys Res Commun* **247,** 100-5.

Sterner-Kock, A., Thorey, I. S., Koli, K., Wempe, F., Otte, J., Bangsow, T., Kuhlmeier, K., Kirchner, T., Jin, S., Keski-Oja, J., and von Melchner, H. (2002). Disruption of the gene encoding the latent transforming growth factor-beta binding protein 4 (LTBP-4) causes abnormal lung development, cardiomyopathy, and colorectal cancer. *Genes Dev* **16,** 2264-73.

Sun, P. D., and Davies, D. R. (1995). The cystine-knot growth-factor superfamily. *Annu Rev Biophys Biomol Struct* **24,** 269-91.

Sun, Z., Jin, P., Tian, T., Gu, Y., Chen, Y. G., and Meng, A. (2006). Activation and roles of ALK4/ALK7-mediated maternal TGFbeta signals in zebrafish embryo. *Biochem Biophys Res Commun* **345,** 694-703.

Suzuki, C., Murakami, G., Fukuchi, M., Shimanuki, T., Shikauchi, Y., Imamura, T., and Miyazono, K. (2002). Smurf1 regulates the inhibitory activity of Smad7 by targeting Smad7 to the plasma membrane. *J Biol Chem* **277,** 39919-25.

Tabin, C. J. (2006). The key to left-right asymmetry. *Cell* **127,** 27-32.

Tabin, C. J., and Vogan, K. J. (2003). A two-cilia model for vertebrate left-right axis specification. *Genes Dev* **17,** 1-6.

Tajbakhsh, S., and Sporle, R. (1998). Somite development: constructing the vertebrate body. *Cell* **92,** 9-16.

Tajima, Y., Goto, K., Yoshida, M., Shinomiya, K., Sekimoto, T., Yoneda, Y., Miyazono, K., and Imamura, T. (2003). Chromosomal region maintenance 1 (CRM1)-dependent nuclear export of Smad ubiquitin regulatory factor 1 (Smurf1) is essential for negative regulation of transforming growth factor-beta signaling by Smad7. *J Biol Chem* **278,** 10716-21.

Takahashi, S., Onuma, Y., Yokota, C., Westmoreland, J. J., Asashima, M., and Wright, C. V. (2006). Nodal-related gene Xnr5 is amplified in the Xenopus genome. *Genesis* **44,** 309-21.

Takahashi, S., Yokota, C., Takano, K., Tanegashima, K., Onuma, Y., Goto, J., and Asashima, M. (2000). Two novel nodal-related genes initiate early inductive events in Xenopus Nieuwkoop center. *Development* **127,** 5319-29.

Tanaka, Y., Okada, Y., and Hirokawa, N. (2005). FGF-induced vesicular release of Sonic hedgehog and retinoic acid in leftward nodal flow is critical for left-right determination. *Nature* **435,** 172-7.

Tanegashima, K., Yokota, C., Takahashi, S., and Asashima, M. (2000). Expression cloning of Xantivin, a Xenopus lefty/antivin-related gene, involved in the regulation of activin signaling during mesoderm induction. *Mech Dev* **99,** 3-14.

Tang, Y., Katuri, V., Dillner, A., Mishra, B., Deng, C. X., and Mishra, L. (2003). Disruption of transforming growth factor-beta signaling in ELF beta-spectrin-deficient mice. *Science* **299,** 574-7.

Thisse, B., Wright, C. V., and Thisse, C. (2000). Activin- and Nodal-related factors control antero-posterior patterning of the zebrafish embryo. *Nature* **403,** 425-8.

Thisse, C., and Thisse, B. (1999). Antivin, a novel and divergent member of the TGFbeta superfamily, negatively regulates mesoderm induction. *Development* **126,** 229-40.

Toyoizumi, R., Mogi, K., and Takeuchi, S. (2000). More than 95% reversal of left-right axis induced by right-sided hypodermic microinjection of activin into Xenopus neurula embryos. *Dev Biol* **221,** 321-36.

Toyoizumi, R., Ogasawara, T., Takeuchi, S., and Mogi, K. (2005). Xenopus nodal related-1 is indispensable only for left-right axis determination. *Int J Dev Biol* **49,** 923-38.

Tsukazaki, T., Chiang, T. A., Davison, A. F., Attisano, L., and Wrana, J. L. (1998). SARA, a FYVE domain protein that recruits Smad2 to the TGFbeta receptor. *Cell* **95,** 779-91.

Turing, A.M., 1952. The chemical basis of morphogenesis. Philos. Trnas. R. Soc. Lond. B237, 37-72.

Vincent, S. D., Norris, D. P., Le Good, J. A., Constam, D. B., and Robertson, E. J. (2004). Asymmetric Nodal expression in the mouse is governed by the combinatorial activities of two distinct regulatory elements. *Mech Dev* **121,** 1403-15.

Watanabe, M., and Whitman, M. (1999). FAST-1 is a key maternal effector of mesoderm inducers in the early Xenopus embryo. *Development* **126,** 5621-34.

Weeks, D. L., and Melton, D. A. (1987). A maternal mRNA localized to the vegetal hemisphere in Xenopus eggs codes for a growth factor related to TGF-beta. *Cell* **51,** 861-7.

Whitman, M. (2001). Nodal signaling in early vertebrate embryos: themes and variations. *Dev Cell* **1,** 605-17.

Whitman, M., and Mercola, M. (2001). TGF-beta superfamily signaling and left-right asymmetry. *Sci STKE* **2001,** RE1.

Williams, P. H., Hagemann, A., Gonzalez-Gaitan, M., and Smith, J. C. (2004). Visualizing long-range movement of the morphogen Xnr2 in the Xenopus embryo. *Curr Biol* **14,** 1916-23.

Wright, C. V. (2001). Mechanisms of left-right asymmetry: what's right and what's left? *Dev Cell* **1,** 179-86.

Wu, G., Chen, Y. G., Ozdamar, B., Gyuricza, C. A., Chong, P. A., Wrana, J. L., Massague, J., and Shi, Y. (2000). Structural basis of Smad2 recognition by the Smad anchor for receptor activation. *Science* **287,** 92-7.

Wylie, C., Kofron, M., Payne, C., Anderson, R., Hosobuchi, M., Joseph, E., and Heasman, J. (1996). Maternal beta-catenin establishes a 'dorsal signal' in early Xenopus embryos. *Development* **122,** 2987-96.

Xu, L., Chen, Y. G., and Massague, J. (2000). The nuclear import function of Smad2 is masked by SARA and unmasked by TGFbeta-dependent phosphorylation. *Nat Cell Biol* **2,** 559-62.

Yamamoto, M., Meno, C., Sakai, Y., Shiratori, H., Mochida, K., Ikawa, Y., Saijoh, Y., and Hamada, H. (2001). The transcription factor FoxH1 (FAST) mediates Nodal signaling during anterior-posterior patterning and node formation in the mouse. *Genes Dev* **15,** 1242-56.

Yamamoto, M., Mine, N., Mochida, K., Sakai, Y., Saijoh, Y., Meno, C., and Hamada, H. (2003). Nodal signaling induces the midline barrier by activating Nodal expression in the lateral plate. *Development* **130,** 1795-804.

Yan, Y. T., Gritsman, K., Ding, J., Burdine, R. D., Corrales, J. D., Price, S. M., Talbot, W. S., Schier, A. F., and Shen, M. M. (1999). Conserved requirement for EGF-CFC genes in vertebrate left-right axis formation. *Genes Dev* **13,** 2527-37.

Yan, Y. T., Liu, J. J., Luo, Y., E, C., Haltiwanger, R. S., Abate-Shen, C., and Shen, M. M. (2002). Dual roles of Cripto as a ligand and coreceptor in the nodal signaling pathway. *Mol Cell Biol* **22,** 4439-49.

Yeo, C., and Whitman, M. (2001). Nodal signals to Smads through Cripto-dependent and Cripto-independent mechanisms. *Mol Cell* **7,** 949-57.

Yin, W., Fang, J., Smiley, E., and Bonadio, J. (1998). 8-Cysteine TGF-BP structural motifs are the site of covalent binding between mouse LTBP-3, LTBP-2, and latent TGF-beta 1. *Biochim Biophys Acta* **1383,** 340-50.

Yokouchi, Y., Vogan, K. J., Pearse, R. V., 2nd, and Tabin, C. J. (1999). Antagonistic signaling by Caronte, a novel Cerberus-related gene, establishes left-right asymmetric gene expression. *Cell* **98,** 573-83.

Yoshioka, H., Meno, C., Koshiba, K., Sugihara, M., Itoh, H., Ishimaru, Y., Inoue, T., Ohuchi, H., Semina, E. V., Murray, J. C., Hamada, H., and Noji, S. (1998). Pitx2, a bicoid-type homeobox gene, is involved in a lefty-signaling pathway in determination of left-right asymmetry. *Cell* **94,** 299-305.

Yost, H. J. (2003). Left-right asymmetry: nodal cilia make and catch a wave. *Curr Biol* **13,** R808-9.

Yu, J. K., Holland, L. Z., and Holland, N. D. (2002). An amphioxus nodal gene (AmphiNodal) with early symmetrical expression in the organizer and mesoderm and later asymmetrical expression associated with left-right axis formation. *Evol Dev* **4,** 418-25.

Yu, X., St Amand, T. R., Wang, S., Li, G., Zhang, Y., Hu, Y. P., Nguyen, L., Qiu, M. S., and Chen, Y. P. (2001). Differential expression and functional analysis of Pitx2 isoforms in regulation of heart looping in the chick. *Development* **128,** 1005-13.

Zhang, J., Houston, D. W., King, M. L., Payne, C., Wylie, C., and Heasman, J. (1998). The role of maternal VegT in establishing the primary germ layers in Xenopus embryos. *Cell* **94,** 515-24.

Zhang, L., Zhou, H., Su, Y., Sun, Z., Zhang, H., Zhang, Y., Ning, Y., Chen, Y. G., and Meng, A. (2004). Zebrafish Dpr2 inhibits mesoderm induction by promoting degradation of nodal receptors. *Science* **306,** 114-7.

Zhou, S., Zawel, L., Lengauer, C., Kinzler, K. W., and Vogelstein, B. (1998). Characterization of human FAST-1, a TGF beta and activin signal transducer. *Mol Cell* **2,** 121-7.

Zhou, X., Sasaki, H., Lowe, L., Hogan, B. L., and Kuehn, M. R. (1993). Nodal is a novel TGF-beta-like gene expressed in the mouse node during gastrulation. *Nature* **361,** 543-7.